TN TDOT Department of Transportation

U.S. Department of Transportation
Federal Highway Administration

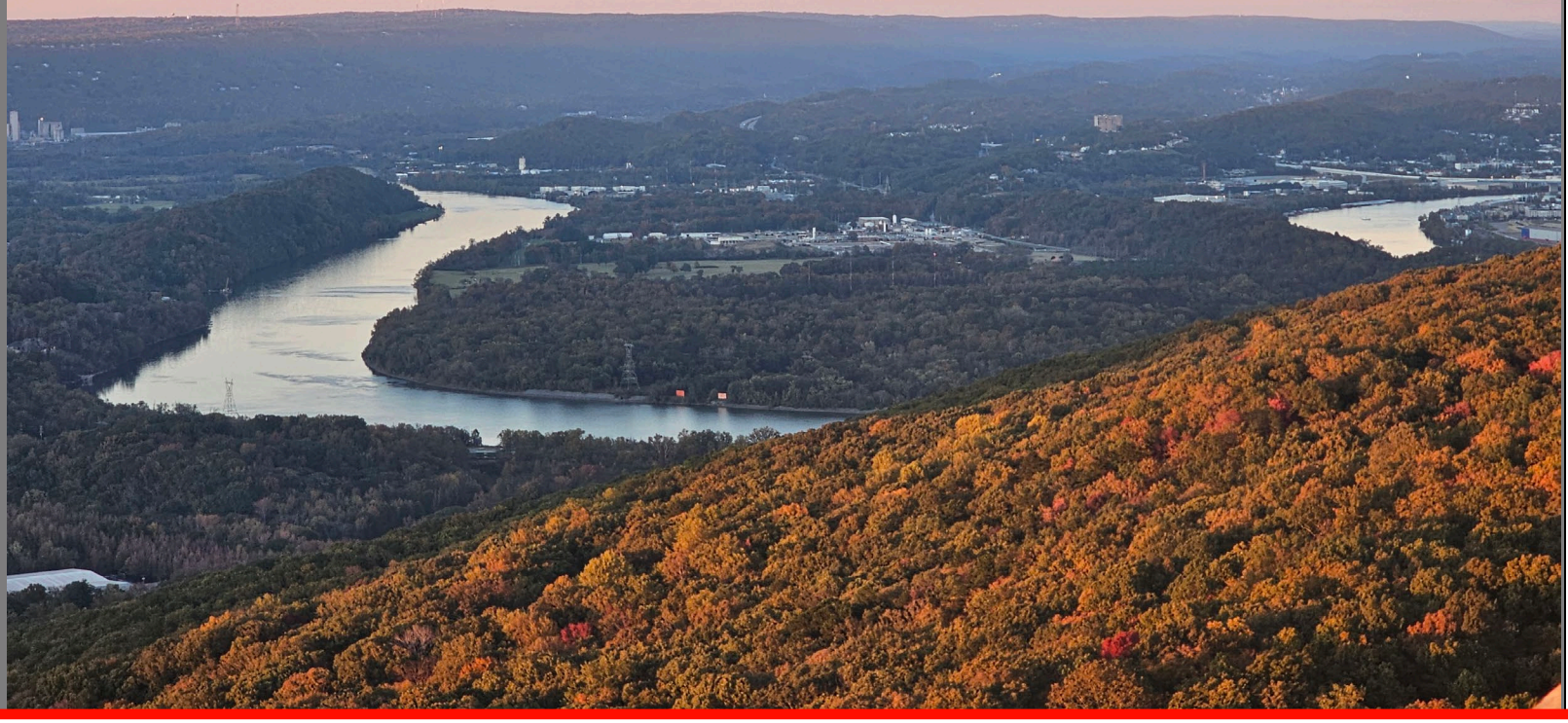

Effects of Extreme Climate Shifts to Pavement Infrastructure in Tennessee

Research Final Report from University of Tennessee at Chattanooga | Dr. Mbakisya Onyango (PI), Dr. Ignatius Fomunung (Co-PI), Dr. Jejal Reddy Bathi (Co-PI), Dr. Joseph Owino (Co-PI), Dr. Yu Liang (Co-PI), Maxine Otieno (RA), Maneesha Vanga (GRA) | September 30, 2025

Sponsored by Tennessee Department of Transportation Strategic, Planning, & Innovation Division & Federal Highway Administration

THE UNIVERSITY OF TENNESSEE CHATTANOOGA
COLLEGE OF ENGINEERING AND COMPUTER SCIENCE

DISCLAIMER

This research was funded through the State Planning and Research (SPR) Program by the Tennessee Department of Transportation and the Federal Highway Administration under ***RES: 2023-11: Effects of Extreme Climate Shifts to Pavement Infrastructure in Tennessee.***

Technical Report Documentation Page

1. Report No. RES 2023-11	2. Government Accession No.	3. Recipient's Catalog No.
4. Title and Subtitle *Effects Of Extreme Climate Shifts to Pavement Infrastructure in Tennessee*		5. Report Date Sept 2025 6. Performing Organization Code
7. Author(s) Dr. Mbakisya Onyango (PI), Dr. Ignatius Fomunung (Co-PI), Dr. Jejal Reddy Bathi (Co-PI), Dr. Joseph Owino (Co-PI), Dr. Yu Liang (Co-PI), Maxine Otieno (GRA), Maneesha Vanga (GRA)		8. Performing Organization Report No.
9. Performing Organization Name and Address University of Tennessee at Chattanooga 615 McCallie Avenue, Dept 2502 Chattanooga, TN, 37403		10. Work Unit No. (TRAIS) 11. Contract or Grant No. RES 2023-11
12. Sponsoring Agency Name and Address Tennessee Department of Transportation 505 Deaderick Street, Suite 900 Nashville, TN 37243		13. Type of Report and Period Covered Final Report September 2025 14. Sponsoring Agency Code
15. Supplementary Notes Conducted in cooperation with the U.S. Department of Transportation, Federal Highway Administration.		

16. Abstract

Resilient pavement infrastructure is a dream of every transportation agency. Many factors affect the health of pavement infrastructure to include extreme climate shifts. This study evaluated the effects of climate shifts to pavement infrastructure in Tennessee. The study used AASHTOWare PMED software to predict distresses on selected pavement sections in Tennessee using historical MERRA climate data (or baseline) and machine learning projected climate scenarios. Results showed that pavement sections of the baseline scenario performed at an acceptable level to the end of design period. Climate data projections used machine learning models to predict five climate inputs: temperature, wind speed, percent sunshine, precipitation, and humidity from 2024 to 2044. NeuralProphet and LSTM models were selected for the study. However, the models did not capture peak temperatures accurately. A hybrid model, based on a Variational Autoencoder (VAE) with LSTM layers, gave more accurate results capturing peak temperatures. The VAE compressed the large climate dataset into a smaller representation to capture seasonal and temporal patterns, and the LSTM encoder learned the sequential climate data and reconstructed the values while keeping these critical weather patterns. Comparative analysis between historical and projected climate data files indicated that the projected climate data predicted distresses that were higher than historical climate data; however, the difference was not statistically significant and did not exceed the distress threshold at the end of design period. This indicates that there is no immediate need to change design and maintenance parameters for Tennessee, but close monitoring of weather events and improving severely distressed sections may be required. Moreover, historical climate data can still be successfully used to design pavements. Tennessee maintenance data showed a state average PSI of 3.35 and strong negative correlation of 68% between PSI and IRI, meaning PSI decreases with increase in IRI.

17. Key Words **Climate change, Climate projection, Machine learning, pavement performance, AASHTOWare PMED.**	18. Distribution Statement No restriction. This document is available to the public from the sponsoring agency at the website http://www.tn.gov/.

19. Security Classif. (of this report) Unclassified	20. Security Classifi. (of this page) Unclassified	21. No. of Pages xxx	22. Price

Acknowledgement

The authors would like to express sincere appreciation to the Tennessee Department of Transportation (TDOT) and Federal Highway Administration for funding this research project. Likewise, appreciation is due to TDOT engineers, technicians and staff from Pavement, Materials and the TDOT Research Office, who continually supported the project and provided relevant information needed for the success of this project. Many thanks are due to graduate and undergraduate students that worked on this project at different times. Finally, and importantly, thanks to the UTC Office of Sponsored Programs and the Office of Budget and Finance for working with the research team and TDOT to make sure that the project was conducted in a timely manner.

Executive Summary

In recent years, the manifestation of weather change events, as seen in extreme rains, hurricanes, and tornadoes, has been both global and local, affecting lives and infrastructure, among other things. The report from the Sixth Assessment Cycle by the Intergovernmental Panel on Climate Change (IPCC) warned that if global warming exceeds 1.5℃ in the coming decades or later, then many human and natural systems will face additional severe risks, such as frequent heat waves, increased drought in some areas, and increased frequency and amount of heavy precipitation in several regions, etc. [13]. These weather changes affect pavement infrastructure negatively. Increased heat waves soften asphalt surfaces, and when coupled with heavy traffic, result in permanent deformation; they may cause bleeding of asphalt and fatigue cracking resulting from asphalt oxidation and hardening. While increased frequency and intensity of precipitation saturates the subgrade, reducing its resilient modulus and pavement load-bearing capacity resulting in undermining structural integrity. Therefore, it is important to study, monitor, and prevent as much as possible the effects of extreme climate change, especially temperature and precipitation. This research was conducted by the University of Tennessee at Chattanooga (UTC) in collaboration with the Tennessee Department of Transportation (TDOT) to study the effect of extreme climate shifts to pavement infrastructure in Tennessee.

The objective of this research was to evaluate the effects of extreme climate shifts on pavement infrastructure in Tennessee and give recommendations. The extreme climate shift in this study is the compounded effects of climate shifts over the design period affecting pavement design rather than a particular extreme weather event. The study identified sixty-six (66) pavement sections, thirty-nine (39) provided by TDOT and twenty-seven (27) from the LTPP website, covering all four TDOT regions. The thirty-nine sections were used for comparative analysis of distresses, and the twenty-seven sections were used for validation of prediction models embedded in the PMED software. MERRA historical climate data, available from 1985 to 2023, was used to project future hourly climate data files for temperature, wind speed, percent sunshine, precipitation, and humidity using machine learning models. Both the historical and projected climate data file, with the selected pavement sections, were input into the AASHTOWare PMED pavement design software version 2.6.2.2 to predict pavement distresses. Statistical analysis methods were used to compare the distresses predicted using historical and projected climate data files. The results were used to highlight the effects of the climate shifts in Tennessee and provide recommendations. Furthermore, maintenance data availed by TDOT was analyzed to assess the pavement performance in Tennessee.

From MERRA historical climate data visualization, no significant trend was observed. The overall hourly peak precipitation (rainfall intensity) for TDOT Region 1 was 1.08 in. in 2022; Region 2 was 1.14 in. in 1989; Region 3 was 1.28 in. in 2023; and Region 4 was 1.46 in. in 1994. The overall peak temperature for TDOT Region 1 was 98.06°F in 1988; Region 2 was 107.24°F in 2012; Region 3 was 109.04°F in 2012; and Region 4 was 110.12°F in 2007. However, the annual average temperature showed a slight increase from 2016 to 2023, but the increase did not exceed the recorded peak annual average temperatures for each region. The climate data projection used machine learning models, where LSTM (Long Short-Term Memory) and NeuralProphet projected closer to the test data, while the XGBoost model projection was far from the test data. Five climate data files were projected from 2024 to 2044 using the NeuralProphet model. After many trials, a

hybrid model based on a Variational Autoencoder (VAE) with LSTM layers was developed. This model captured the peak annual temperatures and showed promising results when compared to other models for long-term hourly temperature predictions from 2024 to 2044.

AASHTOWare PMED software was used for analysis because of its ability to predict pavement performance. The software uses material, traffic, and climate data inputs for design, then uses empirical models to predict distresses in the design/analysis period. The prediction models require local calibration of the coefficients to better predict distresses in the state. LTPP sites in Tennessee with measured distress values were used to validate prediction models. Since some of the distress models have changed since the last calibration, it was determined that only terminal IRI predicted values close to measured values for both flexible and rigid pavements. This showed the importance of local calibration of distress prediction models.

Pavement design methods use historical climate data for design and distress prediction. This research compared the predicted distresses using historical and projected climate data files, leaving all other inputs the same. The results showed an average increase in all predicted distresses using projected climate data of 1.7% for terminal IRI, 36% for total rutting, 37% for bottom-up cracking (three points were outliers), 29% for top-down cracking, and 27% for AC rutting. Although the increase was observed, statistical analysis showed that the difference is not statistically significant. Furthermore, at the end of the analysis period, the thresholds were not exceeded. This indicates that, currently, historical climate data can still be used until better climate prediction methods are developed.

Pavement maintenance data revealed that the state average pavement PSI is approximately 3.35, which is a good condition. Further evaluation indicated a strong negative correlation (68%) between PSI and IRI: PSI decreases with increase in IRI. When comparing PSI and IRI for the four regions, Regions 1 and 2 had a higher median serviceability index while Region 3 exhibited greater variation in PSI with lower-end outliers. Overall, Region 4 had the lowest PSI values indicated by the lowest median and more noticeable low-end outliers, both in terms of roughness and serviceability. While the overall differences were not drastic, the results suggest that Region 3 and Region 4 may require more targeted pavement maintenance due to greater roughness and lower serviceability in several segments.

Key Findings

- Data visualization did not show a specific trend that clearly described climate input patterns. The patterns were almost similar throughout the years with overall peak values of temperature and precipitation in different years for the four TDOT regions. Since pavement design methods consider climate inputs for the design or analysis period, extreme climate shifts in this analysis are not considered as few extreme weather events, but the cumulative effects of climate shifts over the years for the design period. Extremes could be considered by design for the worst condition. For example, using the 1993 Guide for Design of Pavement Structures, climate data could consider poor or very poor drainage coefficients to cater for severe flooding areas, or with PMED software layer modulus could be reduced to represent reduced modulus of soaked pavement layers.
- 20-year climate data was successfully projected using the machine learning NeuralProphet model. The distresses predicted using projected climate data were not statistically

significantly different from those predicted using historical climate data, and the design thresholds were not exceeded at the end of the design period. This implies that, currently, historical climate data are valid to be used for design and analysis of pavement structures.

- Calibration and/or validation of PMED software distress prediction models is crucial for accurate pavement design and analysis. For this study, the difference between measured and predicted IRI was not statistically significant at 95% confidence level for both flexible and rigid pavements. The difference for the rest of the prediction models validated was statistically significant. This included total pavement rutting and fatigue cracking for flexible pavements and transverse cracking for rigid pavements.
- Although the study did not see immediate effects of climate shifts using projected climate data, evidence showed an increase of severe weather events in Tennessee. According to the billion-dollar disaster report released by NOAA [11], Tennessee experienced an increase in severe weather events from one in 1980 to eleven in 2023. These events did not significantly change climate data inputs, but with time they may. It is important for DOTs to start investing in capacity building to manage the effects of climate change. To quantify the capacity building needed, DOTs should establish the status of present infrastructure against the current climate and predict the status of a future infrastructure under expected climate change. Moreover, TDOT should evaluate and document pavement infrastructure health after major weather events to quantify the damage. This will give a clear direction regarding design needs, depending on the frequency of events and the amount of damage recorded.
- Average PSI for Tennessee pavement was 3.35, which is a good condition. From regional comparisons, Region 3 and 4 had lower-end outliers, hence lower performance, indicating the need for focused maintenance, compared to Regions 1 and 2. Region 4 had the lowest mean PSI and IRI.

Key Recommendations

- The historical data trends are not clearly defined, but there is evidence of increased frequency of severe weather events nationally and locally. This increase was not captured by the climate data inputs over the years. It is not recommended to change design parameters but to watch closely and address severely distressed sections accordingly. Since the main climate data inputs affecting pavement design are temperature and precipitation, DOTs may first build capacity to manage and document the current condition of pavement infrastructure and effects of climate change on pavement infrastructure, especially after severe weather events. DOTs should evaluate and document pavement infrastructure health after major weather events to quantify the damage. These records could be evaluated periodically to determine when need arises to improve/change pavement design parameters, using trends of actual events and pavement degradation.
- Tennessee pavements are in acceptable condition at PSI 3.35. It is recommended to locate areas with PSI close to trigger values and upgrade the pavement sections to cater for immediate and long-term needs. TDOT may use the maintenance database to identify problematic areas that are affected by extreme climatic events especially flooding. A cost-

benefit analysis should be performed, and if the findings indicate that the investment would contribute to saving lives in flood scenarios, funding may be justified. Measures that could be considered include (1) increasing performance binder grade for temperature and loading on flexible pavements, (2) using lime/cement-treated subgrades on flood-affected areas, (3) using concrete pavements on evacuation routes and areas prone to flooding with improved subgrade or subbase, (4) adding pavement monitoring devices on routes prone to flooding to alert TDOT of upcoming events, information may be timely sent to road users to alert them to use alternative routes, and (5) locating and establishing evacuation routes for areas prone to flooding.

Limitations:

- AASHTOWare PMED software can be used to analyze pavements with a ground water table close to the road surface, but material effects due to prolonged flooding must be changed manually if pavement layer moduli in wet conditions are known.
- Water table depth values incorporated in this study were obtained exclusively from active sites. However, given that some of these sites were considerably far from the location of the pavement under analysis, there is a significant possibility that the value may not accurately reflect the water table depth at the pavement's location. This could possibly contribute to discrepancies in the predicted distresses.
- The version of the PMED software used in this research study (version 2.6.2.2) had some of the distress prediction models that were not recalibrated to suit Tennessee conditions at the time of analysis. Subsequent investigations using a calibrated software version are expected to produce more accurate and reliable results. Nevertheless, predicted IRI values can be considered reliable based on the findings on the validation of prediction models [26].
- Climate data projection took longer than expected. The NeuralProphet model worked well but could not correctly capture the extremes. In the end, a hybrid model based on a Variational Autoencoder (VAE) with LSTM layers was developed that captured temperatures and the extremes well, but this could not be used in distress prediction because the PMED license expired and was not renewed by the project sponsor.
- The analysis of the projected climate data was performed on 17 pavement sections using v2.6.2.2. The new PMED v3.0 had many problems in predicting distresses. After several consultations with AASHTOWare PMED personnel, the software worked, but it was close to the end of its licensure, which was not renewed. Some of the projected climate data was not used to predict distresses.

Table of Contents

List of Tables

List of Figures

Glossary of Key Terms and Acronyms

AOGCM, Atmosphere-Ocean General Circulation Model

CRCPs, Continuously Reinforced Concrete Pavements

DOTs, Departments of Transportation

DTR, Diurnal Temperature Range

GHG, Greenhouse Gases

GIS, Geographic Information Systems

IPCC, Intergovernmental Panel on Climate Change

JPCPs, Jointed Plain Concrete Pavement

LTPP, Long Term Pavement Performance

MEPDG, Mechanistic-Empirical Pavement Design Guide

MERRA, Modern-Era Retrospective Analysis for Research and Application

ML, Machine Learning

NARCCAP, North American Regional Climate Change Assessment Program

NARR, North American Regional Reanalysis

NOAA, National Oceanic and Atmospheric Administration

PCC, Portland Cement Concrete

PCI, Pavement Condition Index

PMED, Pavement Mechanistic-Empirical Design

RCM, Regional Climate Model

RCP, Representative Concentration Pathway

SRES, Special Report on Emissions Scenarios

TDOT, Tennessee Department of Transportation

UTC, University of Tennessee at Chattanooga

Chapter 1 Introduction

The United States has one of the most extensive road networks globally, serving as the backbone of its economic activity by enabling the efficient movement of goods and people. Within this network, approximately 94% of paved roads are constructed with asphalt [1] while only about 1% of public roads use concrete [2]. However, concrete accounts for nearly 25% of expressways [2], reflecting its superior performance under the heavy truck traffic typical of these corridors, which is characteristic of expressways, as compared to asphalt pavements.

Concrete pavements tend to perform better under heavy truck traffic loads, which is characteristic of expressways.

Pavement performance is strongly influenced by environmental conditions, as the materials used are sensitive to climatic variability affecting their deterioration rate, subsequent maintenance, and life-cycle costs [1]. Traditionally, transportation planners and engineers have relied on historical climate records derived from either weather stations or climate reanalysis [3] to inform pavement design, operations, and maintenance [4]. These approaches assume climate stationarity. With increasing evidence of climate change both globally and locally, the applicability of current design guidelines and standards is increasingly being called into question.

The evidence of climate change is irrefutable, with current trends indicating a high likelihood that these environmental changes will persist well into the future [5]. Anticipated shifts include more frequent extreme heat events, heavier rainfall and storm activity, accelerated sea-level rise, and enhanced localized warming in urban areas due to the Urban Heat Island effect. Each of these stressors poses risks to transportation systems, and pavements in particular, by accelerating deterioration processes and inflating maintenance and life-cycle costs.

Recent research has demonstrated that climate-induced stresses may significantly reduce the service life of pavements [6-8]. Asphalt pavements, for example, lose stiffness as temperatures rise, whereas concrete pavements remain structurally stable but experience thermal expansion and contraction. These temperature-induced gradients can lead to curling and structural challenges, necessitating effective design strategies such as expansion and contraction joints. Understanding how these materials respond under changing climate conditions is therefore essential to ensuring the resilience, durability, and cost-effectiveness of the U.S. roadway system. Since concrete's stiffness is relatively unaffected by temperature, there is a common misconception that this property makes it resistant to the effects of high temperatures associated with climate change. In response to this belief, very little attention has been given to evaluating the performance of concrete pavements in the context of changing climate conditions. Furthermore, because the overall proportion of concrete pavement sections in the U.S. is significantly lower than that of asphalt pavements [1], this disparity has further contributed to the limited focus on assessing the resilience of concrete pavements to climate-related challenges. Addressing this knowledge gap is crucial, given the strategic importance of concrete in expressways and freight corridors where structural reliability is paramount.

Pavement performance is strongly influenced by environmental conditions, as the materials used are sensitive to climate change.

1.1 Problem Statement

While climate change manifestations such as extreme rains are considered a global phenomenon, the impacts tend to be regional and local, as evidenced by recent hurricanes and tornadoes. The institutional capacity of Departments of Transportation (DOTs) is one strategic way to manage the adverse effects of climate change. Much of the capacity lies within the planning, design, construction, operation, and maintenance of civil infrastructure. To quantify the needed capacity building, DOTs should establish the status of present infrastructure against the current climate and predict the status of future infrastructure under projected climate change. In recent years, pavements have increasingly been affected by severe weather changes such as elevated temperatures and severe rainfall, resulting in flooding. In the event of flooding, the rate of pavement deterioration is accelerated due to its submergence underwater, leading to increased frequency of maintenance and a consequent rise in infrastructure costs. Despite noticeable changes in weather patterns, some pavement design parameters have largely remained unchanged and have not been updated to reflect these climatic variations. For example, presently, pavement designers rely on stationary data sets derived from historical climate observations to account for climate factors in their designs [8]. However, the concept of climate change challenges this assumption of stationarity, indicating a need for its consideration in the pavement design process. Insufficient data on projected weather trends and a limited knowledge and/or understanding of how to manipulate the available data may be a contributing factor to the lack of updated design inputs.

As a result, this research study sought to understand the status of current pavement infrastructure, the changing climatic conditions, and their impact on pavements in Tennessee to provide the Tennessee Department of Transportation (TDOT) with considerations for pavement materials and pavement design inputs that account for the changing climatic conditions (if any). The research utilized the AASHTOWare Pavement Mechanistic-Empirical Design (PMED) software and big-data analytics combined with machine learning approaches to quantify the current and future status of selected pavement sections in Tennessee to provide short-term and long-term planning for management of the effects of adverse climate changes on pavements.

1.2 Research Objectives

The overarching objective of this proposed research project was to assess the effects of climate shifts to pavement infrastructure and propose needed modification for pavement design inputs and maintenance strategies (if any) such that TDOT can consider climate changes in the short term and long-term planning of pavement infrastructure projects. While utilizing version 2.6.2.2 of the pavement performance analysis software, AASHTOWare PMED, the specific objectives of this research study were as follows:

1. To evaluate conditions on selected routes in Tennessee using historical climate data files (baseline scenario).
2. To analyze climatic trends within historical climate records specific to Tennessee to develop projected climate data files using machine learning techniques.
3. To evaluate the conditions of the selected routes in Tennessee using developed projected climate data files (projected climate scenario).
4. To statistically compare the predicted pavement performance under the baseline and projected climate scenarios and to quantify the differences, if any.

5. To propose pavement design parameters and maintenance strategies, if necessary, aimed at mitigating the effects of climate shifts, especially rainfall intensity and temperature in Tennessee.

1.3 Significance of the Study

This research quantified the effects of projected climate shifts on various pavement distresses by statistically evaluating and comparing predicted pavement distress values using historical and projected climate data files. Climate data visualization was performed to capture trends of climate data inputs for the years 1982 to 2023 and draw inferences. In addition, machine learning methods were used to predict future climate data inputs. The distress prediction models on PMED software were validated using LTPP sections in Tennessee that had measured distress values available. A comparative analysis of distresses predicted using historical and projected climate data files was performed using 39 pavement sections provided by TDOT, scattered over all four TDOT regions.

1.4 Scope of the Project

This research study used distresses predicted on AASHTOWare PMED to evaluate the performance of various pavement sections in Tennessee using the base scenario, which is the pavement structure in its current situation using historical climate data, in comparison to projected climate scenario. The climate data prediction was performed using machine learning methods.

1.5 Working Definition

While climate projections often highlight extreme events (e.g., unusually high temperatures on selected days), it is important to recognize that such events occur for short durations and are spread over long periods. To better capture this broader shift, including those extremes, we analyzed pavement conditions using long-term continuous historical and machine learning predicted climate data. The overall change itself can be considered extreme, not because of any single event, but due to the persistent, frequent, and measurable shifts in temperature and related variables. In this sense, the extremity lies in the long-term, systemic transformation of the climate rather than in isolated extreme weather events. This framing also aligns with scientific consensus and helps avoid overstating the role of individual events. For this report, “extreme climate” is used for short-term occurrences of extreme weather events, and “climate shift” for long-term continuous effects of climate inputs, as used in pavement design.

1.6 Report Outline

This report is comprised of an introduction, literature review, methodology, results, analysis, and conclusion. The project performed a comparative analysis of pavement distresses obtained using historical and projected climate data files to assess the effects of climate shifts. Climate data files obtained from MERRA climate data sources were utilized as historical climate data and machine learning methods were used to predict the future climate from 2024 to 2044. The analysis indicated that projected climate data increased distresses on the pavement during the analysis period, but the increments did not exceed the current/existing design thresholds.

Chapter 2 Literature Review

Extreme and unanticipated weather occurrences around the globe substantiate the realities of a changing climate. Evidence is building that human induced climate change is changing precipitation and the hydrological cycle, especially the extremes [9]. Global average surface temperatures have increased since 1850, and temperatures have significantly risen in the past 50 years [10]. The sea level has been rising globally and extreme weather events such as floods, hurricanes, and heat waves have become more frequent in many regions [1]. The billion-dollar disaster report released by NOAA National Centers for Environmental Information (NCEI) confirmed more disasters throughout the country in 2023. There were 28 weather and climate disasters in 2023, surpassing the previous record of 22 in 2020, tallying a price tag of at least $92.9 billion. [11]

If no actions are taken to address the root causes of anthropogenic climate change, these effects are likely to continue well into the future, affecting both natural and built environments [12]. The report from the Sixth Assessment Cycle by the Intergovernmental Panel on Climate Change (IPCC) warns that if global warming exceeds 1.5℃ in the coming decades or later, then many human and natural systems will face additional severe risks [13], [7]. Humphrey and Gudipudi assert that climate change will affect every mode of transportation and every region in the United States, presenting infrastructure providers with new and often unfamiliar challenges [4, 7]. Although the damage to buildings and bridges is usually apparent during extreme weather occurrences, the impact on roadways may sometimes not be easy to recognize [14]. However, this does not imply that roadways are unaffected. Pavements are environmentally sensitive infrastructure, and as such, any adverse changes in environmental conditions can have detrimental effects on pavement integrity.

Pavement structures are designed to cater to the present and forecasted traffic needs under current and projected environmental conditions. However, the design uses historical climate records and the assumption that climate conditions remain stationary with time. With escalating concerns regarding climate change, an important question arises: will the existing design methodologies and assumptions remain suitable for future climate scenarios? [10]. A thorough evaluation of the resiliency and adaptability of current pavement design practices is deemed necessary to appropriately respond to the extreme climate patterns driven by climate change.

2.1 Climatic Stressors and their Influence on Pavement Performance

While all climatic factors collectively influence the response and performance of pavements, certain climatic stressors have been observed to have a more pronounced impact compared to others.

2.1.1 Temperature

In the field of pavement research, for example, it has been widely accepted that temperature predominantly affects the asphalt layers [1] and is the most critical climatic factor impacting the performance of flexible pavements [8]. Gudipudi et al., Qiao et al., and Msechu et.al. investigated the effects of climatic factors on flexible pavements and concluded that temperature-related factors, including increases in average annual temperature and seasonal

variations, significantly exacerbated pavement distresses. This was especially observed for longitudinal cracking, fatigue cracking, and AC rutting [7, 15, 16]. Wind speed and depth of water table was found to affect pavement performance to a lesser extent [16]. Concrete pavements are known to be sensitive to fluctuations in daily temperature ranges, as the temperature gradient through the depth of the concrete slab induces stress. These thermal stresses, combined with vehicular loads, contribute to the generation of fatigue damage [17]. A research study by Sen et al. in 2022 revealed that climate change may increase fatigue damage and potentially reduce the service life of concrete pavements [2].

2.1.2 Precipitation

Precipitation and groundwater levels affect the moisture content in pavements, particularly in unbound underlying layers and soil materials [18]. Although precipitation is observed in certain cases to have minimal impact on pavement performance [7, 19], when the ground-water levels are significantly elevated for some pavements, precipitation can be said to be as influential as temperature [20]. This is because a significant increase in ground saturation can reduce the resilient modulus of the subgrade materials, hence, reducing the pavement's load bearing capacity and, overtime, undermining the structural integrity of pavements. For example, following Hurricane Katrina in New Orleans, submerged asphalt pavements were found to have experienced strength losses equivalent to about two inches of new asphalt concrete [14]. In addition, a weaker subgrade for the submerged areas equivalent to nearly one inch of asphalt concrete was identified. However, minimal damage was observed in Portland Cement Concrete (PCC) pavements [14]. Another study justifying the resiliency of rigid pavements to flooding is that by Khan et al. [21], in addition to an article written by Joy Powell (2018) [22].

2.1.3 Wind Speed and Freeze-Thaw Cycles

Other climatic stressors known to impact pavement performance are wind speed and freeze-thaw cycles. While increasing wind speeds can potentially lower pavement surface temperatures, which is beneficial for pavement longevity (assuming very low temperatures are not involved), extreme winds from tornadoes and hurricanes can potentially bring debris and cause significant damage to pavements [1]. Climate change may prolong thaw cycles, leading to extended periods of high moisture content in pavements, resulting in rapid development of distresses such as rutting and stripping [1]. Conversely, it may reduce frost occurrence, especially in areas with mild winters, potentially mitigating pavement deterioration in the spring [1]. In certain instances, percent sunshine and relative humidity have been observed to influence the performance of flexible pavements, albeit to a lesser degree [23]. A 2k factorial sensitivity analysis conducted by Onyango et. al., reported that relative humidity and percent sunshine had no effect on the predicted pavement distresses [24].

2.2 Pavement Performance Analysis Software Packages

In the field of pavement design and performance analysis, various software tools are available to facilitate this process. Examples include WINPAS, PAVEXpress, KENPAVE, MXROAD Suite, and StreetPave.

With regards to incorporating different climate scenarios while analyzing the performance of pavements, a more recent and widely utilized software is the AASHTOWare Pavement Mechanistic-Empirical Design (PMED). Developed and released in 2004, this software

was designed to address the shortcomings of the empirical approach of designing pavements based on the 1993 AASHTO Guide for Design of Pavement Structures. The software was also set to operationalize the mechanistic-empirical procedures outlined in the Mechanistic-Empirical Pavement Design Guide (MEPDG).

PMED considers detailed design inputs in material characteristics, traffic loading, and climatic inputs [25] to analyze the performance of a model pavement structure over a specified design life. The software is intricately embedded with the Enhanced Integrated Climatic Model (EICM) which comprehensively accounts for all environmental factors influencing pavement performance [26], modeling and predicting heat and moisture flow in the pavement layers and subgrade throughout the pavement's years of service [27]. PMED software offers users the flexibility to utilize existing historical climate data files sourced from actual weather stations on the ground, the North American Regional Reanalysis (NARR), or the Modern-Era Retrospective analysis for Research and Applications (MERRA). Additionally, users can freely develop and implement custom climate data files, provided they conform to the hourly climatic data (HCD) format. This capability enhances the flexibility and applicability of the software for diverse climatic conditions and specific project requirements.

The National Centers for Environmental Prediction (NCEP) initiated the NARR program as a long-term dataset that is dynamically consistent with high frequency and resolution starting from 1979. The data produces real-world conditions, including wind speed, temperature, and pressure data from surface observations, and moisture data from radiosondes. However, NARR has fewer and scattered stations. For instance, the state of Tennessee has 12 NARR stations, 5 of which are concentrated near the Knoxville area. [28] [29] [30] [31]. MERRA is a reanalysis dataset based on the Goddard Earth Observation System (GEOS-5), released by NASA in 2010. MERRA is comprised of real time climate data observations, collected from ground, ocean, satellite, and atmospheric observations that are uniformly gridded and currently operating at 0.625^{o} longitude and 0.5^{o} latitude special resolution. Currently, MERRA data ranges from 1985 to 2024 [29] [31, 32]

2.3 Sources of Future Climate Data

Increased emission of greenhouse gases (GHG) into the atmosphere is primarily attributed to human-driven industrial activities, which retain more solar energy in the atmosphere, thus increasing global temperatures [33] contributing to climate change. As a result, future GHG emissions and temperature increases are linked to societal development in climate projection estimates [10]. After evaluation of previously developed 1992 emission scenarios, the IPCC [34] released a Special Report on Emissions Scenarios (SRES) in 2000, describing a wide range of a new set of future scenarios and the potential GHG emissions corresponding to each scenario [34]. Subsequently, in 2007 [35], the Representative Concentration Pathways (RCPs) was released to replace the SRES. RCPs represent a set of four pathways developed as a basis for long-term and near-term modeling experiments and they are named according to radiative forcing target level for 2100 [36]. For example, RCP 2.6 is a low forcing level, RCP 4.5/6 is a medium forcing level, and RCP 8.5 corresponds to a very high forcing level.

2.3.1 Existing Climate Data Projections by Different Programs

Several programs have been developed to generate simulations based on emission scenarios outlined in the SRES reports by the IPCC and subsequent development of RCPs. These simulations are developed on a global scale and therefore require downscaling to be applicable on a local scale. Additionally, the predicted data must be converted into an hourly climatic data format to ensure compatibility with the PMED software.

The North American Regional Climate Change Assessment Program (NARCCAP), for example, is an international program that produces high resolution climate change simulations to serve the needs of United States, Canada, and northern Mexico [37]. NARCCAP's atmosphere-ocean general circulation models (AOGCMs) have been forced with the SRES A2 emissions scenario for the 21st Century. The regional climate models (RCMs) nested within the AOGCMs are for the current period (1971-2000) and for the future period (2041-2070), at a spatial resolution of 50km. The North America Co-ordinated Regional Climate Downscaling Experiment (NA-CORDEX) generates climate data outputs at a spatial resolution of 25km/50km, covering most of North America. Outputs from different RCMs are driven using different RCPs. Historical scenarios run from 1950-2005 and future scenarios (RCP- based) run from 2006-2100. Datasets developed by the Climate Impacts Group contain historical and projected hydro-climatic data at various spatial scales covering the Pacific Northwest and regions extending beyond the Pacific Northwest.

The Climate Explorer tool, which was built to support the U.S. Climate Resilience Toolkit, provides interactive graphs and maps containing climate projection simulations under RCP 4.5 and 8.5. The graphs and maps of historical (1950-2009) and projected (2010-2090) temperature, precipitation, and related climate variables cover every county in the United States. The highest resolution is on a daily scale (either average maximum or minimum values), as illustrated in Figure 2.2.

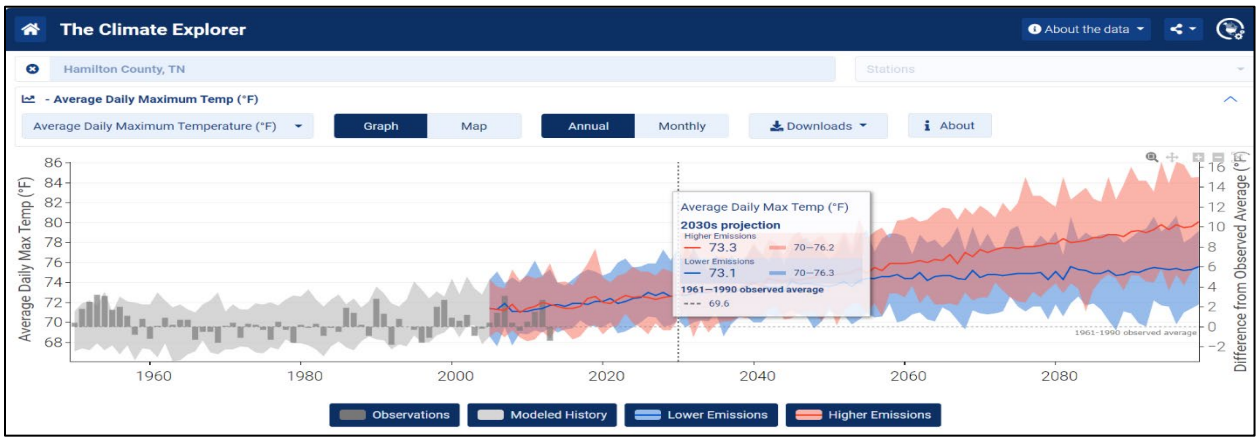

Figure 2.1 Sample temperature graph for Hamilton County from Climate Explorer

While these methods are promising as an attempt to quantify the future, some of the disadvantages associated with the use of existing projected climate data simulations are (1) Inability to simulate future conditions with complete certainty, (2) Both downscaling methods (dynamic and statistical) are active research areas and require appropriate expertise to implement, hence no single consistent approach, (3) Certain climate datasets require approval

for access, (4) Spatial and temporal resolutions of the global and regional models are too course, with limited ability to capture local scale variations, which hinders their direct application in localized studies, and (5) Numerous RCM-AOGCM model combinations make it difficult to pick the best model to implement in a research study.

2.3.2 Machine Learning and Artificial Intelligence

Big data analytics is another research domain that utilizes artificial intelligence (AI) and machine learning (ML) techniques to train, validate, and calibrate different models that can predict future climate data. To be effective, this technique requires a large training dataset and the examination of different algorithms and models before selecting one that exhibits a high level of accuracy in terms of its predictions.

Existing research has demonstrated the application of machine learning techniques for predicting future climate conditions. For instance, Piryonesi et al. [38] developed a decision support tool for predicting the pavement condition index of asphalt roads in Ontario and Texas in two, three, five, and six years. After examining several algorithms (two decision trees, k-nearest neighbors (k-NN), naïve Bayes classifier, naïve Bayes coupled with kernel estimator, random forest, and gradient boosted trees) and using a large training dataset of more than 3000 road sections from LTPP, a proposed tool was developed from the last three algorithms, as they had the highest level of accuracy. Park and Lee [39] employed three machine learning algorithms—k-nearest neighbor, random forest, and support vector machine—to develop a predictive framework for forecasting future rainfall and tidal levels, enabling the assessment of coastal flooding risks under climate change impacts in South Korea.

2.3.2.1 ML for climate data predictions

In recent years, AI and ML have become essential tools for addressing complex challenges in climate prediction, infrastructure planning, and numerous other domains [40]. Climate prediction involves the analysis and forecasting of intricate temporal and spatial patterns in climate systems [41]. ML has proven to be a transformative tool in climate science, offering enhanced capabilities for tasks such as short-term and seasonal weather forecasting, downscaling simulations to higher resolutions, and accelerating computationally expensive model parameterizations [42]. The ability of ML to process vast, high-dimensional datasets is particularly advantageous in climate research, where data from diverse sources such as satellites, weather stations, and ocean buoys must be integrated. Machine learning techniques have gained prominence as they can process large, high-dimensional datasets, uncover hidden patterns, capture nonlinear dependencies, and adapt dynamically to changing data distributions [42]. These strengths make ML well-suited for addressing complex phenomena, including temperature, precipitation, and wind speed predictions, across varying time horizons.

2.3.2.2 ML models for climate data projections

Numerous ML models are used for data prediction, some successfully. Facebook created prophet as a data prediction model, but its performance was poor, leading to the creation of NeuralProphet [43], which captures non-data linearity and utilizes deep learning principles. For climate prediction, NeuralProphet's decomposition of time series data into interpretable components like trend, seasonality, and residuals proves invaluable. This feature allows for detailed analysis of variables such as temperature, precipitation, and wind speed, which are

critical for understanding climate impacts on infrastructure [43]. Its ability to combine interpretability, accuracy, and scalability positions it as a critical component in the arsenal of modern forecasting methodologies [44].

Long Short-Term Memory (LSTM) is an improved version of a recurrent neural network designed by Hochreiter & Schmidhuber [45]. The name is made in analogy with long-term memory and short-term memory and their relationship, studied by cognitive psychologists since the early 20th century [46]. It is aimed at mitigating the vanishing gradient problem commonly encountered by traditional RNNs [47]. LSTM architecture is capable of long-term dependencies in sequential data, which makes them well suited for tasks like speech recognition and time series forecasting [40]. These are also used in CNN (Convolutional Neural Networks) for image and video analysis. Figure 2.3 shows the architecture of LSTM.

XGBoost stands for Extreme Gradient Boosting. It is used to solve data science problems [48]. XGBoost initially started as a research project by Tianqi Chen [42] as part of the Distributed (Deep) Machine Learning Community (DMLC) group. While the XGBoost model often achieves higher accuracy than a single decision tree, it sacrifices the intrinsic interpretability of decision trees [49]. XGBoost has become a go-to model for structured data due to its regularization techniques, feature importance analysis, and handling of missing data. XGBoost's strength lies in feature engineering and its ability to provide insights into variable importance, which is invaluable for understanding climate drivers. It is a parallelized and carefully optimized version of the gradient boosting algorithm. Parallelizing the whole boosting process improves the training time significantly [50]. It is an advanced implementation of gradient boosting that is optimized for speed and performance boosting and involves building a sequence of decision trees, where each subsequent tree corrects the errors of its predecessor. XGBoost extends this concept by introducing features such as regulation, parallel processing, and awareness, making it highly efficient for large datasets.

2 Deep Neural Network (DNN) is used to predict pavement deterioration according to the historical/predictable climatic and traffic data. The temporal pattern of climatic data and traffic data is formulated using the Transformer neural network [51]. A critical assessment of the DNN architecture is made in comparison with alternative machine learning models such as linear regression, MLP, and decision tree, [52].

Machine learning presents a promising approach for predicting future climate patterns. However, the accuracy of such predictions is largely dependent on the quality of the training dataset and the robustness of the algorithm or model employed. One of the limitations of this approach is that the occurrence of extreme weather events is usually scattered in a year. As a result, the historical climate data records a limited number of such occurrences. Consequently, the predictive model may underrepresent the frequency and intensity of such events in future scenarios. On the other hand, future climate conditions may end up being positively influenced by human interventions, resulting in the reduction in greenhouse emissions. Machine learning models have limited capacity to integrate this uncertainty into their predictions, thereby limiting the comprehensiveness of their predictions.

2.4 Pavement Performance Analysis (Methods and Results)

To quantify the effects of climate change and extreme weather occurrences on pavement infrastructure, several researchers investigated the effects of different climatic stressors on pavement distresses while employing different climate data sources, performance analysis procedures, and software packages, as highlighted below.

Gudipudi et al. [7] used AASHTOWare PMED software to assess the impact of climate change on pavement structural performance in the United States, under both historical and projected climate data. The projected climate data were sourced from the Climate Analytics Website. Results indicated increases in fatigue cracking and AC rutting in flexible pavement sections under projected temperature data, with more pronounced increases observed in AC rutting. For rigid pavement sections, increases in joint faulting and decreases in transverse cracking were observed. The inclusion of precipitation and temperature data did not show any substantial differences in pavement performance.

The inclusion of precipitation and temperature data did not show any substantial differences in pavement performance.

Meagher et al. [8] presented a method to assess the impacts of climate change on the performance and deterioration of flexible pavements using the PMED software. MEPDG historical climate data files and NARCCAP projected temperature change simulations were used while all other inputs remained the same. Results showed that differences in alligator cracking were predicted to be less than 5% while increases in AC rutting ranged between 4% to 16% for both pavement types.

In response to Hurricanes Katrina and Rita in New Orleans, the Louisiana Department of Transportation and Development (LaDOTD) contracted Fugro Consultants to analyze the extent of structural damage on state highways in New Orleans. It was found that the strength loss in asphalt pavements was equal to about two inches of new asphalt concrete, and thinner asphalt pavements were weaker than thicker pavements. In addition, a weaker subgrade equivalent to about one inch of asphalt concrete was observed in submerged pavements. However, very little damage was detected to the PCC pavements [14].

Piryonesi et al. [38] developed a machine learning-based decision support tool to predict the future pavement condition index of asphalt roads in Ontario and Texas in two, three, five, and six years. The analysis revealed lower levels of deterioration in Ontario compared to higher deterioration rates in Texas. The authors concluded that climate change may either exacerbate or alleviate road deterioration depending on the geographic location.

While investigating flood impacts on typical arterial and collector Jointed Plain Concrete Pavements (JPCPs) in Ontario, [53] utilized the AASHTOWare PMED software to carry out pavement performance analysis. In comparing historical and predicted climate data, results indicated lower damage ratios and pavement life loss in arterial JPCPs than collector JPCPs.

Another study by Sen et al. [2] to investigate the effects of climate change and urban heat islands on the deterioration of concrete roads considered thick (250mm) and thin (175mm) JPCP pavements in Phoenix, AZ and Boston, MA. The study used PMED software for pavement damage

analysis, along with NAAR historical climate data files, and the daily minimum and maximum air temperatures were uniformly and independently increased for climate change. The damage in JPCP was observed to have a positive correlation with the change in the diurnal temperature range (DTR). Furthermore, it was observed that increasing the thickness of the JPCPs increased the sensitivity to changes in DTR.

From this review it is evident that climate change could potentially accelerate pavement deterioration and ultimately reduce pavement service life. Although the degree of change in pavement distresses varies across research studies, there is a consistent message that an increase in distresses is anticipated with climate changes. A 2010 project by the National Cooperative Highway Research Program (NCHRP) identified the Southeast Region as one of the key areas for analysis while reviewing the potential impacts of regional climate change on the highway system. This is because more extreme climate events are expected in this area [54]. Given that Tennessee is one of the states located in the Southeast region, it is imperative to thoroughly examine the potential implications of extreme weather events on the transportation infrastructure here to adequately provide the Department of Transportation with informed strategies for addressing these challenges. Overall, integrating projected climate data into pavement designs going forward could potentially lead to the development of more robust pavements, capable of withstanding extreme weather occurrences.

Chapter 3 Methodology

In this research study thirty-nine (39) selected rigid, composite, and flexible in-service pavement sections in Tennessee were analyzed to evaluate the potential effects of climate shifts on their performance. The pavement performance analysis was carried out using the AASHTOWare PMED software (version 2.6.2.2). The selected pavement sections, provided by TDOT personnel, were distributed across all the four regions in Tennessee as classified by TDOT. MERRA climate data was used as the historical climate data, and machine learning models projected future climate data files. Pavement input parameters were entered into the PMED software, which is embedded with empirical distress prediction models. The resulting pavement distresses, derived from the use of historical climate data files, were then statistically compared to those arising from the use of projected climate data files. This comparison aimed to identify any differences in distress patterns. Based on the findings, recommended strategies are subsequently proposed to address the variations observed. A summary of the above outlined procedure is illustrated in Figure 3.1.

Furthermore, the distress prediction models were validated using twenty-seven (27) LTPP sections (with measured distresses) to assess the accuracy of the prediction models, using both local (statewide) and global (default) inputs. The data input for pavement analysis is outlined in section 3.1.

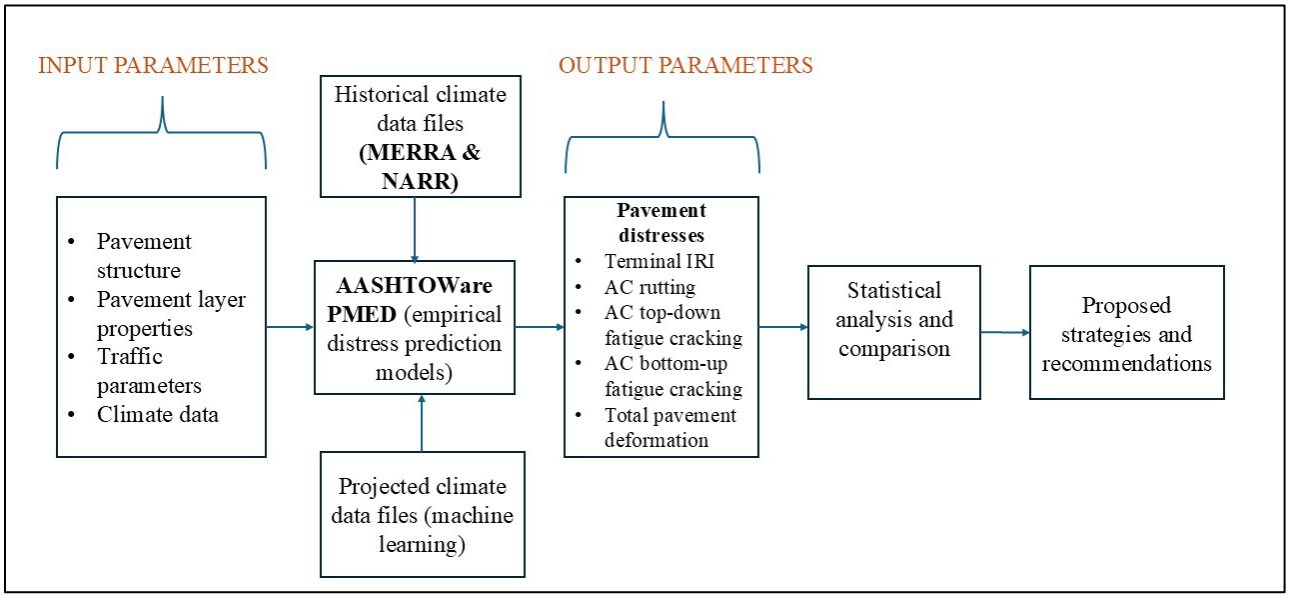

FIGURE 3-1 Summary of research methodology

3.1 Pavement Distress Analysis

The analysis of the effect of climate shifts on Tennessee pavements was performed using pavement distresses predicted from the historical climate data files and projected climate data files. AASHTOWare PMED software version 2.6.2.2 was used for distress prediction, a machine learning model (NeuralProphet) was used for climate data file projections, and statistical models were used to compare the effects of climate changes on predicted stresses.

3.1.1 Data Sources for Distress Predictions

AASHTOWare PMED uses hierarchical input data for pavement analysis. Level 1 data, which corresponds to actual project/field data, was provided by TDOT or obtained from the LTPP website. Level 2 data, which pertains to regional (statewide) information, was sourced from different published research reports and relevant articles specific to the state of Tennessee (Appendix A). Level 3 data, comprised of default values, was available within the AASHTOWare PMED. A combination of level 1, level 2, and level 3 data was employed in this research study (Table 3.1). A detailed description of the inputs utilized, and their respective sources, are provided in the sections below.

TABLE 3-1 Input levels for pavement distress prediction

PMED Input	***Input Hierarchy Level***	***Example of input data***
Local distress model calibration factors	Level 2	Local calibrated coefficients
	Level 3	Default coefficients
Materials properties	Level 2	Statewide properties, such as asphalt mixes.
	Level 3	Material properties not readily available
Traffic Input parameters	Level 1	AADTT
	Level 2	Vehicle distribution factors
	Level 3	No. of axels per truck etc.
Climate	Level 2	MERRA climate data source
	Level 3	Depth of water table

3.1.2 Pavement General Information

Data pertaining to pavement types and their locations, year of construction and/or rehabilitation, layer materials, and layer thicknesses were provided by TDOT or obtained from the LTPP website. Thirty-nine (39) pavement sections provided by TDOT were used for climate shifts analysis and twenty-seven (27) LTPP sections for validation of PMED prediction models.

TABLE 3-2 TDOT and LTPP Pavement sections information by TDOT Regions

Region	***Sections***		***Flexible***	***Rigid***	***Composite***	***Functional Class***							
	TDOT	***LTPP***				***1***	***2***	***6***	***7***	***11***	***12***	***14***	***16***
1	6	4	9	0	1	3	1	1	2	2	0	1	0
2	9	13	21	1	0	0	17	1	0	0	0	0	4
3	18	2	18	1	1	0	2	4	10	1	1	0	2
4	6	8	5	8	1	9	4	0	0	1	0	0	0
Total	39	27	53	10	3	12	24	6	12	4	1	1	6

Of the thirty-nine (39) pavement sections, two (2) were rigid, three (3) were composite (rigid pavement with asphalt overlay), and thirty-four (34) were asphalt. Of the twenty-seven (27) LTPP pavement sections, eight (8) were rigid and nineteen (19) were flexible. The analysis was performed on these sections as new constructions. Table 3.2 summarizes the pavement section information; more details of the TDOT pavement sections are provided in Appendix A. Figure 3.2 is a diagrammatic representation of the distribution of the pavement sections across the state of

Tennessee. The red markers represent the asphalt pavements, the purple markers represent the composite pavements, and the green markers represent the concrete pavements.

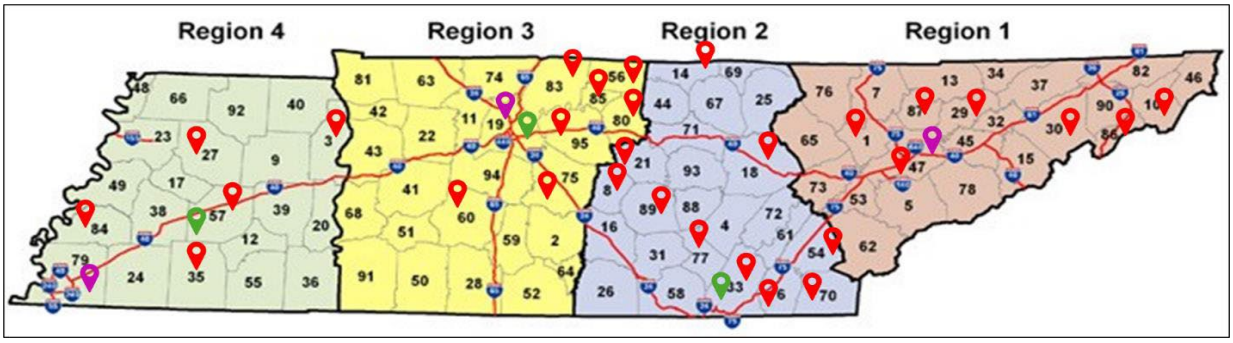

FIGURE 3-2 Distribution of pavements analyzed in Tennessee

3.1.2 Pavement Analysis Period

The analysis period, based on the pavement type, conformed to recommendations in TDOT's 2025 Pavement Design Guide and is summarized in Table 3.3 [55].

TABLE 3-3 TDOT pavement design guidelines [55]

Construction type	***Design period***
New Construction	20 years
Major Reconstruction	20 years
Asphalt Rehabilitation	15 years minimum
PCC rehabilitation (CPR)	15 years minimum
Temporary Pavement	Anticipated life of the temporary lane plus one year

3.1.3 Pavement Structural and Layer Properties

Structural and layer properties and performance grade of asphalt concrete used on the pavement sections were provided by TDOT or obtained from LTPP database. In case of missing data, especially on layer material properties, software default values were utilized. Tables 3.4 to 3.7 show the layer properties of four sections: I-275 in Knox County (Region 1), SR 111 in Hamilton County (Region 2), I-40 in Benton County (Region 3), and SR 141 in Macon County (Region 4).

TABLE 3-4 Design input for I-275 in Knox County- Urban Interstate (Region 1)

Layer	***Material***	***Thickness***	***AADT***	***PG of asphalt***	***% Trucks in design lane***	***Depth of water table***
Asphalt overlay	OGFC	1.25"	71180	76 -22	60%	8.74
PCC	JPCP	10.00"				
Base	Crushed stone w CaCl	5.00"				
Subgrade	A-7-5 (CBR 3.5)	Semi-Infinite				

TABLE 3-5 Design input for SR 111 in Hamilton County – Rural Principal Arterial (Region 2)

Layer	*Material*	*Thickness*	*AADT*	*PG of asphalt*	*% Trucks in design lane*	*Depth of water table*
Asphalt	D mix	1.25″	11480	70 -22	85%	107.57ft
Asphalt	B modified	2.00″				
Asphalt	A mix	3.50″				
Asphalt	A-S mix	3.50″				
Base	Mineral aggregates	10.00″				
Lime treated Subgrade	A-7-6 (CBR= 5.9)	Semi-Infinite				

TABLE 3-6 Design input for SR 141 in Macon County – Rural Major Collector (Region 3)

Layer	*Material*	*Thickness*	*AADT*	*PG of asphalt*	*% Trucks in design lane*	*Depth of water table*
Asphalt	Surface treatment	1.25″	1470	64 -22	100%	7.92ft
Asphalt	Binder	2.00″				
Base	Crushed stone	4.00″				
Subgrade	A-7-5 (CBR= 8.8)	Semi-Infinite				

TABLE 3-7 Design input for I-40 in Benton County- Rural Interstate (Region 4)

Layer	*Material*	*Thickness*	*AADT*	*PG of asphalt*	*% Trucks in design lane*	*Depth of water table*
Asphalt	OGFC	1.25″	34250	76 -22	65%	15.38ft
Asphalt	BM2 mix	2.00″				
Asphalt	A mix	8.00″				
Asphalt	A-S mix	3.50″				
Base	Crushed stone	12.00″				
Subgrade	A-4 (CBR= 5.4)	Semi-Infinite				

3.1.4 PMED Calibration Coefficients

Local calibration coefficients used in this research study were derived from a previous study by the University of Tennessee at Knoxville [56], and are presented in Table 3.8.

TABLE 3-8 Summary of MEPDG Local Calibration Coefficients for Tennessee [56].

Distress model	C_1	C_2	C_3
Alligator cracking	1.023	0.045	6000
Longitudinal cracking	6.44	0.27	204.54
Rutting	β_{r1} = 0.111	β_{BS} = 0.196	β_{SG} = 0.722
IRI (national defaults)	C_1 = 40; C_2 = 0.4; C_3 = 0.008; C_4 = 0.015		

Calibration coefficients were developed using PMED software (version 2.2) [56]. Due to software updates, local calibration for coefficients C_1 and C_3 were used for the alligator cracking distress model while default values were used for the coefficient C_2, since the software version (2.6.2.2) has two separate inputs for the coefficient C_2, which are dependent on the thickness of the second AC layer. Likewise, version 2.6.2.2 has three coefficients for AC rutting (β_{r1}, β_{SB}, β_{SG}.), while v.2.2 had only one coefficient value (β_{r1}). As a result, default values were used for the other two coefficients. The rutting calibration coefficients (β_{BS}, β_{SG}) pertain to the subgrade and subbase respectively.

For concrete pavements, global coefficients, which are program default values, were used because they have not been locally calibrated for the state of Tennessee. Table 3.9 presents the coefficients used for concrete pavements.

TABLE 3-9 Global Calibration Coefficients for JPCP [57]

Distress model	***C_4***	***C_5***
Alligator cracking	0.52	-2.17
Longitudinal cracking	C_1 = 0.595; C_2 = 1.636; C_3 = 0.00217; C_4 = 0.00444; C_5 = 250; C_6 = 0.47; C_7 = 7.3; C_8 = 400	
IRI	*J1* = 0.8203; *J2* = 0.4417; *J3* = 1.4929; *J4* = 25.24	

3.1.5 Performance Criteria and Reliability Levels

Performance threshold values serve as benchmarks for pavement maintenance decisions and judging the adequacy of pavement design to ensure desired performance over the design period. The threshold values typically reflect the pavement condition at which rehabilitation or reconstruction is triggered [26]. These values may differ based on varying state regulations and agency policies. The initial IRI value utilized in this study was 43 in./mi., as was previously determined in a study by Zhou et al. for the state of Tennessee [58]. Other threshold values were applied according to recommendations highlighted in the Third Edition of the MEPDG Design Guide [57], a summary of which is presented in Table 3.10. Pavement reliability levels utilized were as per TDOT's 2019 Pavement Design Guidelines [55], as follows: 95% for Interstates and Principal Arterials, and 90% for local streets and roads.

TABLE 3-10 Summary of Threshold Values at the end of Design Life [57]

Pavement Type	***Performance Criteria***	***Threshold value at end of design life***		
		Interstate	***Primary***	***Secondary***
New AC pavements and overlays	AC bottom-up cracking (%)	10	20	35
	Total rut depth (in)	0.4	0.5	0.65
	AC thermal cracking (ft/mi)	500	700	700
	IRI (in/mi)	160	200	200
New JPCP and overlays	Mean joint faulting (in)	0.15	0.2	0.25
	IRI (in/mi)	160	200	200
	Transverse slab cracking (%)	10	15	20

Default threshold values of 25% and 0.25 inches were used for AC top-down fatigue cracking and AC rutting, respectively.

3.1.5 Traffic Volume Adjustment Factors

Site specific traffic adjustment factors for the pavement sections were provided by TDOT or obtained from LTPP sites. In the case of missing information, either level 2 or 3 data was used. A statewide linear traffic growth factor of 1.34% used in Tennessee was adopted for this study as recommended in [59]. Additionally, the vehicle-class distribution factors, monthly adjustment factors, and axles per truck were applied in accordance with the guidance provided in a report by Onyango et. al [59], also presented in Appendix A. The operational speed was applied according to the Tennessee Code Annotated 55-8-152 and is summarized as follows: Interstates and limited access freeways (70 mph), Divided highways (65 mph), Undivided and two-lane roads (55 mph), and residential streets (30 mph). Default values for axle configuration, lateral wander, and wheelbase were used.

3.1.6 Climate Data

The AASHTOWare PMED software utilizes climate data files in the hourly climatic data (hcd) format. Based on the findings of their study, Msechu et al. [24] recommended the use of MERRA climate data within the AASHTOWare PMED, for the design and performance analysis of Tennessee pavements. AASHTO has also adopted MERRA as climate data files for asphalt pavement analysis. Furthermore, MERRA data has more stations (49 in the state of Tennessee as compared to NARR (12 stations, 5 are in the Knoxville area) [24]. As a result, MERRA climate data files were employed in this research to assess the performance of asphalt and composite pavements. At the time of analysis, MERRA historical climate files had coverage from 1985-2023. For the analysis of concrete pavements, NARR historical climate data files were utilized. At the time of analysis, their coverage was from 1979-2015. MERRA climate data files were downloaded from the Long Term Pavement Performance (LTPP) database, and NARR historical climate data files were downloaded from AASHTOWare PMED database [60]. Climate data from the station closest to the location of the pavement was used under analysis.

Water table depth values incorporated in this study were obtained from active sites within the National Water Information System (NWIS) Mapper (Water Resources of the United States—National Water Information System (NWIS) Mapper (usgs.gov). The values selected were based on the nearest source to the pavement under analysis.

3.2 Validation of Prediction Models

Distress prediction utilized the AASHTOWare PMED software, which is Mechanistic-Empirical in nature. The AASHTO 1993 design guide serves us well, but it lacks climate data inputs and pavement performance prediction, which is available on the PMED software. Likewise, most civil engineering structural designs use mechanistic design methods. On the contrary, pavement design is highly empirical and is currently moving from empirical (AASHTO 93) to Mechanistic - Empirical (PMED) pavement designs. The ultimate goal is to have a mechanistic pavement design method. The PMED method encompasses traffic input, material characteristics, and climate data inputs. These inputs undergo mechanistic pavement analysis and empirical performance prediction. The AASHTOWare PMED performance prediction models were developed and calibrated using national data; it is important to locally calibrate the coefficients and validate them periodically. Tennessee calibrated design coefficients using PMED version 2.2 [57]; however, some of the coefficients on the current version (v.6.2.2) are not locally calibrated. The

research team decided to validate some of the distress prediction models using AASHTOWare PMED version 2.6.2.2 and measured distresses on LTPP site. The study used local (statewide) and global (nationwide) calibration coefficients along with twenty-seven (27) LTPP sections in Tennessee, with measured pavement performance data. This study performed a statistical analysis to establish the accuracy of the predicted data and the reliability of the calibration coefficients in comparison to measured pavement performance data. Section 4.2 presents the findings from this analysis.

3.3 Machine Learning Climate Data Prediction

The projected/predicted climate data files utilized in this research study were developed using machine learning models. After reviewing different prediction models such as Long Short-Term Memory (LSTM), XGBoost, Facebook Prophet, NeuralProphet, and using MERRA climate data sources, it was determined that NeuralProphet predicted climate data better on a long-term basis compared to the other two models tested. LSTM predicted better on the short-term basis but was not very good on long term data (20 years).

For climate prediction, NeuralProphet's decomposition of time series data into interpretable components like trend, seasonality, and residuals proved invaluable. This feature allowed for detailed analysis of variables such as temperature, precipitation, and wind speed, which were critical for understanding climate impacts on infrastructure. Its ability to combine interpretability, accuracy, and scalability positions it as a critical component in the arsenal of modern forecasting methodologies. NeuralProphet stands for Neural Networks + Prophet.

Facebook Prophet focused on additive regression models for forecasting with seasonality and trend decomposition. Neural Networks captured [61] nonlinearities, and NeuralProphet introduced deep learning principles. Key features of NeuralProphet include: (1) Trend Decomposition, which breaks the time series into trend, seasonality, and residuals. (2) Seasonality models deal with multiple seasonalities (e.g., hourly, daily, weekly, yearly) using Fourier series. (3) Lagged Regressors add historical lagged values as features for autoregression. (4) Event handling accounts for special events or holidays with user-defined effects. (5) Flexible Neural Network Layers allows fine-tuning to capture nonlinearities in time series data.

3.3.1 Architecture of NeuralProphet

The architecture combines traditional [62] statistical models and neural networks to handle both linear and nonlinear aspects of time series data. The core of NeuralProphet lies on an additive model that combines several key components [62]:

$$y(t) = g(t) + s(t) + h(t) + \epsilon(t) \qquad (3.1)$$

y of t equals g of t plus s of t plus h of t plus epsilon t

Where:y(t): predicted value at time t; g(t): trend function; s(t): seasonal components modeled using Fourier series; h(t): effects of holidays or special events; ϵt: Residual noise.

Trend Modeling is given by equation (3.2):

$$\mathrm{g(t)} = \mathrm{k} + \mathrm{mt} + \sum_{i=1}^{n} a_i \ \sigma(\mathrm{t} - \mathrm{ti}) \qquad (3.2)$$

Where: k: Intercept; m: growth rate; σ(t−t_i): logistic growth function or piecewise linear trend changes at change points t_i;

Equation 3.3 represents model seasonality [62]:

$$s(t) = \sum_{\{n=1\}}^{N} \left(a_n \cos\left(\frac{2\pi nt}{P}\right) + b_n \sin\left(\frac{2\pi nt}{P}\right)\right) \quad (3.3)$$

Where: P: Period of seasonality (e.g., daily = 24, yearly = 365); N: Number of harmonics; $a_{n,}b_n$: Learnable coefficients.

Seasonal patterns are periodic, and Fourier series was ideal for modeling periodicity. Fourier series decomposes any periodic function into sine and cosine waves. Equation 3.4 accounts for Holiday Effects (h(t)). Special events like holidays can introduce sudden, irregular effects. NeuralProphet incorporates user-defined events [62]:

$$h(t) = \sum_{\{i=1\}}^{E} \delta_i \, 1(t = t_i) \quad (3.4)$$

Where: E: Number of events; δ_i: Impact of the event t_i; 1(t=t_i): Indicator function, equal to 1 if t=t_i ,0 otherwise.

The Autoregressive Component (AR(t)) is defined by equation 3.5:

$$AR(t) = \sum_{\{l=1\}}^{L} w_l y(t - l) \quad (3.5)$$

Where: L: Number of lags; w_l: Learnable weights.

Neural Network Component: NeuralProphet uses **feedforward neural networks** to model nonlinear patterns. The neural network operates on:

$$\mathrm{X} = [\mathrm{g(t)}, \mathrm{s(t)}, \mathrm{h(t)}, \mathrm{AR(t)}] \quad (3.6)$$

Dense Layers:

The input X is passed through dense layers

$$z_1 = \sigma(W_1 \mathrm{X} + b_1)$$
$$z_2 = \sigma(W_2 z_1 + b_2)$$

Where: W_1, W_2: $weight\ matrices$; b_1, b_2: $bias\ matrices$; σ: Activation function (e.g., ReLU or tanh).

Output Layer, which is the final prediction is given in equation 3.7.

$$y_{pred=} W_{out}\, z_2 + b_{out} \quad (3.7)$$

Optimization:

The model parameters (W, b,a_n,b_n ,δi) are optimized using equation 3.8. The optimization uses gradient-based methods like **Adam Optimizer** for faster convergence.

$$L = \frac{1}{N} \sum_{i=1}^{N} (y_i - y_{pred}, \mathrm{i})^2 \quad (3.8)$$

Where: L: Mean Squared Error (MSE) loss; y_i: Actual value; y_{pred}, i: Predicted value.

3.3.2 Prediction Model Selection

The method below (Figure 3.4) was used to select the NeutralProphet model out of the three models tested. Modal training used MERRA climate data for the years 1985 to 2022 and testing utilized 2022-2023 data for testing the model. The model was then used to predict climate data files including temperature, wind speed, percent sunshine, precipitation, and humidity.

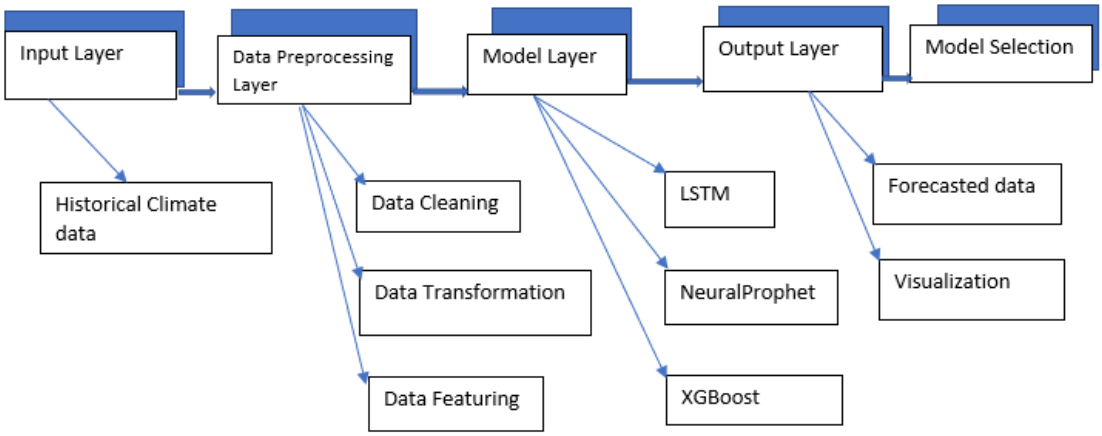

FIGURE 3-3 Method used to select the climate prediction model

Chapter 4 Results, Analysis and Discussion

The overarching objective of this proposed research project was to assess the effects of climate shifts on pavement infrastructure and propose needed modification for pavement design inputs and maintenance strategies (if any) such that TDOT can consider climate changes in the short term and long-term planning of pavement infrastructure projects. Analysis utilized 39 pavement sections in Tennessee, MERRA historical climate data files, and machine learning projected climate data files together with version 2.6.2.2 of the pavement performance analysis software, AASHTOWare PMED.

MERRA climate data files are comprised of five variables, temperature, precipitation, wind speed, percent sunshine, and humidity. Machine learning visualization methods were used to analyze the hourly climate data of each variable, for thirty-eight (38) years (1985 to 2023).

This chapter presents the results, analysis, and discussions, as per inputs outlined in the methodology section in Chapter 3. An assessment of MERRA historical climate data files was conducted to visualize trends on climate variables over time. This assessment was critical as it impacts the nature of the projected climate data files. The historical climate data, used as input on machine learning models, projected the future climate data files. The historical ML projected climate files and PMED software were used to predict pavement distresses, and statistical methods were used to assess the pavement performance using the historical and projected climate data files.

This chapter presents (1) data visualization and inference, (2) validation of prediction models, (3) results of climate data projections using machine learning models, (4) comparative analysis of predicted distresses using historical and projected climate files predicted, (5) pavement maintenance recommendations, and (6) discussion and conclusion. Pavement distresses, resulting from the use of historical, extreme, and projected climate data files, are statistically compared and a comprehensive discussion of the findings is provided.

4.1 Historical Data Analysis and Visualization

Data visualization of MERRA climate stations was performed to illustrate the overarching trends in climatic variables over time and draw inferences that could help TDOT in pavement design and planning moving forward. MERRA climate data files are comprised of five variables, temperature, precipitation, wind speed, percent sunshine, and humidity. Machine learning visualization methods were used to analyze the hourly climate data of each variable for thirty-eight (38) years (1985 to 2023). Presented below are four historical MERRA climate data files, randomly selected from each of the four TDOT regions. Results for other individual climate files utilized during this research are presented in Appendix B of this report. Figures 4.1 to 4.20 show graphical representations of the trends in climate variables over the years (1985 to 2023) for temperature, precipitation, wind speed, percent sunshine, and humidity.

Temperature values (Figures 4.1 to 4.4) and humidity values (Figures 4.17 to 4.20) from the climate data files exhibit slight variation across all four regions, whereas percent sunshine

(Figure 4.13 to 4.16) remains nearly consistent in all four regions throughout the analysis period. Precipitation (Figures 4.5 to 4.8) for Region 1 appears to be generally lower throughout the analysis period compared to Regions 2, 3, and 4. Furthermore, a higher hourly precipitation is observed in recent years for Regions 3 and 4 (Figure 4.7 and 4.8). The analysis indicates that Region 3 experienced the highest wind speeds, up to 20 mph (Figure 4.11), while Regions 1, 2, and 4 have wind speeds of less than 10 mph (Figures 4.9 – 4.12). These graphs provide a basic overview of the distinct climatic patterns observed across the state over the years using hourly climate data. Analysis was further performed using annual averages of temperature and precipitation to provide an in-depth understanding of the historical climate data trends (Figures 4.21 and 4.22). Temperature and precipitation were selected because they are the climate data inputs that affect the pavement performance the most. Figures 4.21 and 4.22 illustrate variations in annual averages of temperature and precipitation, respectively, throughout the analysis period (1985 to 2023) across the four TDOT regions.

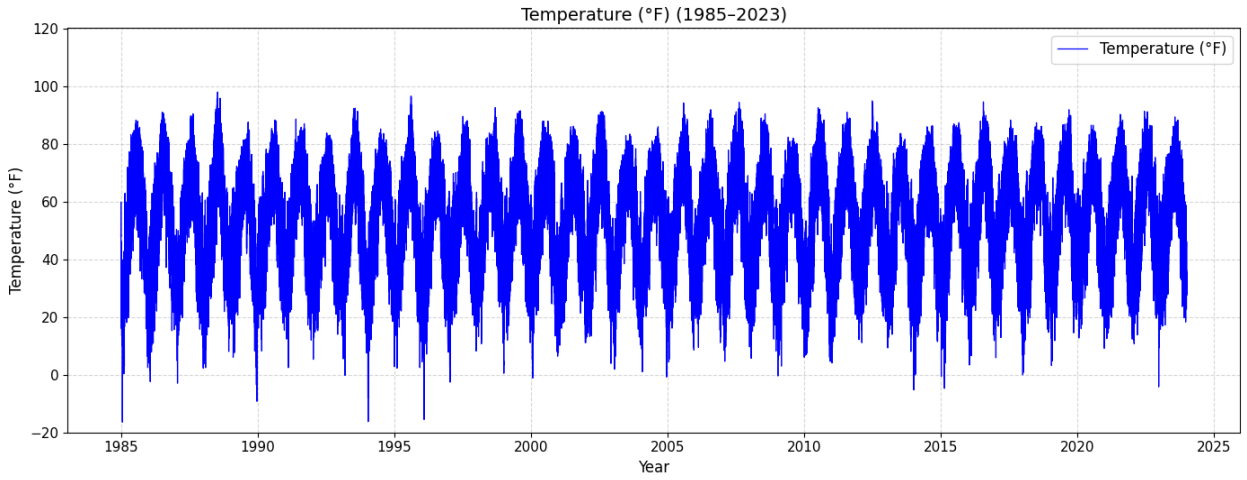

FIGURE 4-1 Trends for station 140126 (Region 1) – Temperature

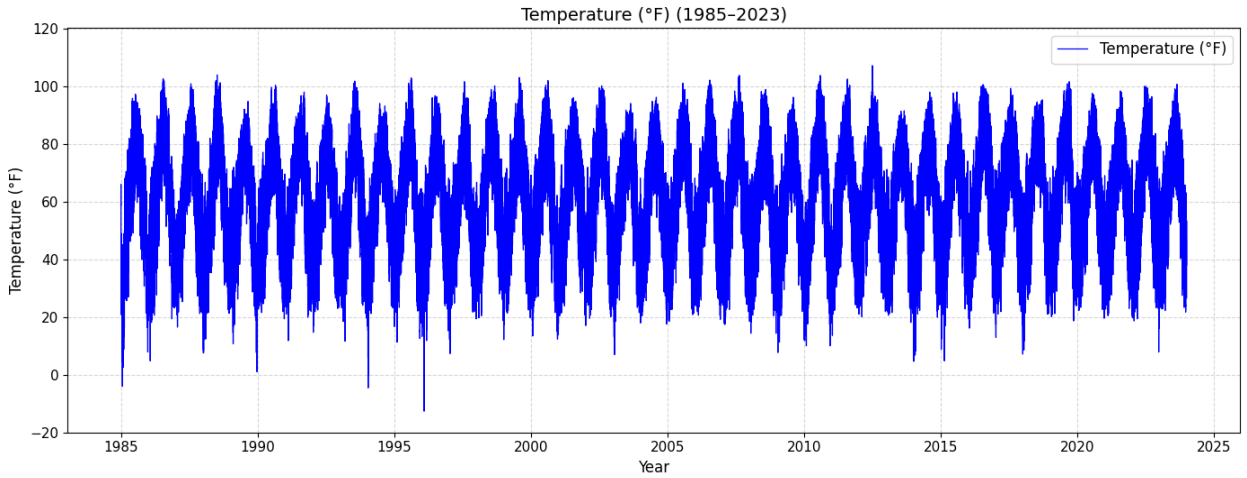

FIGURE 4-2 Trends for station 138393 (Region 2) – Temperature

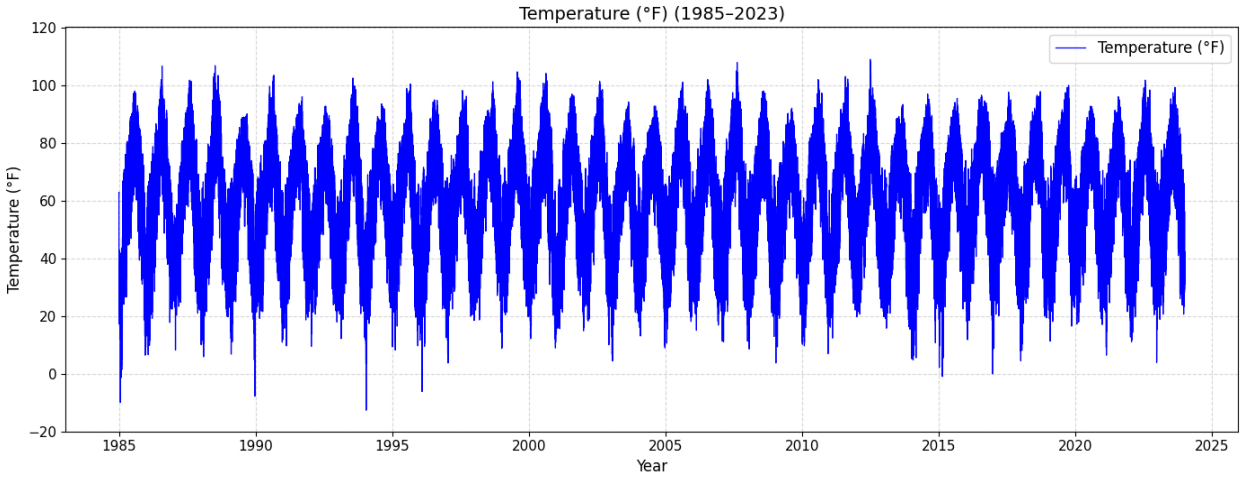

FIGURE 4-3 Trends for station 139542 (Region 3) – Temperature

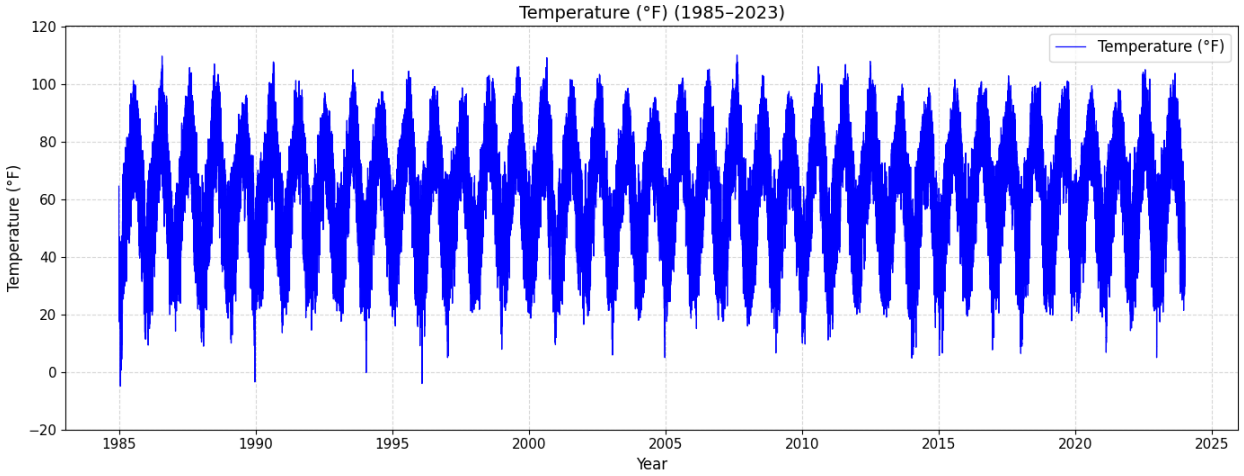

FIGURE 4-4 Trends for station 138387 (Region 4) – Temperature

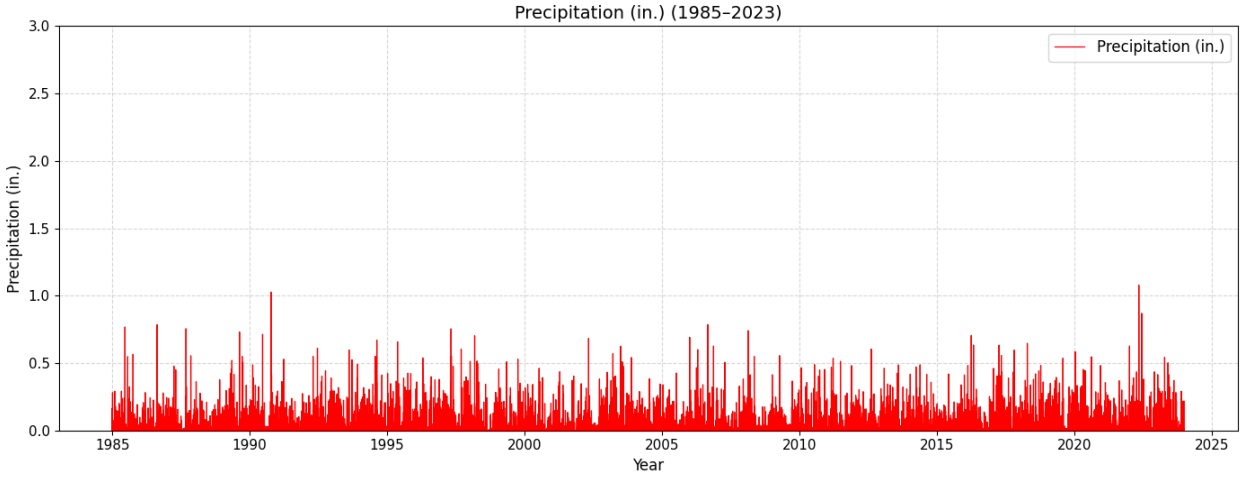

FIGURE 4-5 Trends for station 140126 (Region 1) – Precipitation

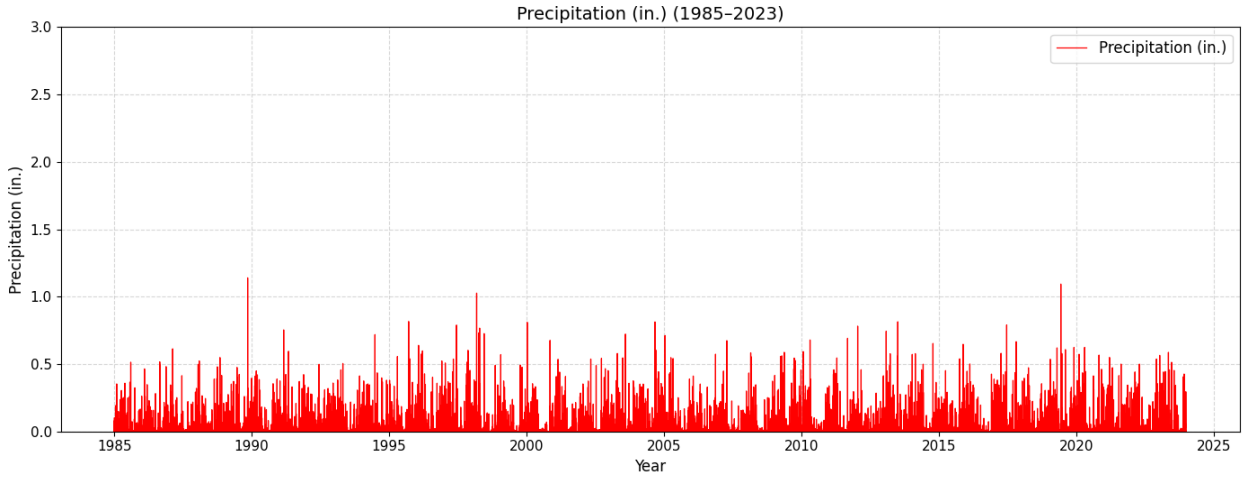

FIGURE 4-6 Trends for station 138393 (Region 2) – Precipitation

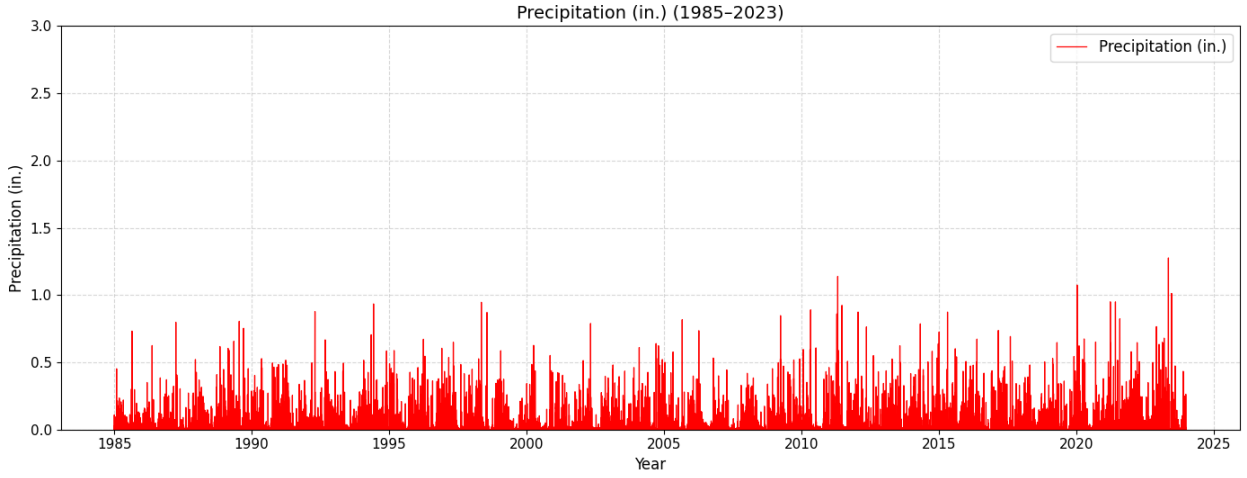

FIGURE 4-7 Trends for station 139542 (Region 3) – Precipitation

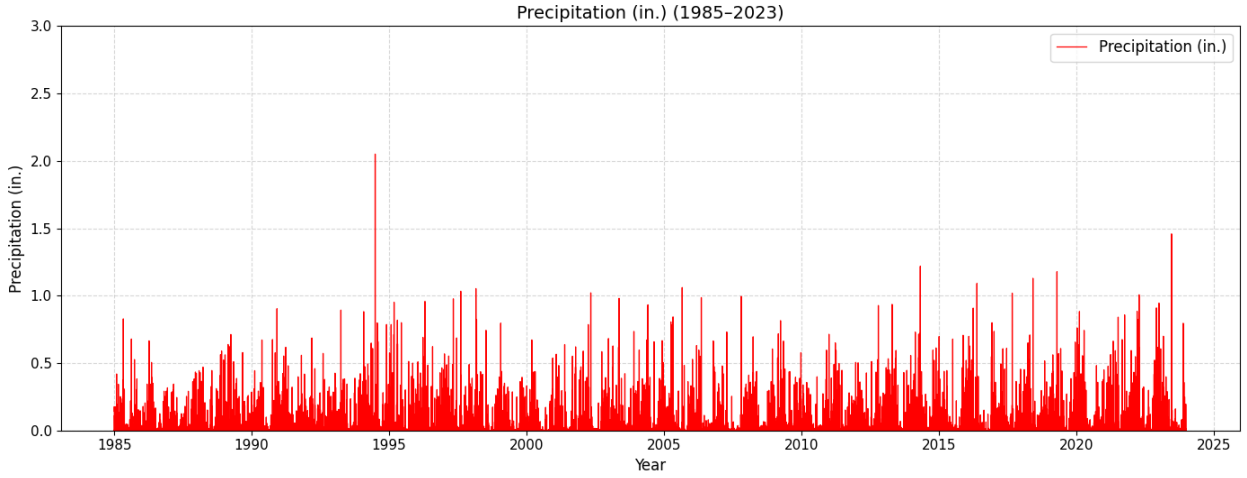

FIGURE 4-8 Trends for station 138387 (Region 4) – Precipitation

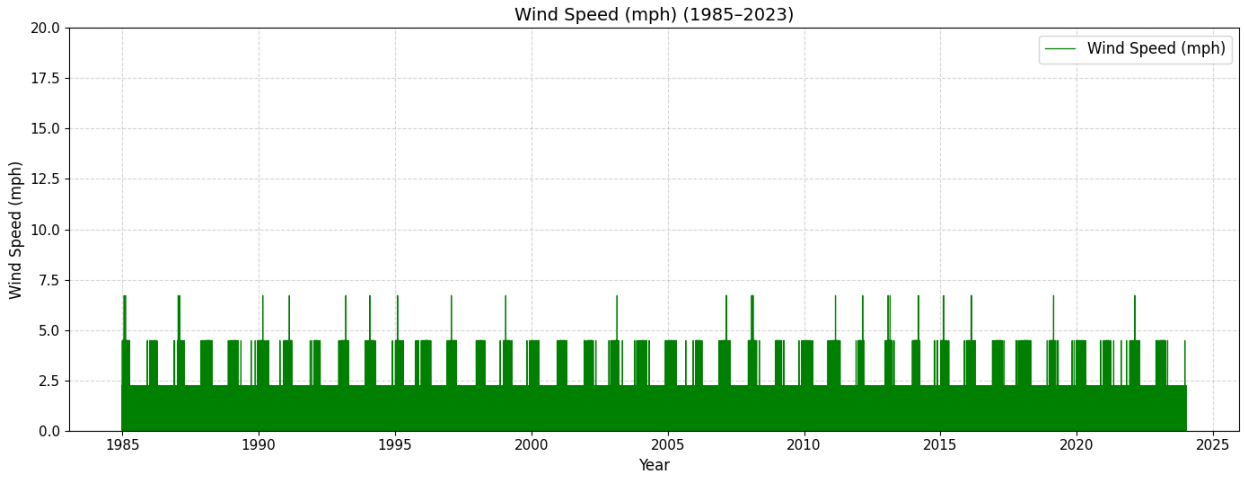

FIGURE 4-9 Trends for station 140126 (Region 1) – Wind speed

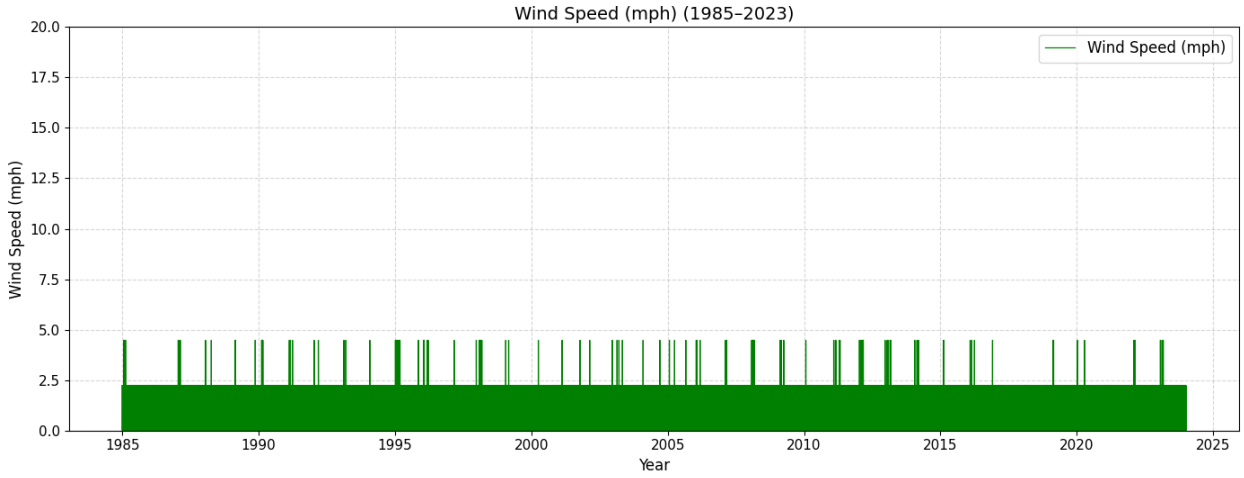

FIGURE 4-10 Trends for station 138393 (Region 2) – Wind speed

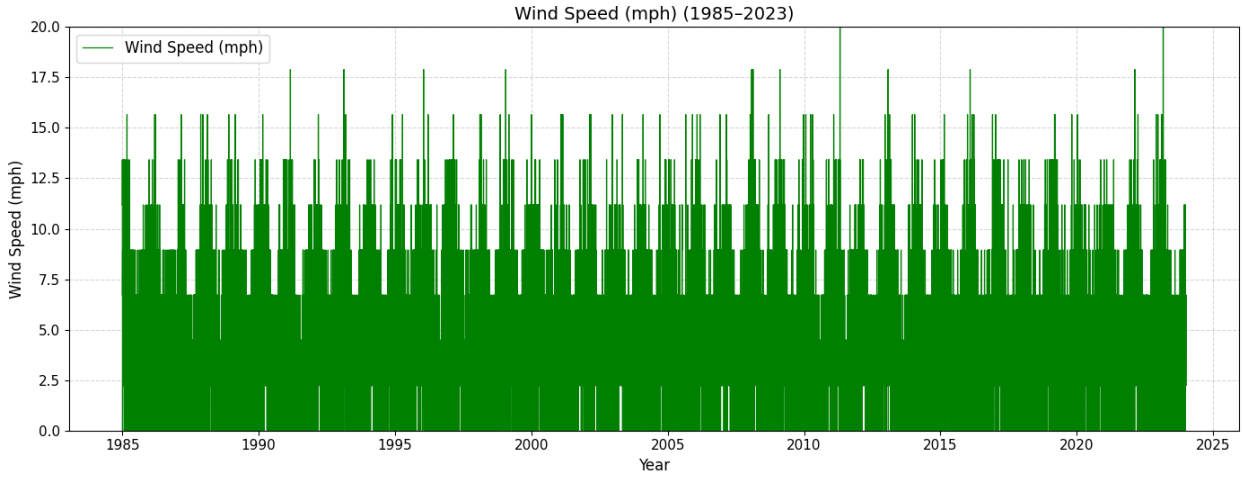

FIGURE 4-11 Trends for station 139542 (Region 3) – Wind speed

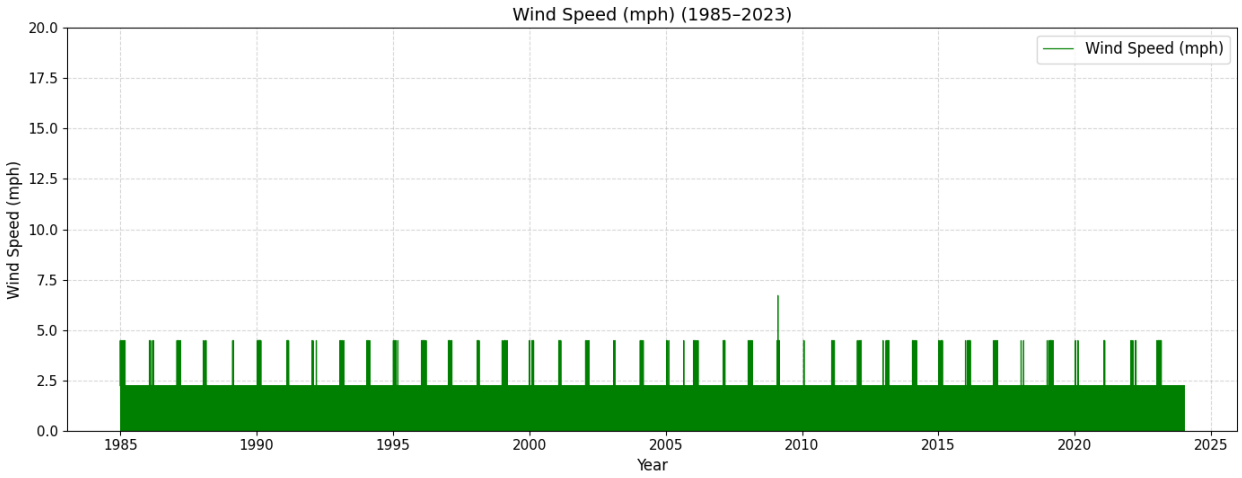

FIGURE 4-12 Trends for station 138387 (Region 4) – Wind speed

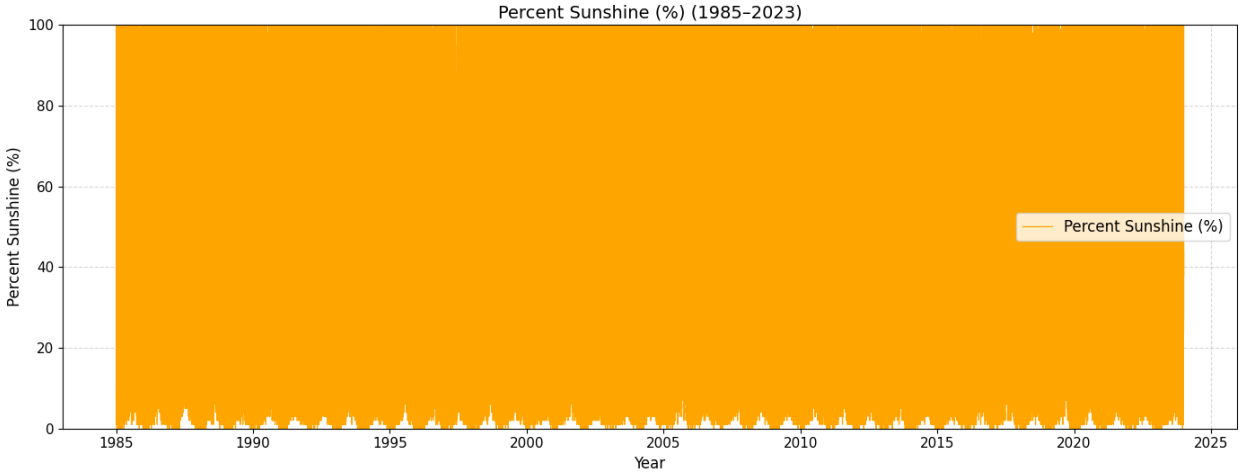

FIGURE 4-13 Trends for station 140126 (Region 1) – Percent sunshine

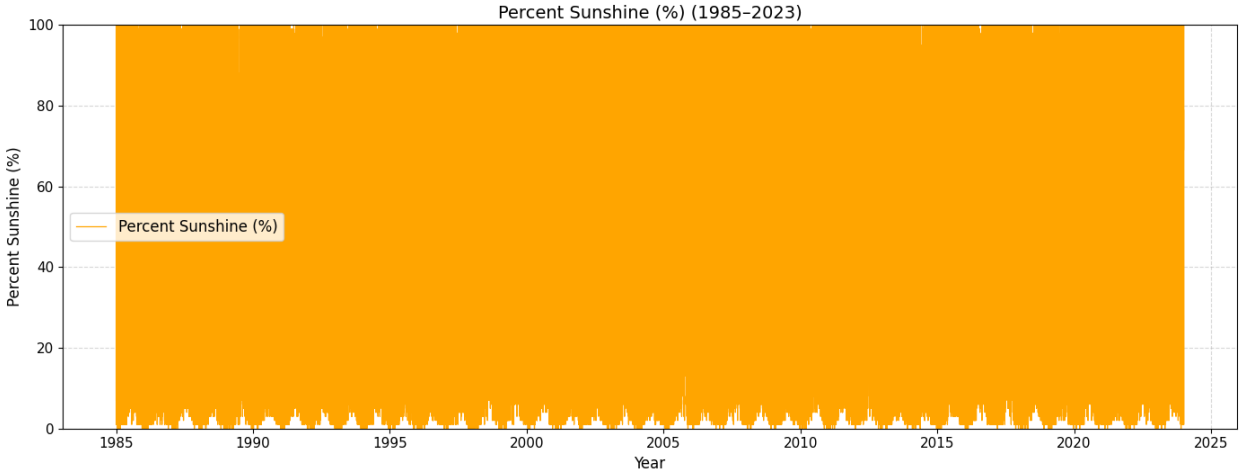

FIGURE 4-14 Trends for station 138393 (Region 2) – Percent sunshine

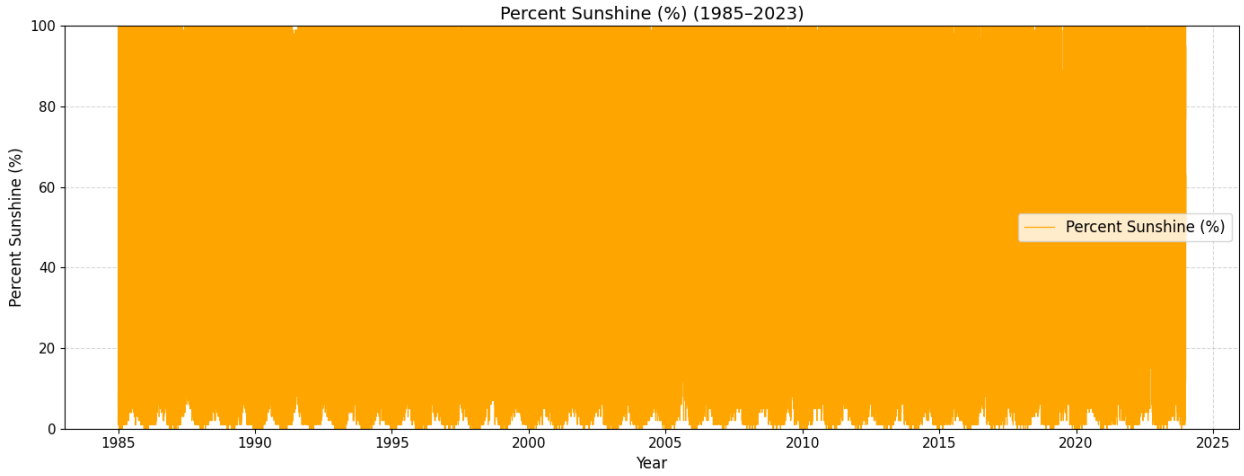

FIGURE 4-15 Trends for station 139542 (Region 3) – Percent sunshine

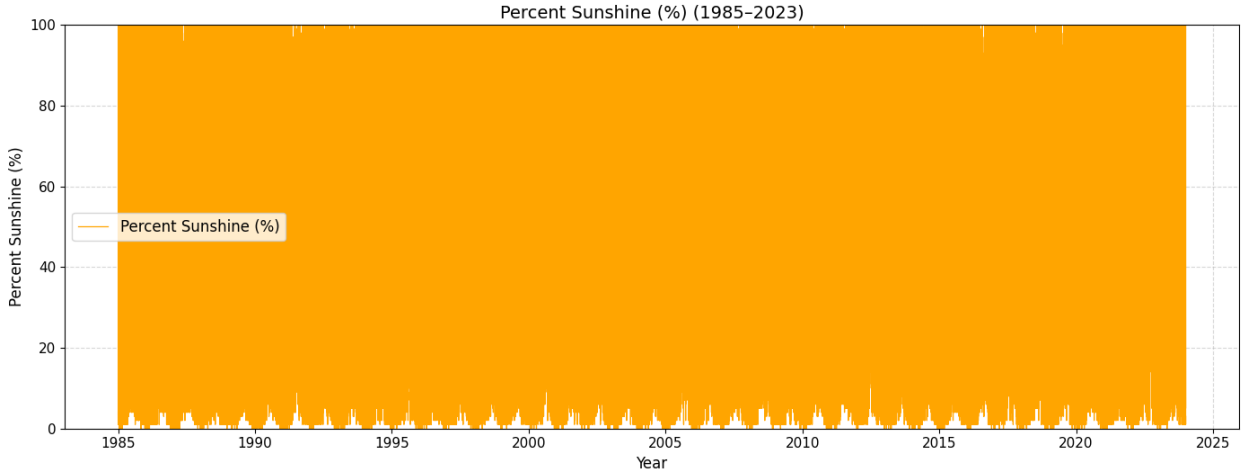

FIGURE 4-16 Trends for station 138387 (Region 4) – Percent sunshine

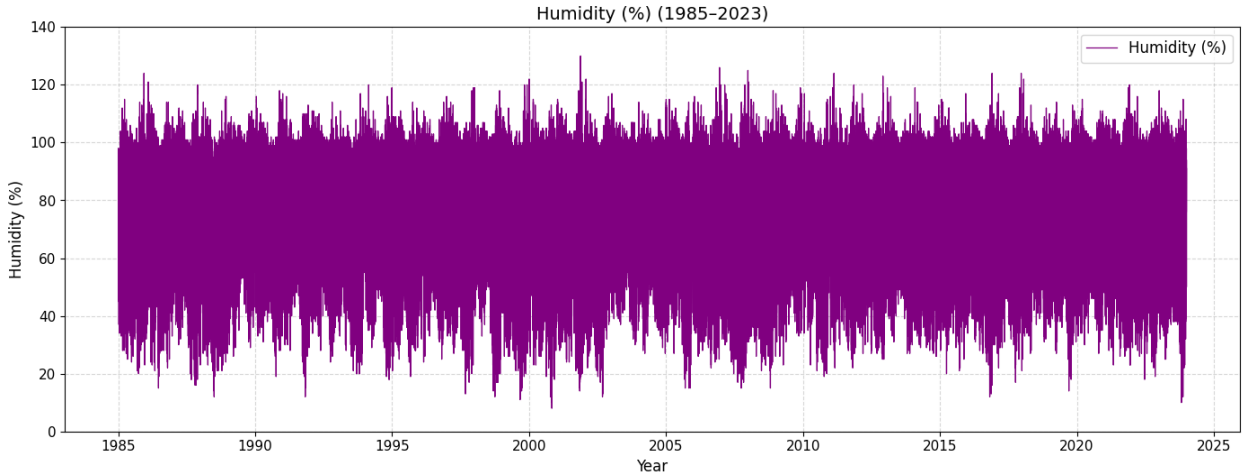

FIGURE 4-17 Trends for station 140126 (Region 1) – Humidity

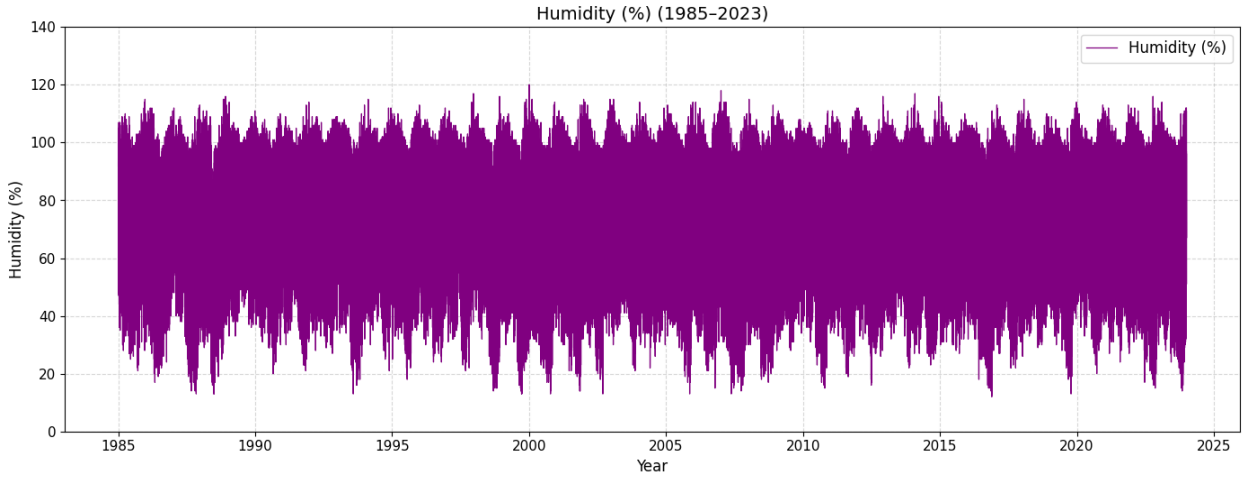

FIGURE 4-18 Trends for station 138393 (Region 2) – Humidity

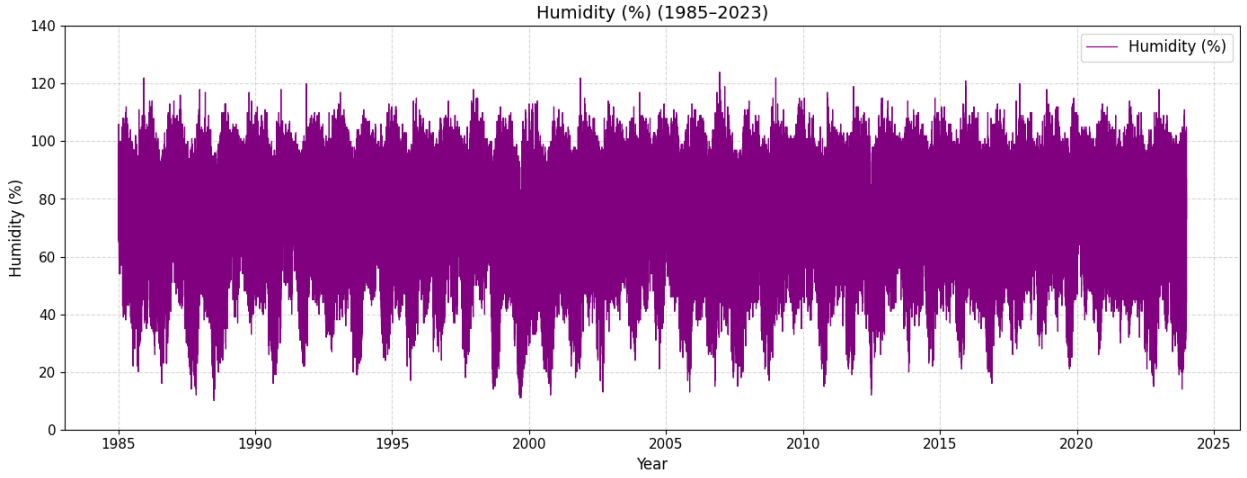

FIGURE 4-19 Trends for station 139542 (Region 3) – Humidity

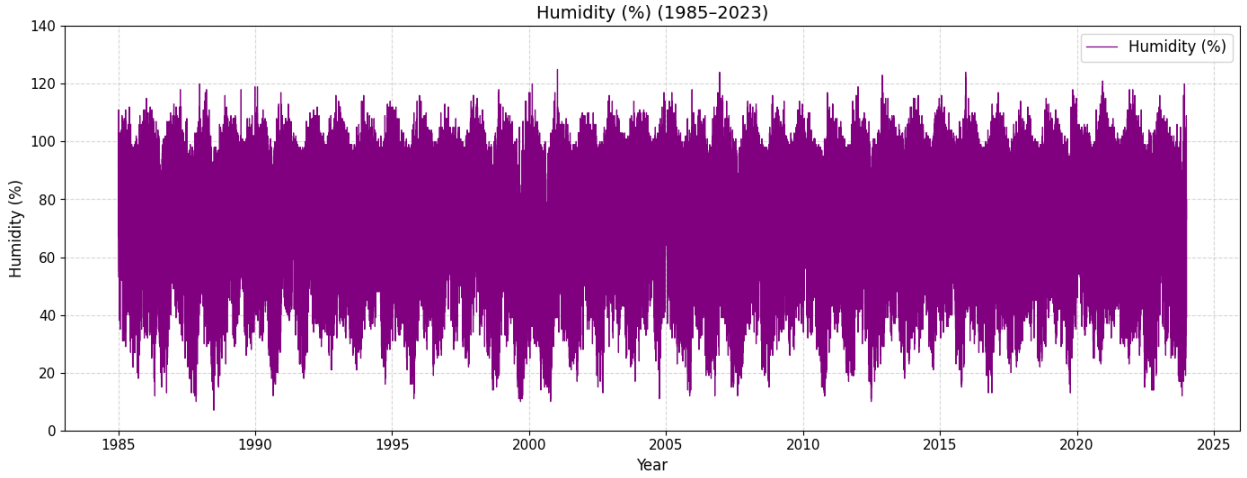

FIGURE 4-20 Trends for station 138387 (Region 4) – Humidity

The annual average temperature (Figure 4.21) and precipitation (Figure 4.22) were obtained by taking the averages of annual temperature or precipitation of all stations analyzed for that region. From the regional annual average temperatures (Figure 4.21), Region 1 exhibits lower temperatures, averaging below 59°F, compared to the Regions 2, 3, and 4. This could be due to the higher elevation of most areas in Region 1. Conversely Region 4 exhibits slightly higher temperatures compared to Regions 1, 2, and 3. Regions 2 and 3 are close to the state average temperatures (black dotted line). All regions indicated consistently higher annual average temperatures in the last six years from 2016 to 2023. Precipitation data (Figure 4.22) indicated that Region 1 exhibits slightly lower precipitation values, in comparison to data from Regions 2, 3, and 4. Likewise, Region 4 demonstrated lower precipitation value observed in some years, although the range remains closely aligned with those of Regions 2 and 3. A high variability exists in annual average precipitation trends in all the regions. No specific trend is observed from the historical data.

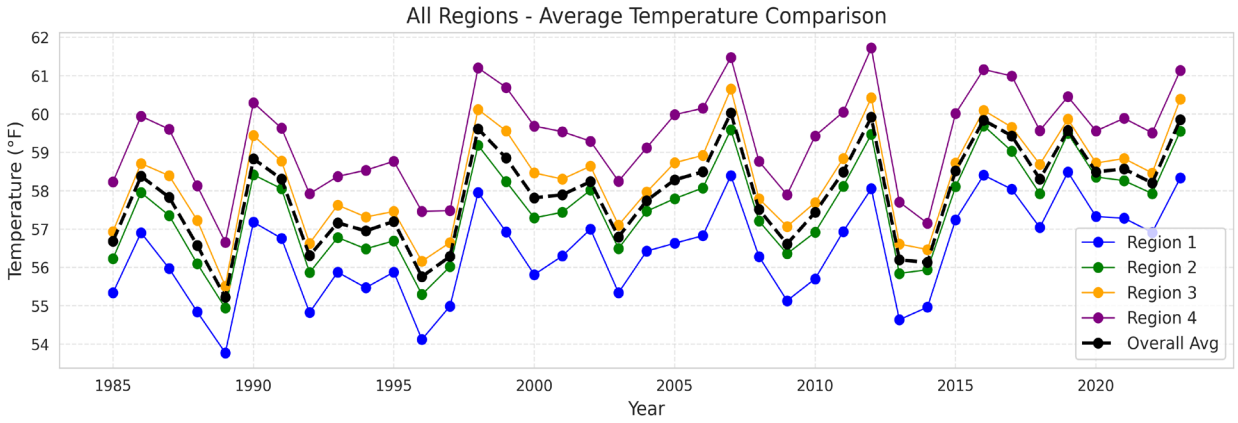

FIGURE 4-21 Annual average temperature for all stations from each TDOT Regions, 1, 2, 3 and 4.

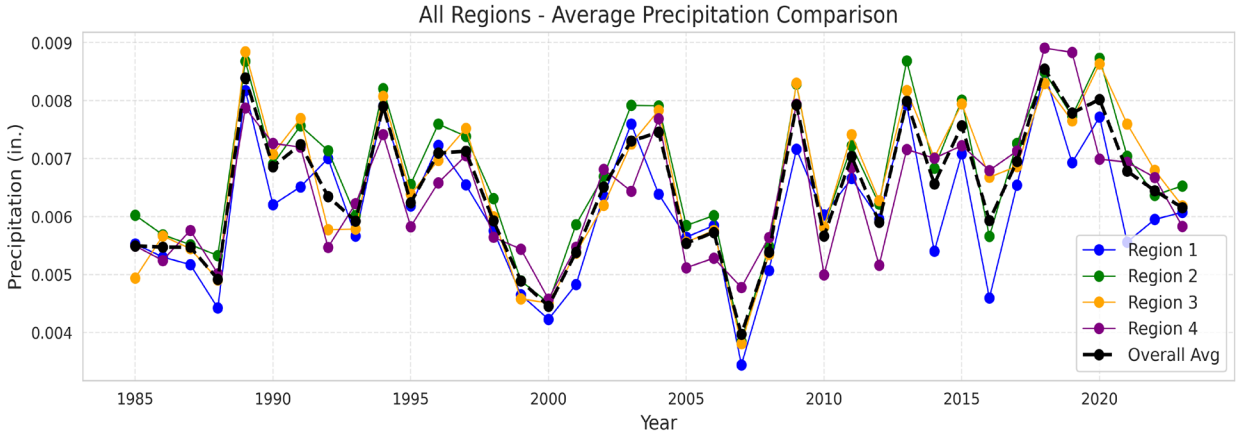

FIGURE 4-22 Annual average precipitation for all stations from each TDOT Regions 1, 2, 3 and 4.

An in-depth analysis of the dataset was further conducted, focusing primarily on temperature and precipitation, to extract critical information such as the highest recorded values

of these climatic variables and the corresponding years in which these extremes occurred. This analysis was performed using data from the same stations in section 4.1.1 depicted in Figures 4.1 to 4.20, with the results presented in Figures 4.23 to 4.26 for temperature and Figures 4.27 to 4.30 for precipitation. The numbers presented in the figures depict the month of the occurrence.

4.1.2 Annual Peak Temperatures

For each Figure, the first graph illustrates daily maximum temperatures with annual peaks highlighted with red dots, while the second graph displays the overall peak temperature during the analysis period, the numbers represent the month of occurrence, the highest temperature is shown by a green dot (Figures 4.23 – Figure 4.26).

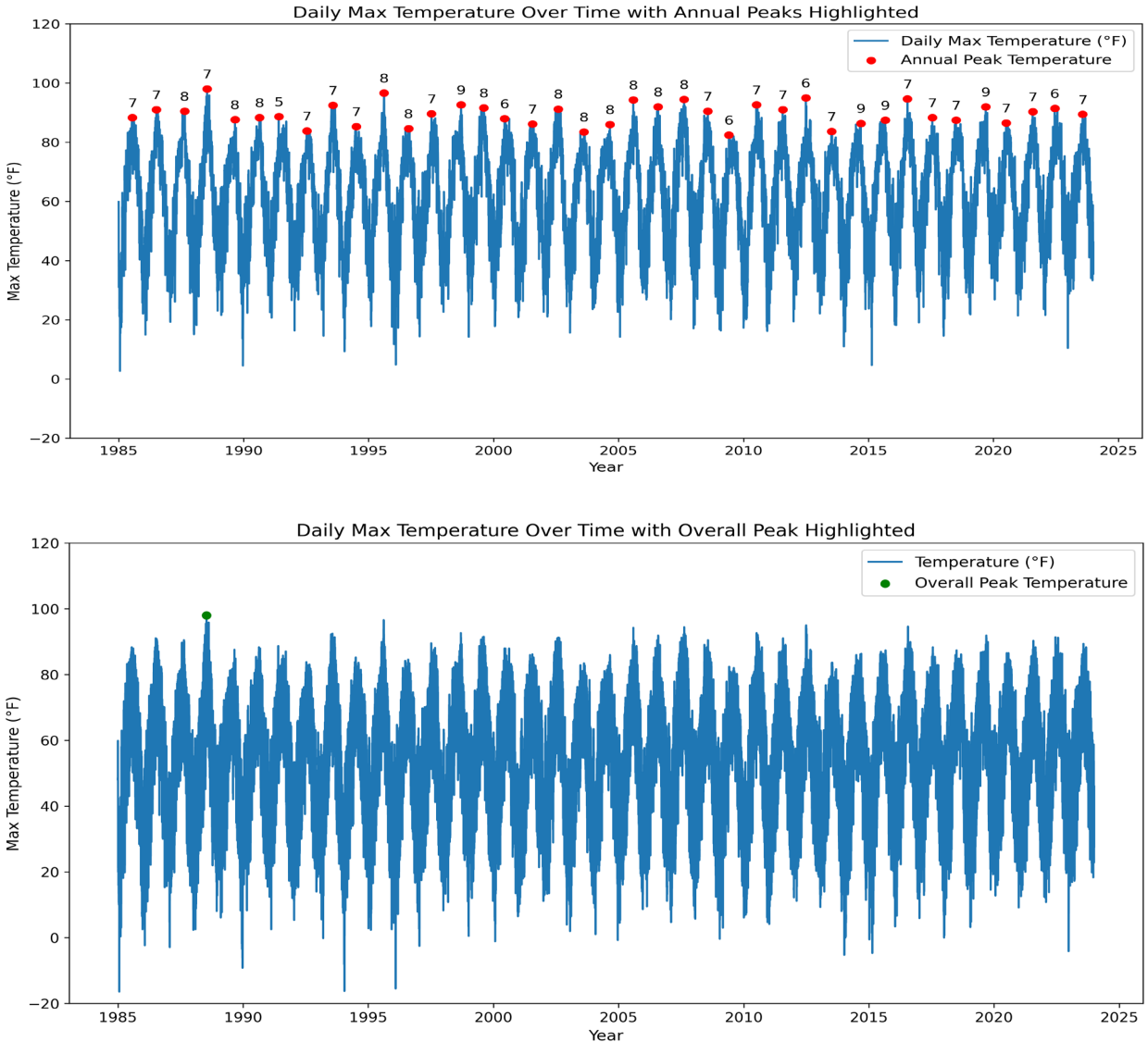

FIGURE 4-23 Temperature data for station 140126 (Region 1)

Overall peak temperature for station 140126 in Region 1 occurred in 1988, with a temperature of 98.06°F. The peak temperature in 2023 for this station was 89.42°F.

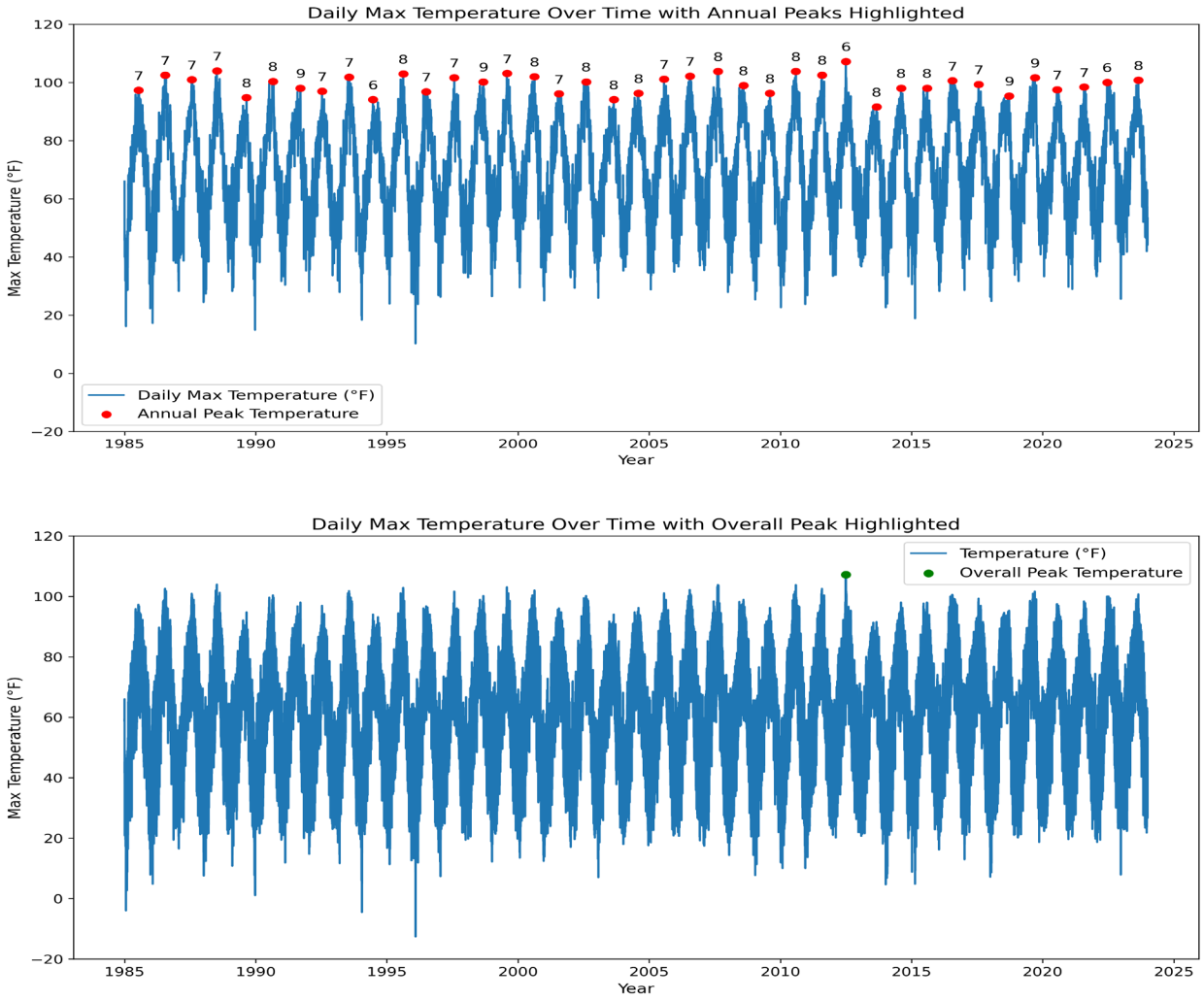

FIGURE 4-24 Temperature data for station 138393 (Region 2)

Overall peak temperature for station 138393 in Region 2 occurred in 2012, with a temperature of 107.24°F. The peak temperature in 2023 for this station was 100.76°F.

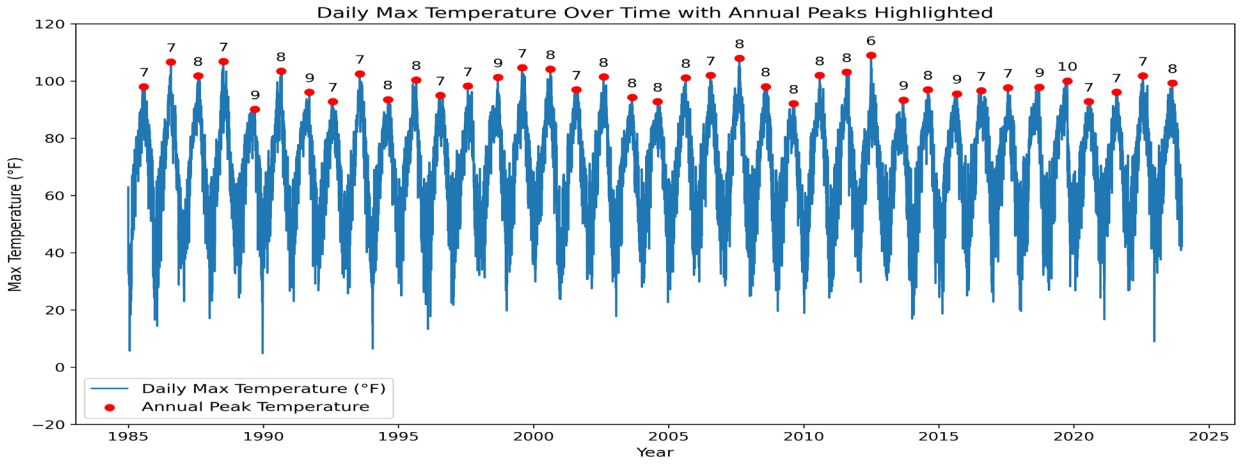

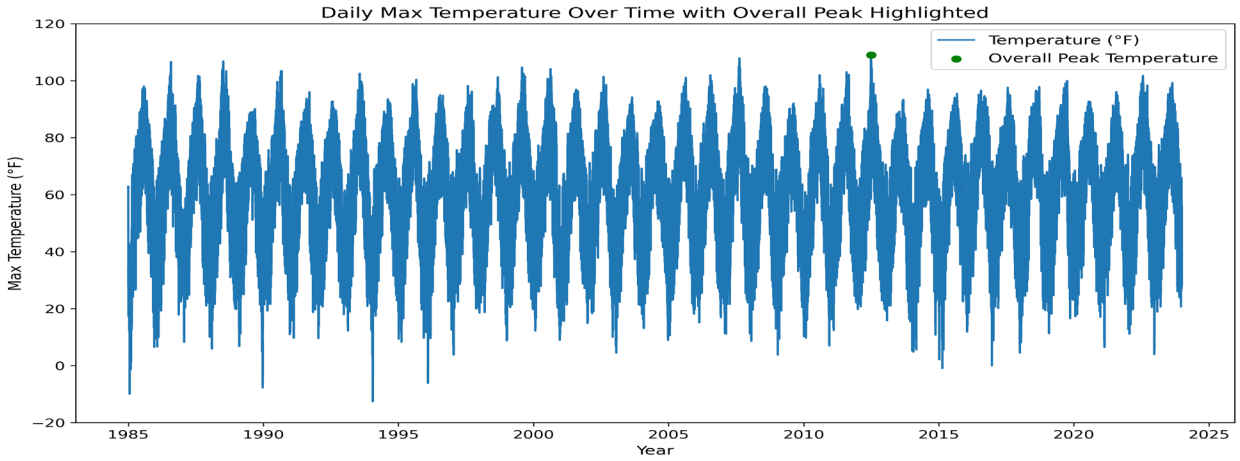

FIGURE 4-25 Temperature data for station 139542 (Region 3)

Overall peak temperature for station 139542 in Region 3 occurred in 2012, with a temperature of 109.04°F. The peak temperature in 2023 for this station was 99.32°F.

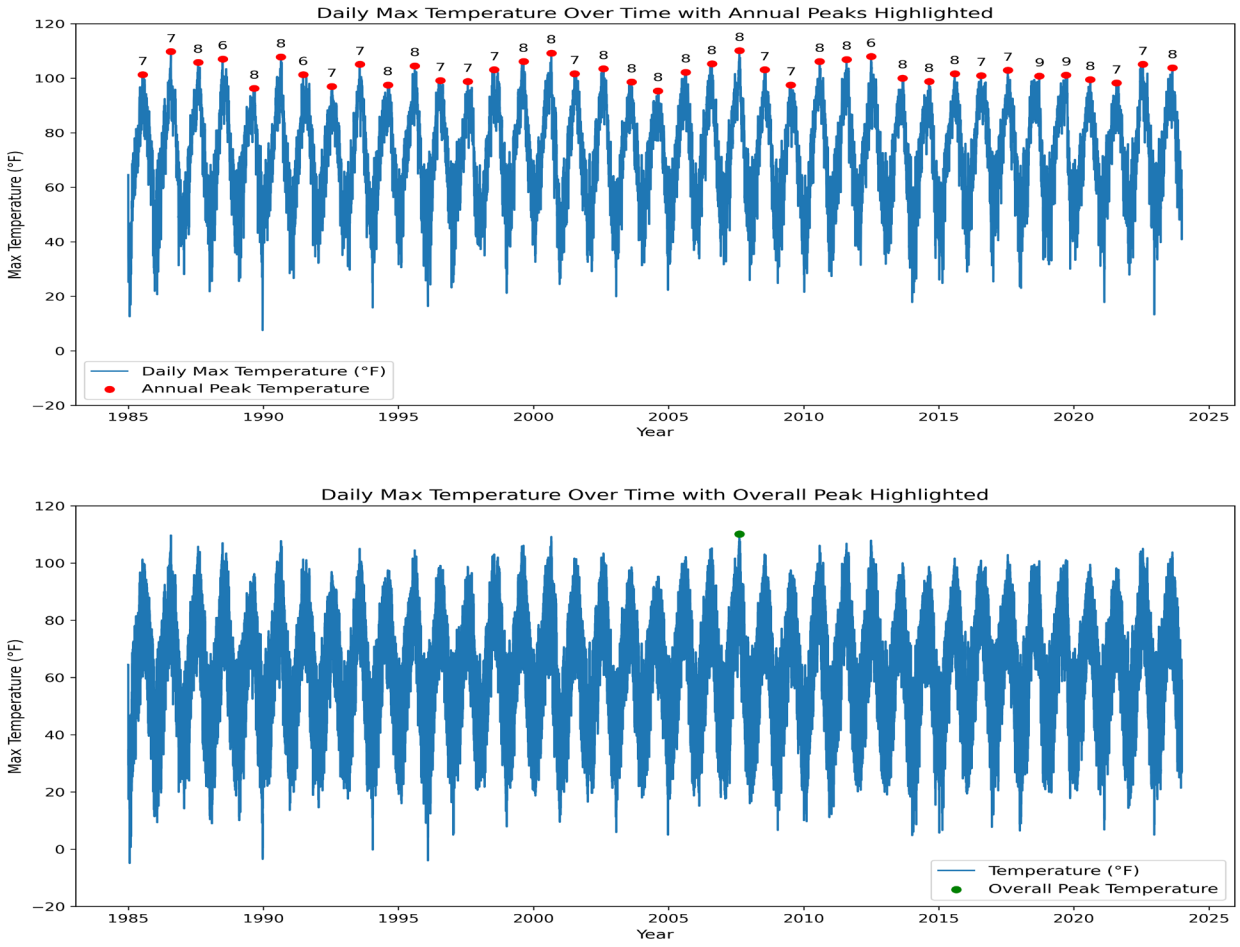

FIGURE 4-26 Temperature data for station 138387 (Region 4)

Overall peak temperature for station 138387 Region 4 occurred in 2007, with a temperature of 110.12°F. The peak temperature in 2023 for this station was 105.08°F.

A high variability exists with regards to temperature data and as a result it is very difficult to establish a uniform trend (as to whether it is uniformly increasing or decreasing with time).

4.1.2 Annual Peak Precipitation

As in the case with temperature, the first graph illustrates daily maximum precipitation with annual peaks in red dots, while the second graph displays the overall peak precipitation during the analysis period, the green dot indicating all time highest peak for the analysis period (Figures 4.27 to Figure 4.30). The numbers presented in the figures depict the month of the occurrence.

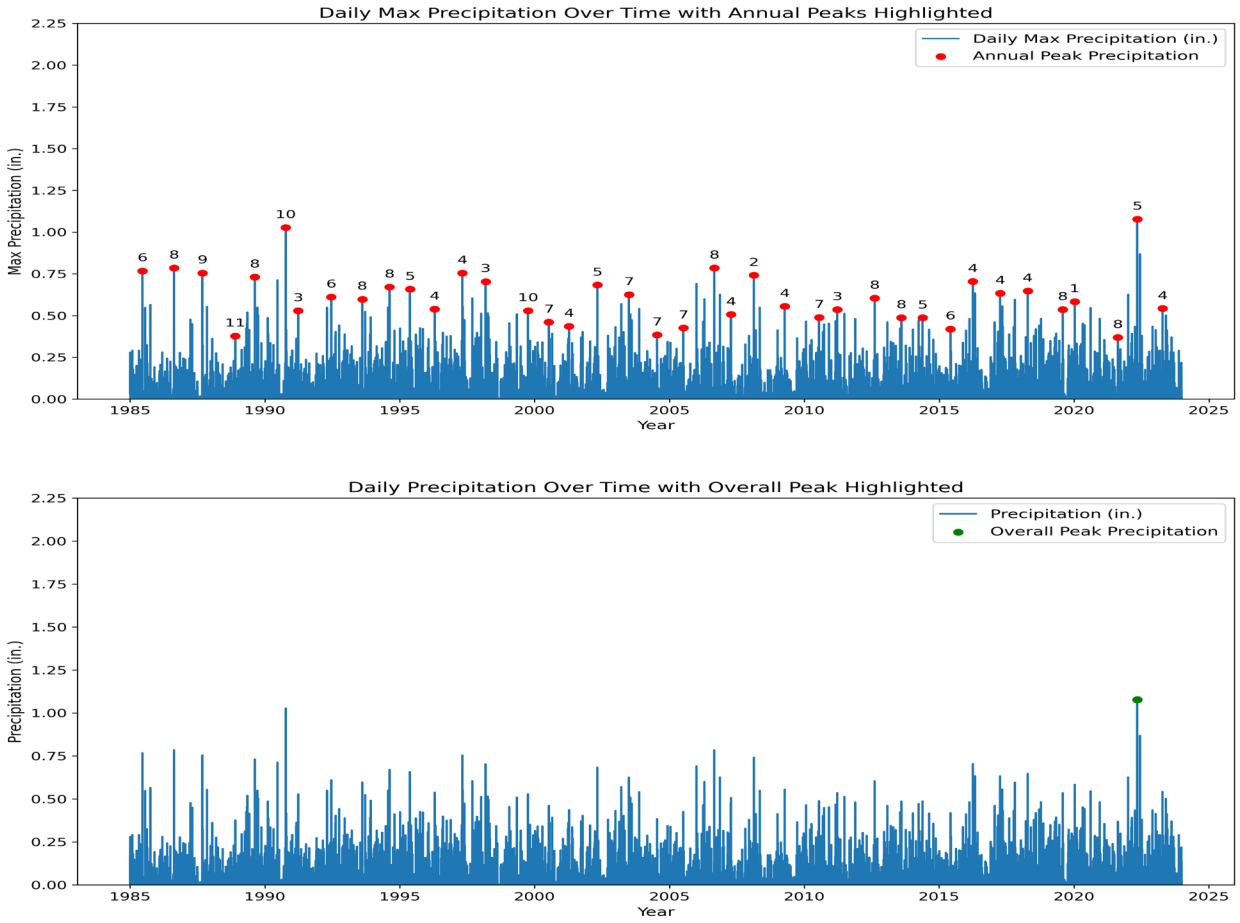

FIGURE 4-27 Precipitation data for station 140126 (Region 1)

Overall peak precipitation for Station 140126 in Region 1 occurred in 2022, with a depth of 1.08 in/hr. The peak precipitation in 2023 for this station was 0.54 in/hr. (Figure 4.27).

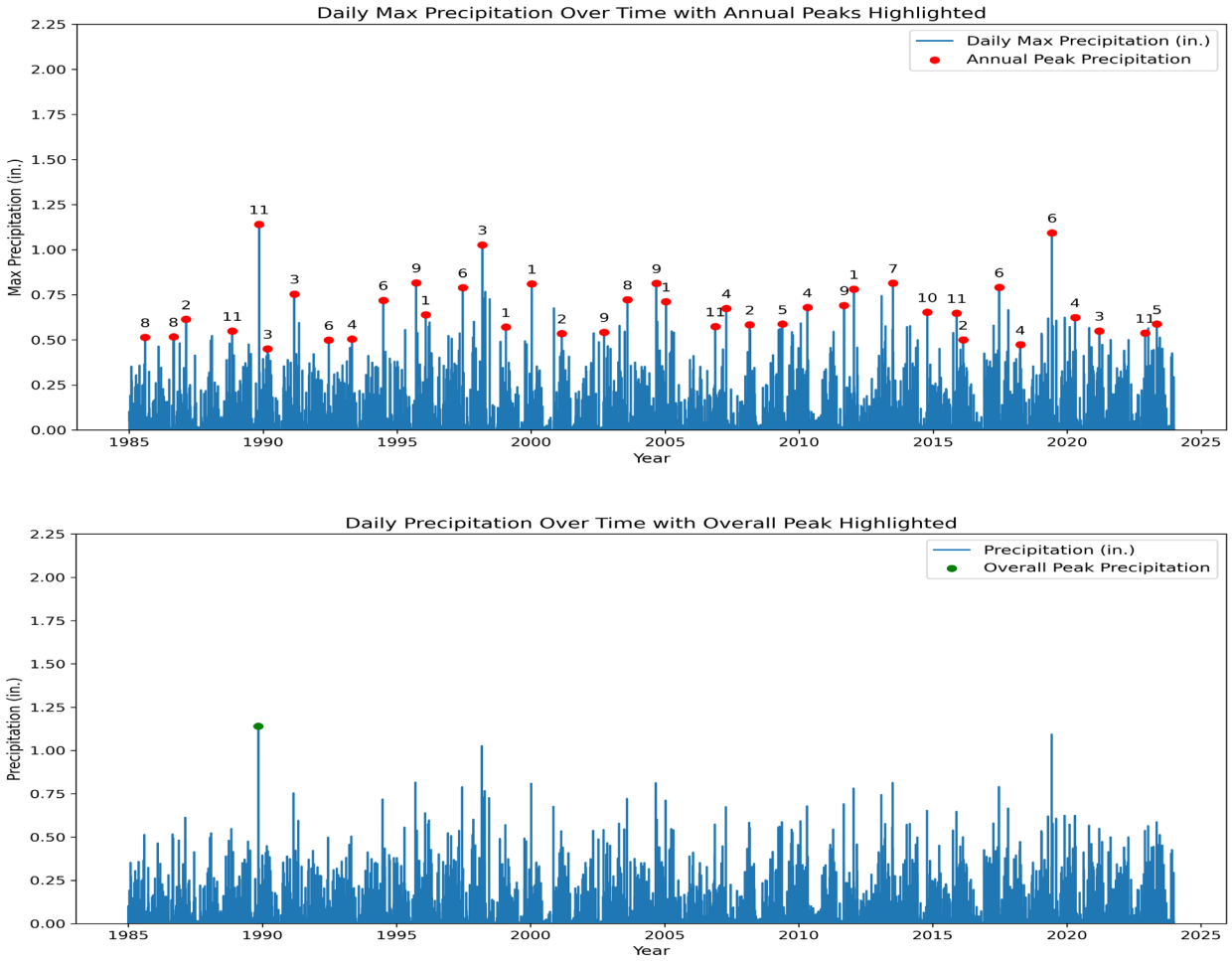

FIGURE 4-28 Precipitation data for station 138393 (Region 2)

Overall peak precipitation for Station 138393 in Region 2 occurred in 1989, with a depth of 1.14 in/hr. The peak precipitation in 2023 for this station was 0.59 in/hr.

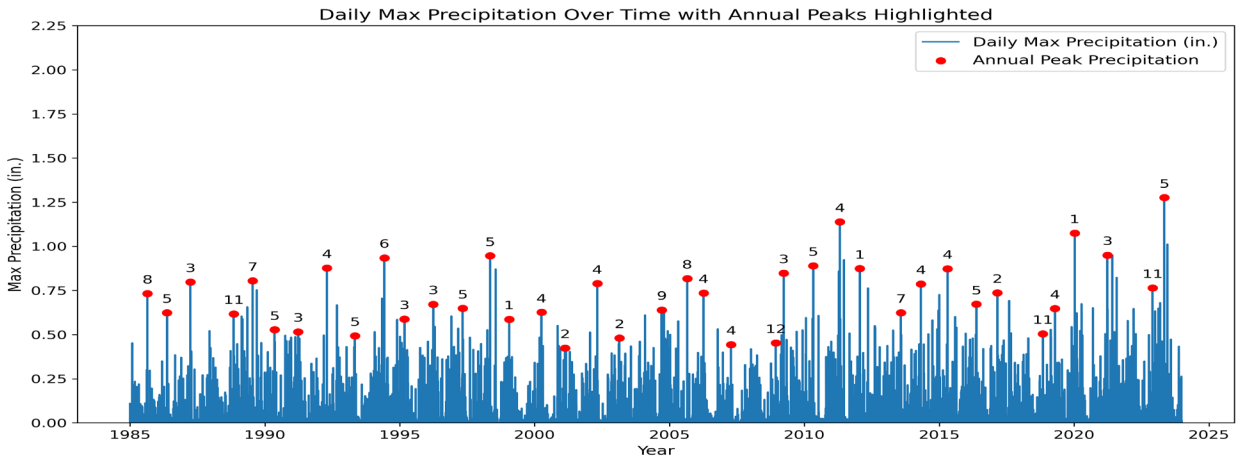

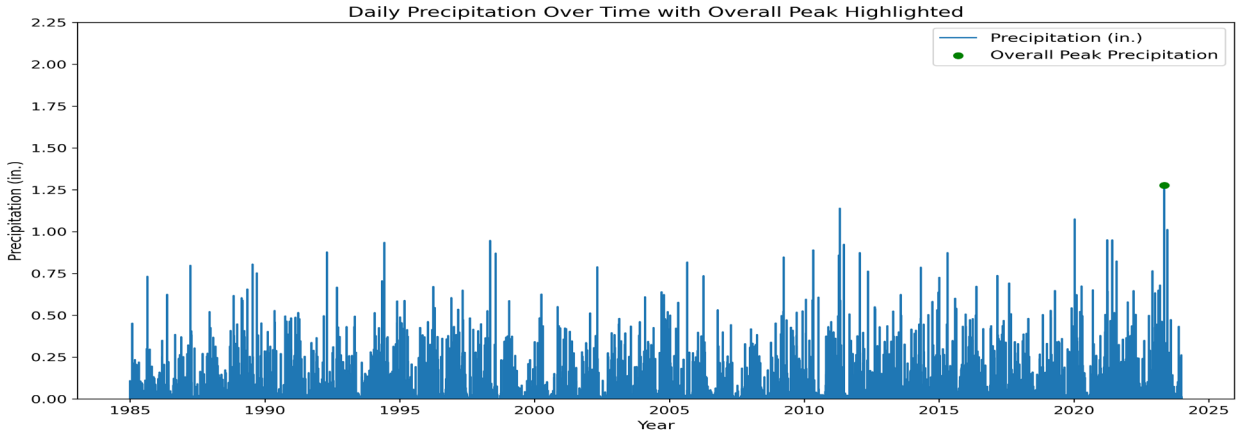

FIGURE 4-29 Precipitation data for station 139542 (Region 3)

Overall peak precipitation for Station 139542 in Region 3 occurred in 2023, with a depth of 1.28 in/hr.

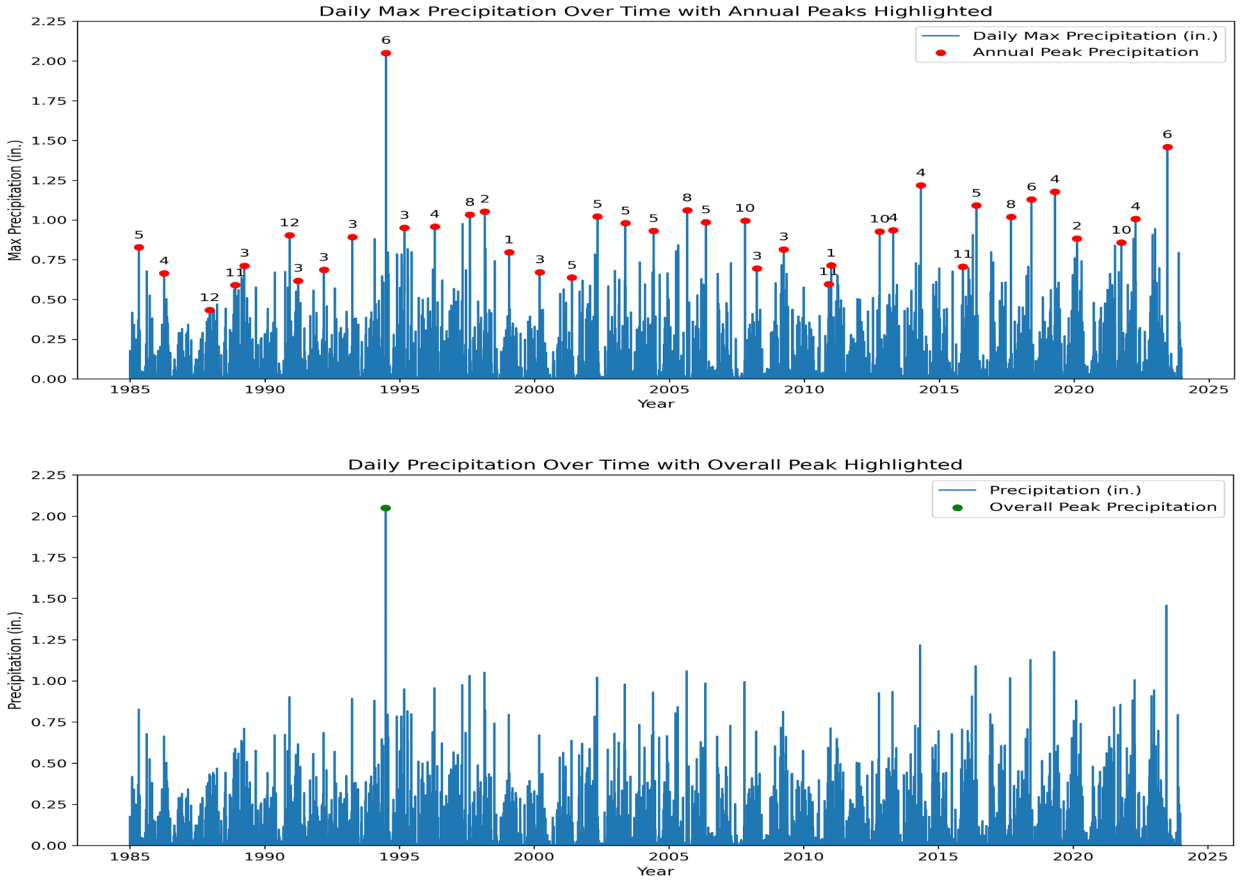

FIGURE 4-30 Precipitation data for station 138387 (Region 4)

Overall peak precipitation for Station 138387 in Region 4 occurred in 1994, with a depth of 2.05 in/hr. The peak precipitation in 2023 for this station was 1.46 in/hr.

4.1.3 Section Discussion and Conclusion

From the visualization of historical climate data, no specific trend can be inferred. The peak temperatures and precipitation occurred in different years for the four regions. Table 4.1 shows the summary of overall peak temperature and precipitation and the peak values in 2023. The overall highest temperature in the state was in 2007 (110.12°F) and overall highest precipitation was in 1994 (2.05 in./hr.). Although Regions 3 and 4 indicated higher peak precipitation in 2023, it did not exceed the overall peak precipitation in 1994. This indicates that the perceived increased frequency of weather events in recent years has not increased the climate inputs beyond the highest recorded values over the years. Therefore, designing for the overall climate shift over the years is more practical. Extreme weather events may be used to determine the recurrence period for design purposes.

TABLE 4-1 Overall peak values for temperature and precipitation

Region	Temperature			Precipitation		
	Year	Overall peak	2023 peak	Year	Overall peak	2023 Peak
Region 1	1988	98.06°F	89.42°F	2022	1.08 in./hr.	0.54 in./hr.
Region 2	2012	107.24°F	100.76°F	1989	1.14 in./hr.	0.59 in./hr.
Region 3	2012	109.04°F	99.32°F	2023	1.28 in./hr.	1.28 in./hr.
Region 4	2007	110.12°F	105.08°F	1994	2.05 in./hr.	1.46 in./hr.

4.2 Validation of Prediction Models

Validation of the empirical distress prediction models embedded in the AASHTOWare PMED software was performed using Tennessee design inputs and measured distress data from the Long Term Pavement Performance Database (LTPP) [26]. This procedure was conducted to assess the reliability of the software in predicting pavement distresses using global (national average or default) and local (statewide) calibration coefficients. The Tennessee local calibration of distress prediction models was performed using AASHTOWare PMED v2.2, while this study utilized v2.6.2.2. Some of the distress prediction models have been updated or changed, therefore it was important to evaluate the reliability of the distress prediction models. Distress models updated on v2.6.2.2 are:

1. Alligator cracking model: PMED software v2.6.2.2 has two separate inputs for the coefficient C_2, which are dependent on the pavement thickness of the second layer, while V2.2 had only one coefficient. The AC layer local calibration for coefficients C_1 and C_3 were used, and default values were used for coefficient C_2.
2. Version 2.6.2.2 has three coefficients for AC rutting (β_{r1}, β_{SB}, β_{SG}), while v.2.2 had only one coefficient value (β_{r1}). As a result, default values were used for the other two coefficients (β_{BS}, β_{SG}) pertain to the subbase and subgrade respectively.
3. Due to software updates, AC thermal cracking model is completely new, therefore, default coefficient values were used.
4. Global coefficients were used for rigid pavement because of lack of local calibration of coefficients.

This analysis compared actual distress data for 27 Tennessee pavement sections, derived from the LTPP database to the corresponding predicted distresses using default and previously

generated local calibration coefficients. The validation process was as outlined on Figure 4.31 [26]. Figure 4.32 shows the LTPP sites used for validation.

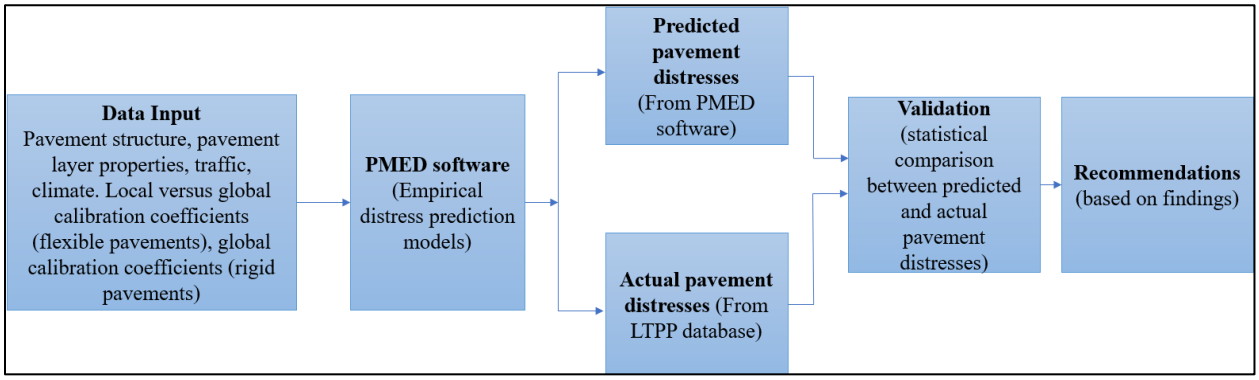

FIGURE 4-31 Validation process of PMED distress prediction models [26]

Three flexible pavement distresses, terminal IRI, fatigue cracking (bottom-up cracking) and total pavement rutting and two rigid pavement distresses, IRI, and transverse cracking were validated depending on the available measured distress data on LTPP website.

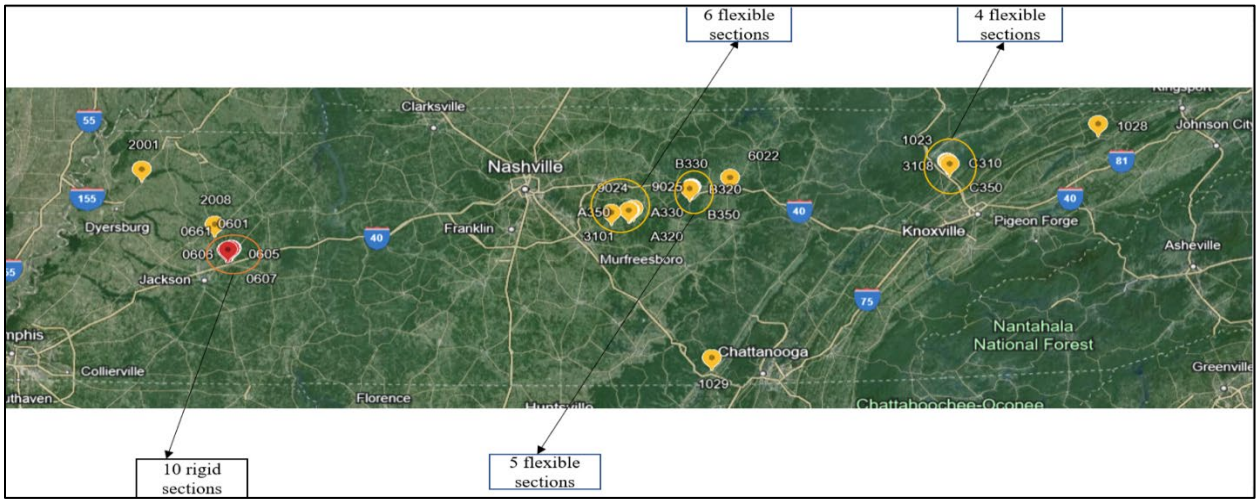

FIGURE 4-32 Distribution of LTPP pavement sites

Statistical evaluations, including the paired t-test and Wilcoxon Signed Rank's Test, were conducted to evaluate the degree of similarity between the measured and predicted distresses. Based on the available data, the study established that for both flexible and rigid pavements, the differences between measured and predicted IRI values were not statistically significant when using local calibration coefficients for flexible pavements or default coefficients for rigid pavements. This suggests that the IRI prediction model provides satisfactory estimates of pavement roughness. However, for flexible pavement distresses, such as total rutting and alligator cracking, the differences between measured and predicted distress values were statistically significant regardless of the calibration coefficients utilized indicating a need for model improvement in this area.

In the case of rigid pavement sections, although IRI predictions remained statistically consistent with measured data, the cracking model underestimated the magnitude of transverse cracking. These findings highlight the importance of local calibration in improving model accuracy. More data is recommended to enable a more comprehensive and robust evaluation of the distress prediction models. Additionally, given frequent revisions and enhancements of the PMED software, methods of making the local calibration procedure easier, such as automating the process, are recommended for local agencies looking to adopt the software.

4.2.1 Section Summary

Table 4.2 below summarizes the findings from the validation of prediction models for flexible pavements. Local calibrated coefficients predicted distresses that were statistically significantly different from the measured values except for IRI model for flexible pavements. Similarly using global coefficients, only predicted IRI for rigid pavements was not statistically significantly different from measured values at 95% confidence level. This emphasizes the importance of local calibration of prediction models coefficients.

TABLE 4-2 Validation of distress prediction models

Distress	Means Statistically significantly different?			
	Local Coefficients		Global coefficients	
Flexible pavements				
IRI		NO	YES	
Alligator cracking	YES		YES	
Total rutting	YES		YES	
Rigid pavements				
IRI				NO
Transverse cracking			YES	

Concrete pavements used only global coefficients because local calibration was not performed. Predicted IRI values were not statistically different from measured values, but the model underestimated the magnitude of transverse cracking.

Given frequent revisions and enhancements of the PMED software, methods of making the local calibration procedure easier, such as automating the process, are recommended for local agencies looking to adopt the software.

4.3 Results of Climate Data Projections

Climate data projections were performed using XGBoost, NeuralProphet, and LSTM Machine Learning models. These models projected the future climate data for 20 years (2024 – 2044) for all climate data files (to include temperature, precipitation, percent sunshine, wind speed, and humidity). The forecasting process was long with each file taking at least 8 hours to process. The projected climate data are formatted as required by AASHTOWare PMED software, then used in the software to predict distresses that are compared to those obtained from the historical climate data files (base scenario).

Figures 4.33 to 4.40 below show the predicted temperature for 20 years for four stations, each from one TDOT region. The prediction used the NeuralProphet model to generate the forecasted climate data files. This model is great at spotting patterns in data over time, like

seasonal changes, and was chosen because it handles long-term forecasts well. To create these projections, we gathered historical climate data and then cleaned and organized this data, normalizing it to ensure consistency. NeuralProphet model data was trained on the yearly, weekly, and daily patterns, running it for 500 epochs, meaning it went through the data 500 times to refine its predictions for the 2024–2044 forecast.

FIGURE 4-33 Historical temperature data for station 140126 (Region 1)

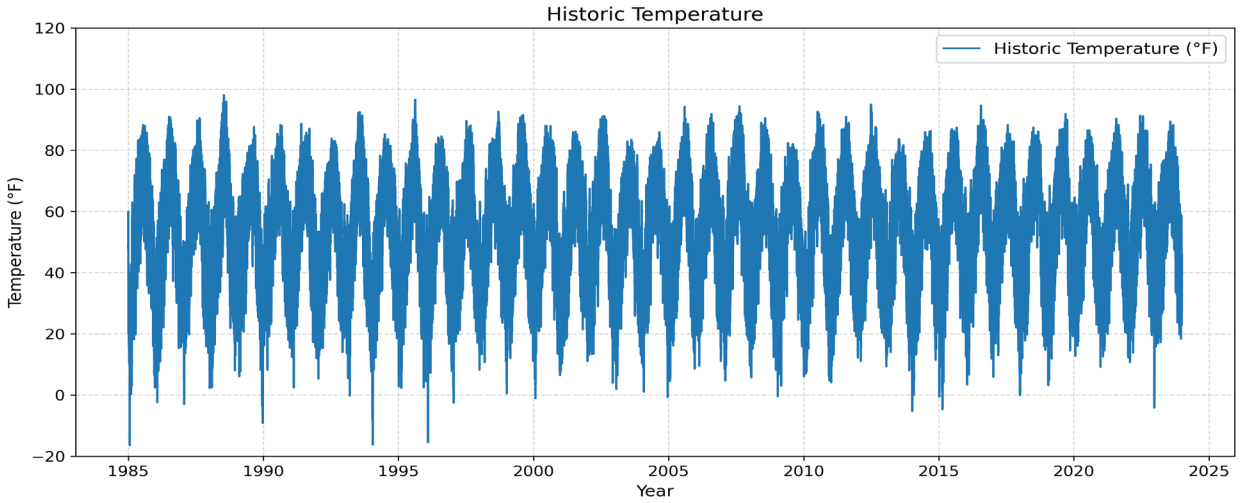

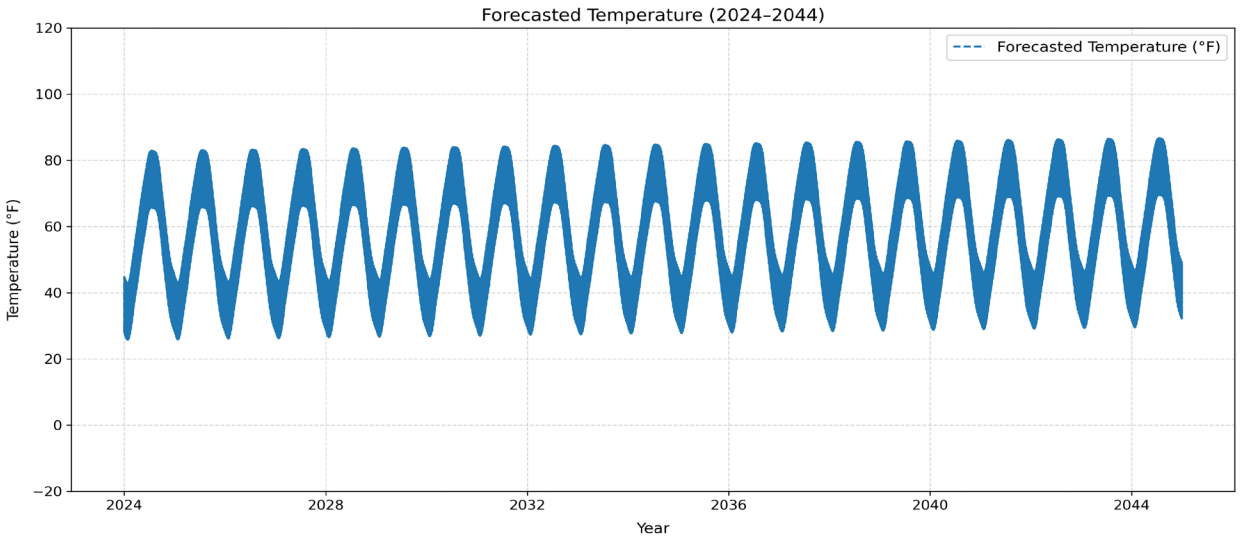

FIGURE 4-34 Forecasted temperature data for station 140126 (Region 1)

For all the figures, the first figure shows the historical temperature data from 1985 to 2023, displaying the natural fluctuations over the years. The second figure shows the forecasted temperature data from 2024 to 2044, illustrating how temperature might vary in the upcoming decades based on model predictions. The model was trained on data with temperatures ranging between approximately 30°F and 90°F, captured these patterns, which is why the forecasts stay within a similar range. However, the data suggests a gradual year-by-year increase in

temperature. This trend is consistent across all predictions for the four regions, as shown in Figures 4.35 to 4.40.

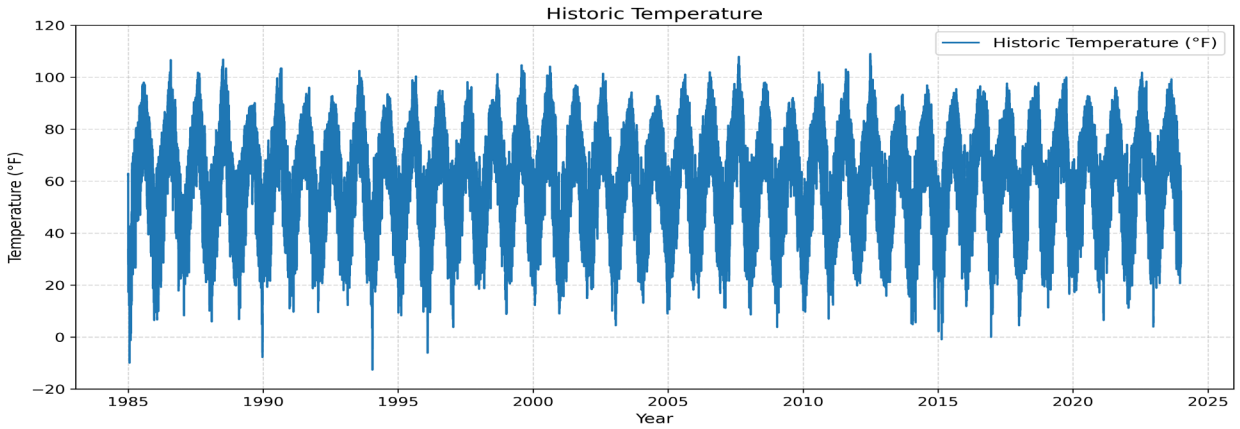

FIGURE 4-35 Historical temperature data for station 139542 (Region 2)

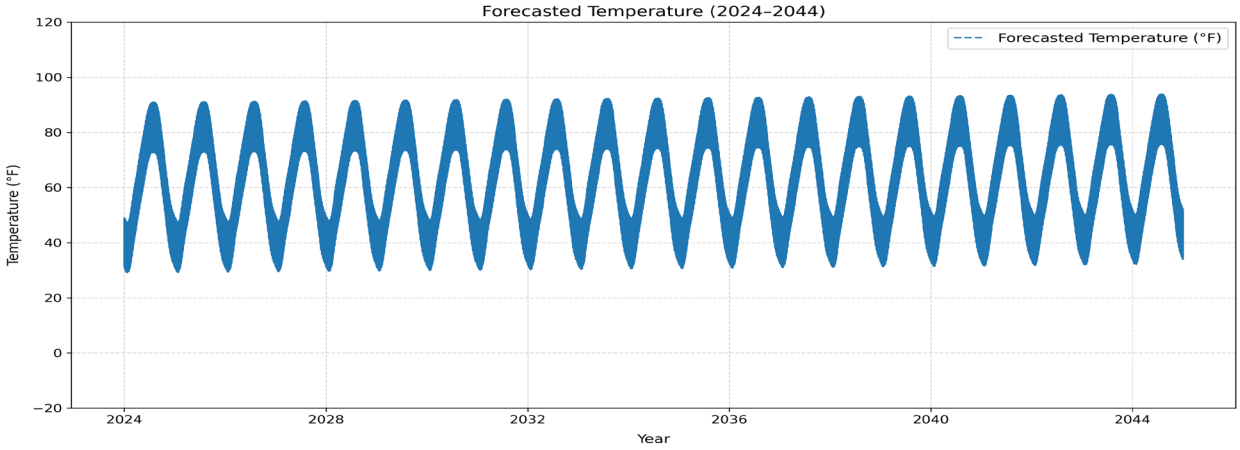

FIGURE 4-36 Forecasted temperature data for station 139542 (Region 2)

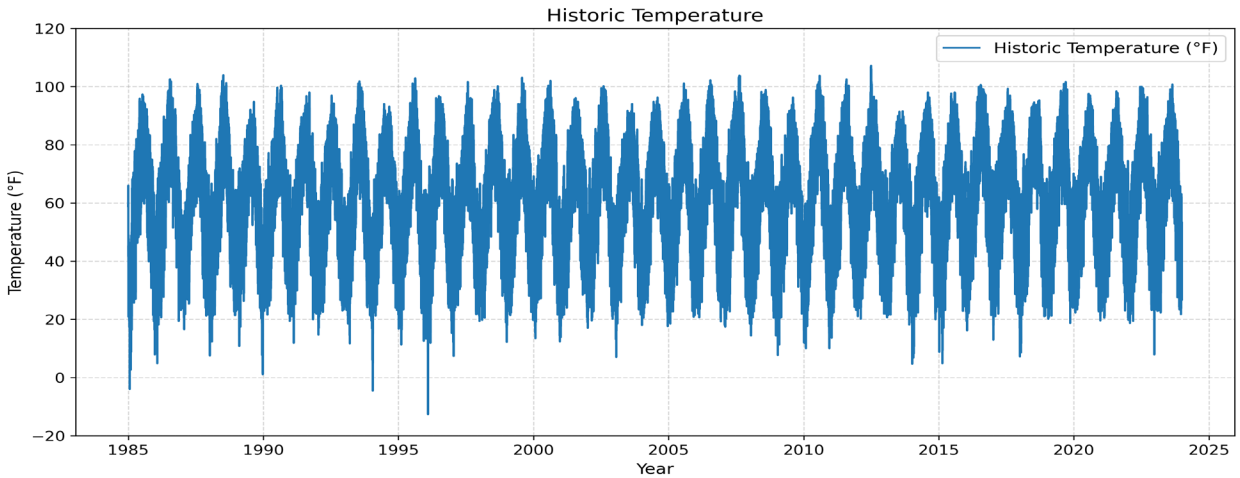

FIGURE 4-37 Historical temperature data for station 138393 (Region 3)

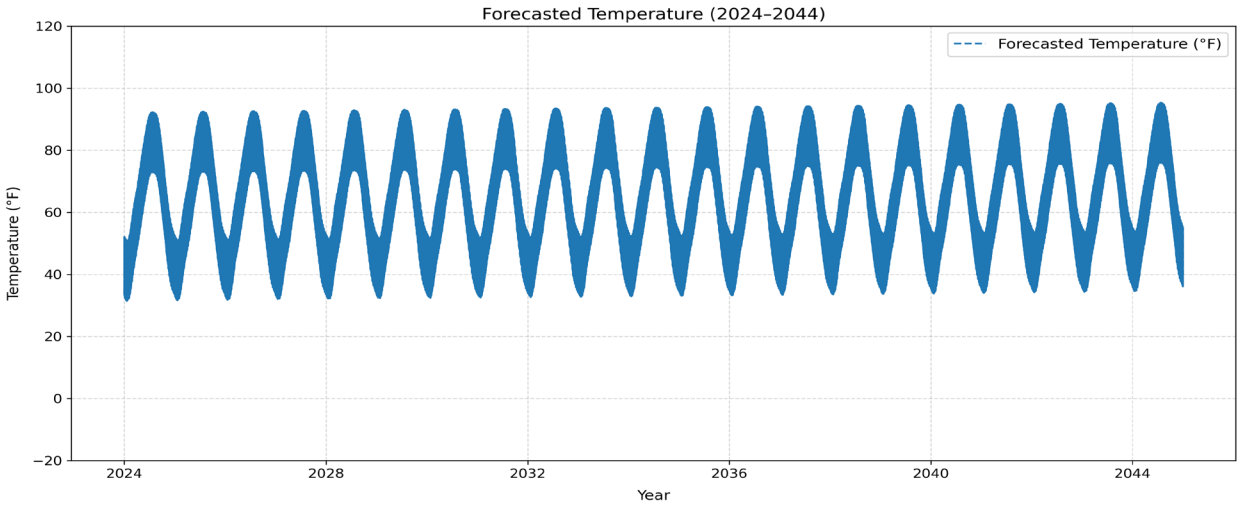

FIGURE 4-38 Forecasted temperature data for station 138393 (Region 3)

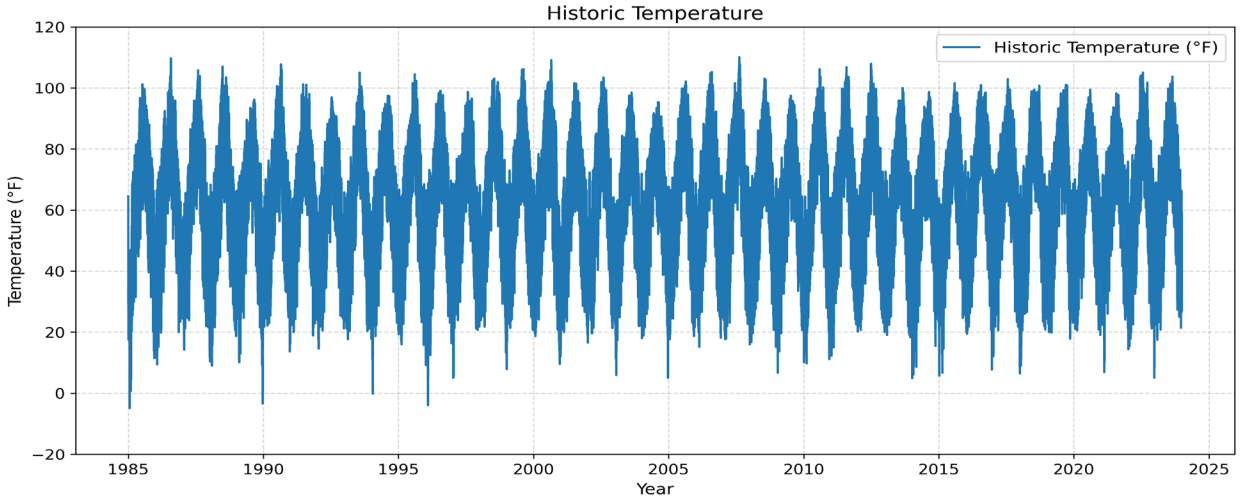

FIGURE 4-39 Historical Temperature data for station 138387 (Region 4)

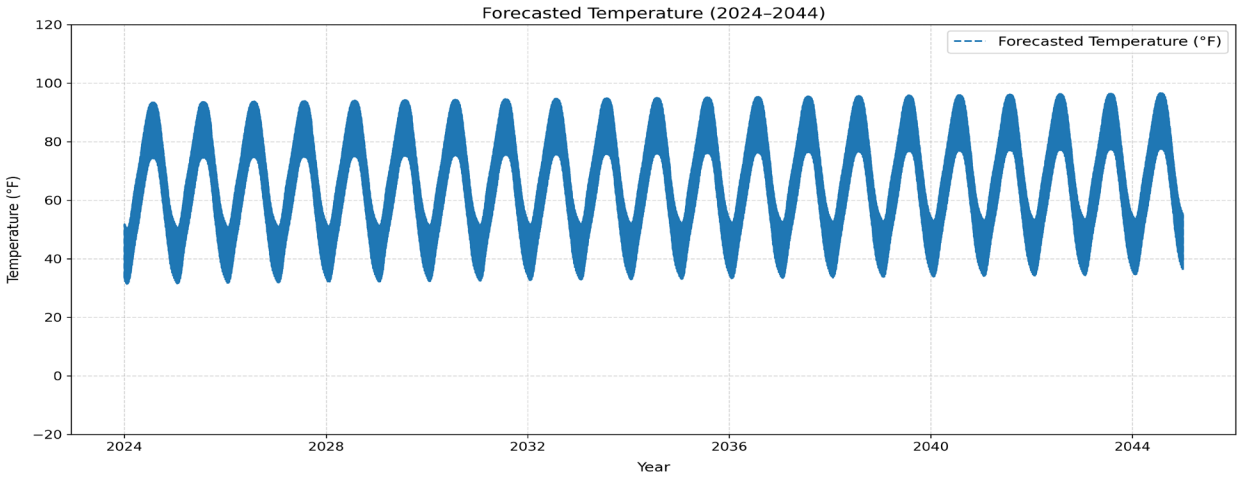

FIGURE 4-40 Forecasted Temperature data for station 138387 (Region 4)

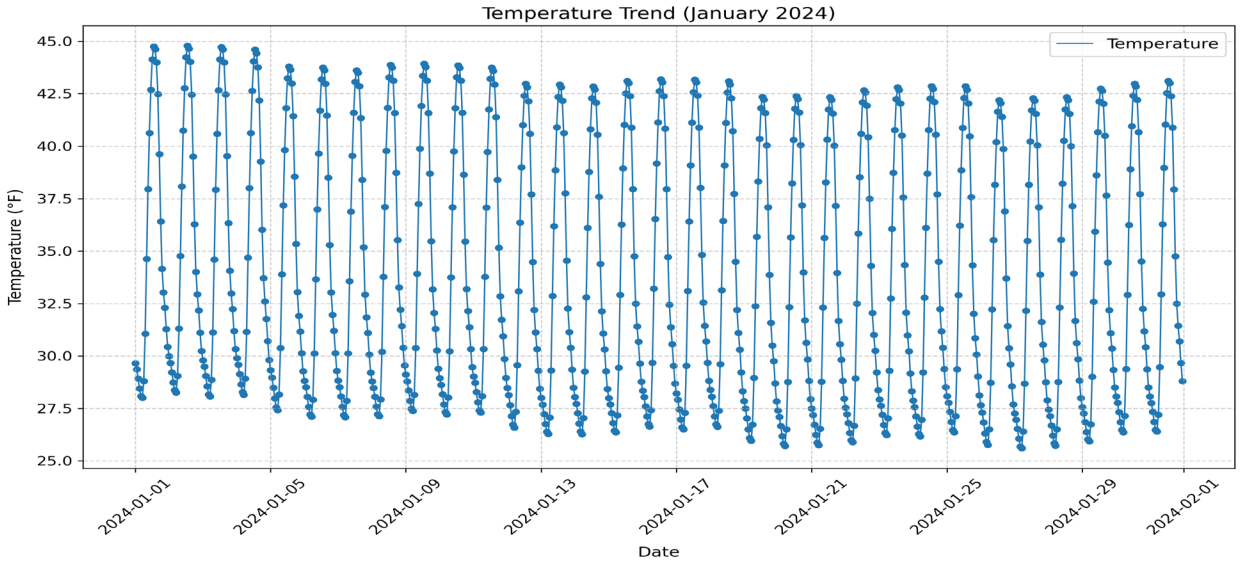

FIGURE 4-41 Projected temperature data for station 140125 for one month

Figure 4.41 illustrates the temperature trend for a subset of data over one month, from January 1, 2024, to February 1, 2024, with hourly temperature readings marked by dots and connected by lines. This graph shows the temperature fluctuating between approximately 25°F and 45°F, with a general pattern of rising to around 45°F during the day and slightly decreasing by the end. This daily variation supports why the 20-year temperature forecast (2024 – 2044) stays within the 30°F to 90°F range. The model trained on historical data with similar daily and seasonal cycles, learns these natural fluctuations and projects future temperatures within a comparable range, reflecting the observed trends like the daily highs and lows seen here.

A further comparison was performed for one month comparing predicted and historical data using LSTM (Long Short-Term Memory). Figure 4.42 shows the comparison of the projected and actual temperature data for 8 years using the LSTM model, which shows that the model closely predicted the actual temperature. Figure 4.43 shows the one-year temperature projection using XGBoost, indicating that the predicted temperature did not capture the peak temperatures.

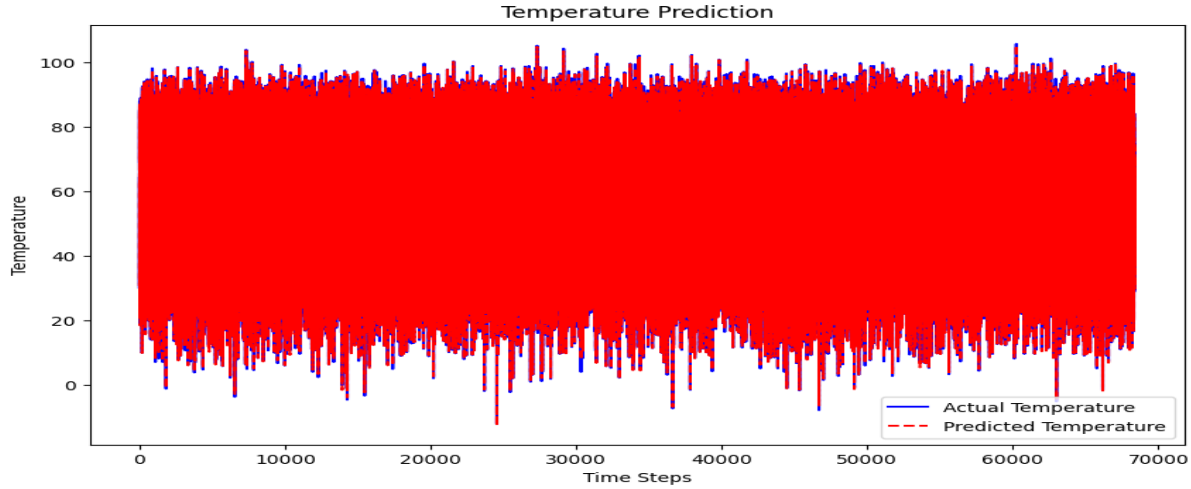

FIGURE 4-42 Projected temperature data for 140126 using LSTM for 8 years

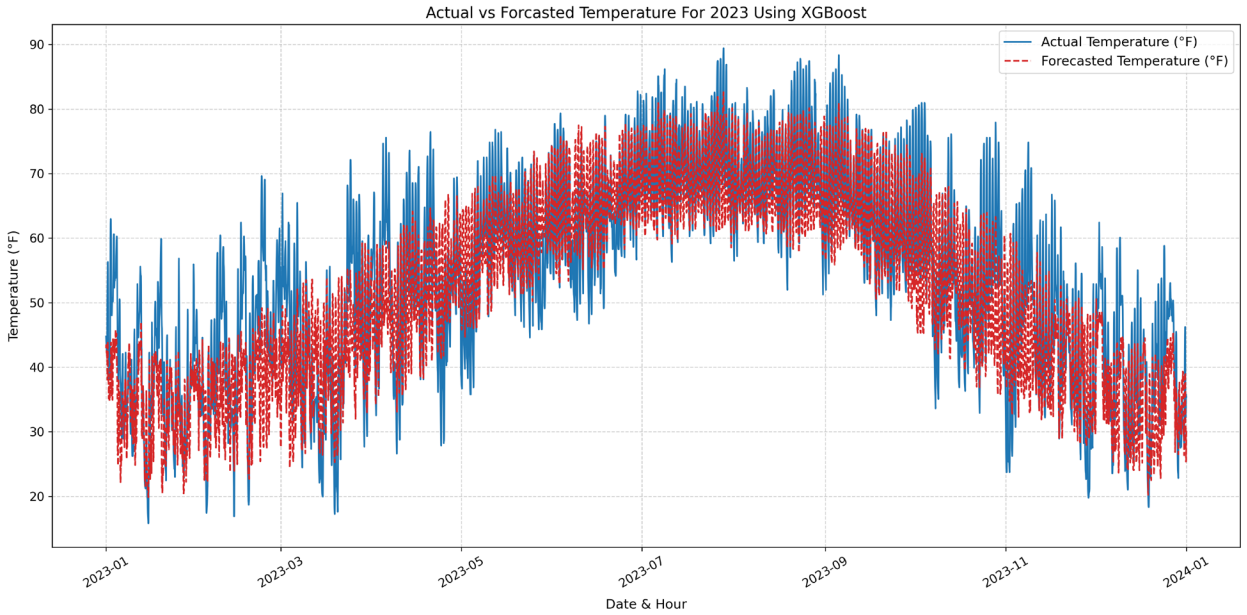

FIGURE 4-43 Projected temperature data for 140126 using XGBoost

4.3.1 Hybrid VAE-LSTM Model for Temperature Projection

After trying many different models for climate forecasting (XGBoost, NeuralProphet, and LSTM) the research team developed a hybrid model based on a Variational Autoencoder (VAE) with LSTM layers. This model gave more accurate results when compared to other models for long-term hourly temperature predictions from 2024 to 2044.

The VAE-LSTM hybrid works in two stages. First, the VAE compresses the large climate dataset into a smaller representation that captures the most important seasonal and temporal patterns. Within this VAE, the LSTM encoder is responsible for learning the sequential climate data (daily, monthly, and yearly cycles). Then, the decoder reconstructs the values while keeping these critical weather patterns.

During the forecasting process, two steps were manually included to ensure realistic values. If the model predicted sudden unrealistic hourly jumps (≥30°F), they were automatically corrected using forward or backward filling. If there were any spikes during dataset preparation, they were smoothed by averaging neighboring hours. These steps made sure the projected data were clear and realistic. Furthermore, because hourly temperature changes greater than 30°F are rare, the correction can be considered valid.

For the other variables (windspeed, percent sunshine, precipitation, and humidity), historical seasonal patterns (1985 to 2005) are used and extended across the projection period, since these variables remain relatively stable compared to temperature.

The final projected climate data (175,200 hourly rows for 20 years) were formatted in the required PMED HCD structure and validated for completeness. Figures 4.44 to 4.51 show the historical and projected temperature using the VAE-LSTM hybrid model.

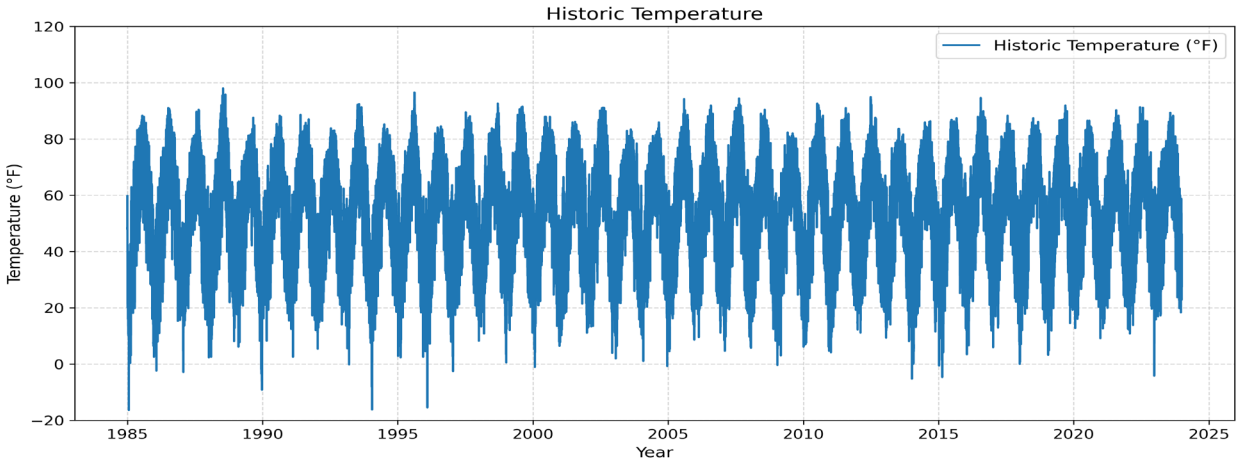

FIGURE 4-44 Historic temperature data for station 140126 (Region 1)

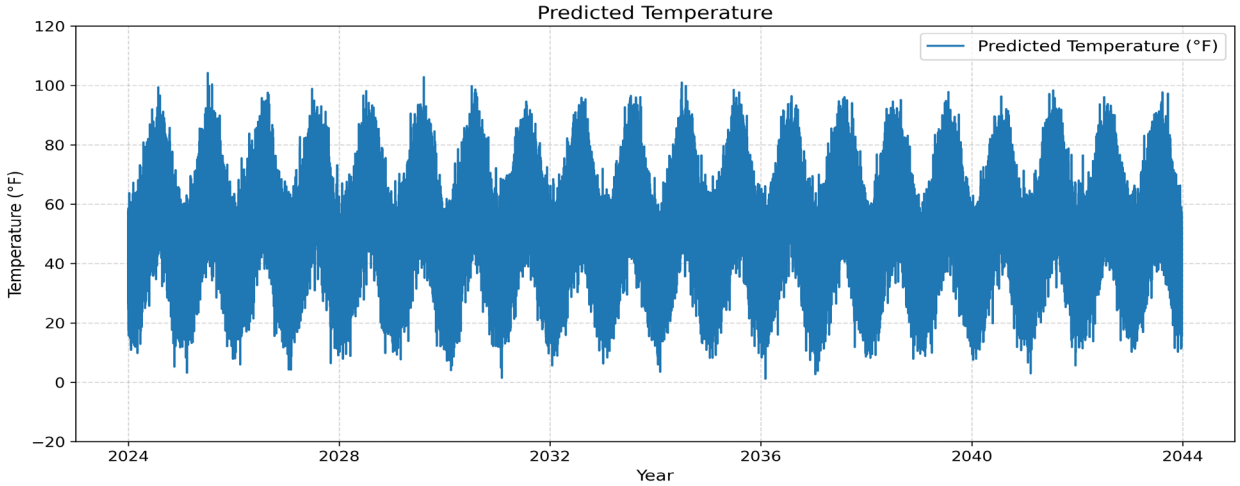

FIGURE 4-45 Projected temperature data for station 140126 (Region 2)

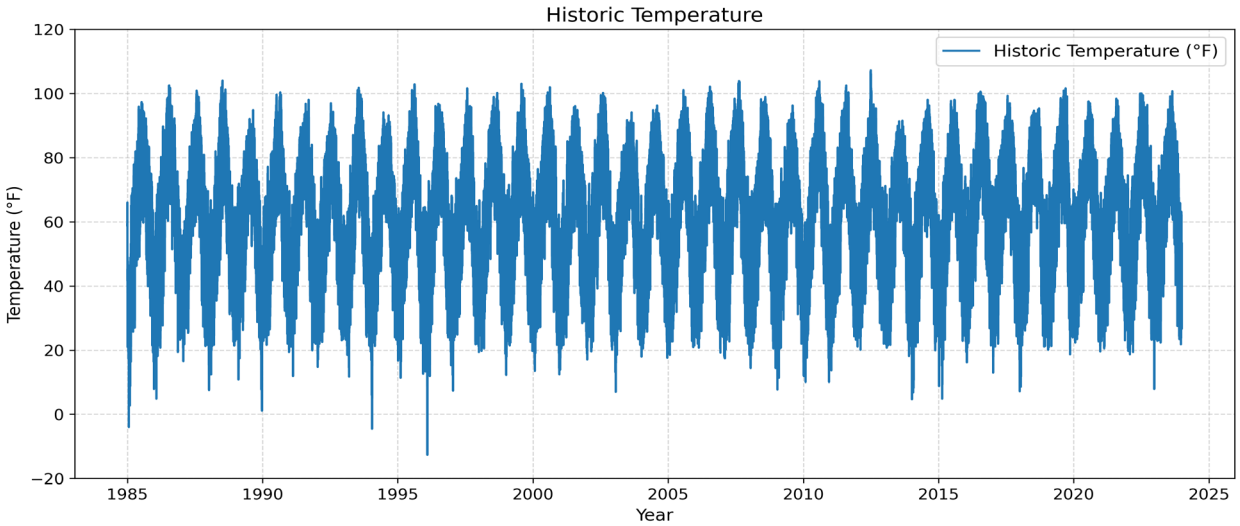

FIGURE 4-46 Historic temperature data for station 138393 (Region 2)

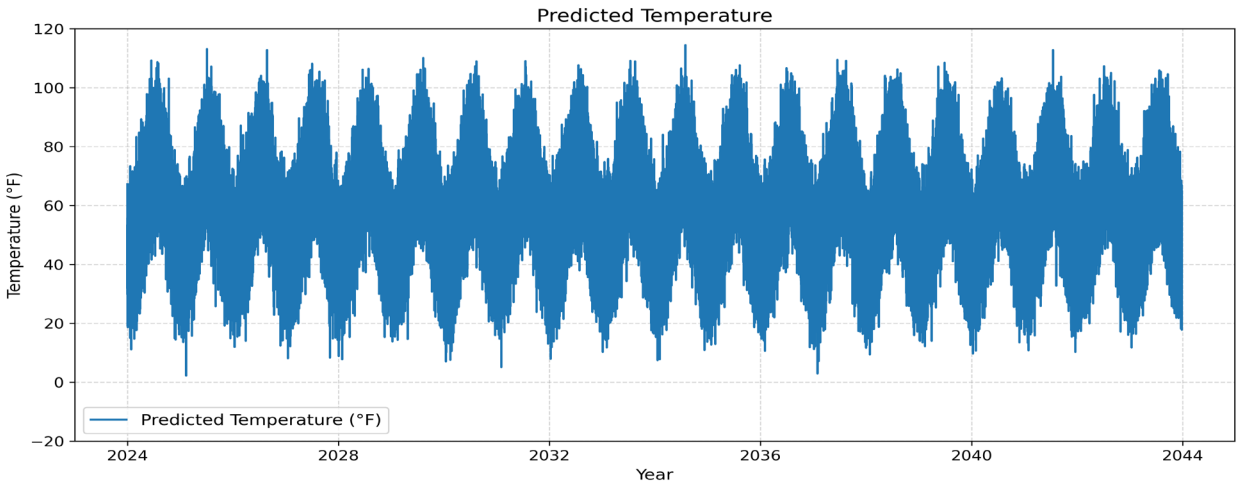

FIGURE 4-47 Projected temperature data for station 138393 (Region 2)

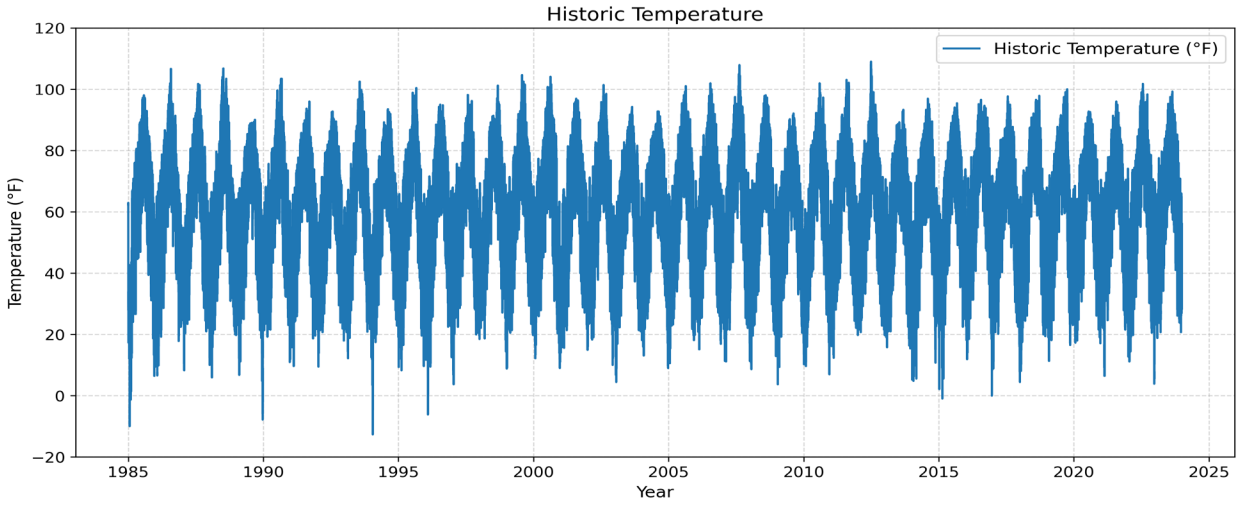

FIGURE 4-48 Historic temperature data for station 139542 (Region 3)

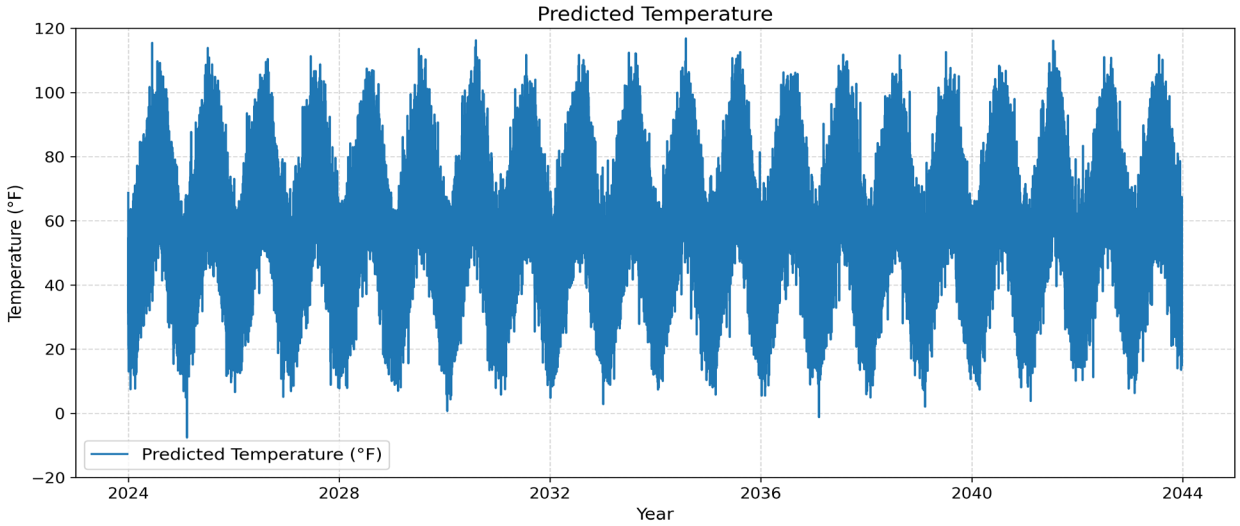

FIGURE 4-49 Projected temperature data for station 139542 (Region 3)

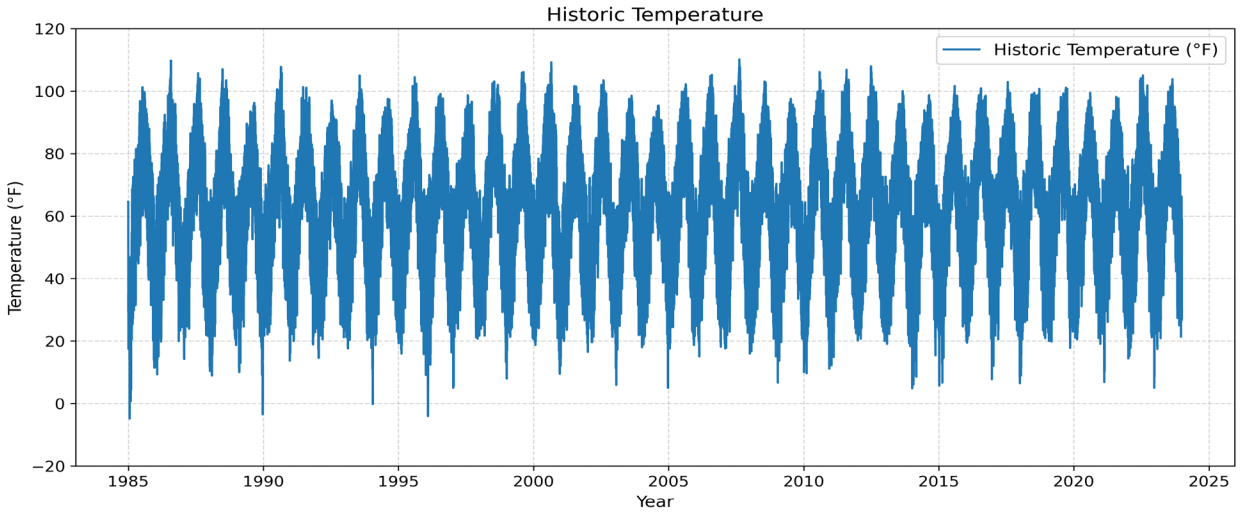

FIGURE 4-50 Historic temperature data for station 138387 (Region 4)

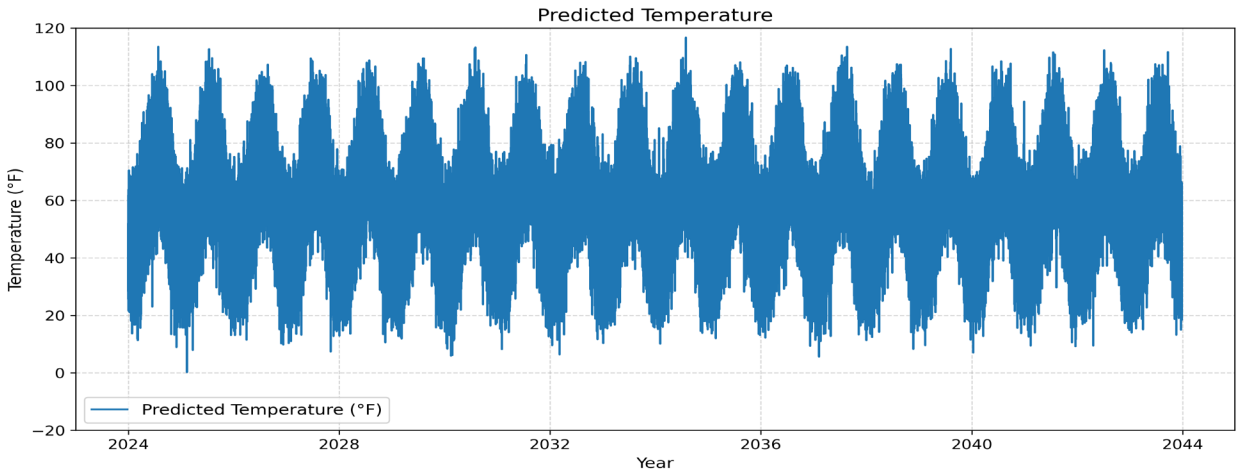

FIGURE 4-51 Projected temperature data for station 138387 (Region 4)

4.3.2 Section Summary

- Data was trained using the NeuralProphet model on the yearly, weekly, and daily patterns, running it for 500 epochs, meaning it went through the data 500 times to refine its predictions for the 2024–2044 forecast.
- The NeuralProphet model was trained on data with temperatures ranging between approximately 30°F and 90°F, which is why the forecasts stay within a similar range. However, the data suggests a gradual year-by-year increase in temperature.
- After many trials, a hybrid model based on a Variational Autoencoder (VAE) with LSTM layers was developed. This model gave more promising results when compared to other models for long-term hourly temperature predictions from 2024 to 2044.
- In the Hybrid model, the VAE acts as a pre-processor, compressing the raw climate data into a lower-dimensional latent space where irrelevant variations are minimized and essential features are retained. This ensures that the LSTM receives cleaner, more structured inputs, allowing it to learn patterns across hours, days, and years. The decoder part of the VAE then helps reconstruct meaningful outputs from the LSTM's predictions.

- The hybrid model results were not used for distress prediction because by the time the model was completed, the PMED software had expired, and the project sponsor opted to not renew the license, and the project was at closure, with no funds for the license renewal.
- Although this model could not be directly applied for distress prediction due to PMED software limitations, its performance highlights the potential of deep learning hybrids for next generation climate forecasting.

4.4 Comparative Analysis of Predicted Distresses using Historical and Projected Climate Data Files

The effect of climate change on pavement performance was analyzed using the AASHTOWare PMED software. The primary goal was to compare the pavement distresses generated using historical climate data and those generated using machine-learning projected climate data. The scenarios include:

1. Baseline scenario, which predicted pavement performance using thirty-nine (39) in service sites provided by TDOT, using historical climate data.
2. Machine learning projected climate data in comparison to the baseline scenario using the same in service sites provided by TDOT.

4.4.1 Predicted Pavement Distresses using Historical Climate Data - Base Scenario

The pavement performance or distress prediction was performed using AASHTOWare PMED to establish a baseline that was compared to distresses obtained using projected climate data. A total of 39 in service pavement sections provided by TDOT distributed across all four TDOT regions were used for this analysis. The sections are comprised of a combination of concrete, composite, and flexible pavements of different functional classes. Their structural, material, and traffic data characteristics were either provided by TDOT, or in the case of missing information, either local (regional) or default software values were utilized.

Figure 4.52 shows the selected 39 sites in Tennessee provided by TDOT. Detailed information of the sections is provided in Appendix A. AASHTOWare PMED input parameters were provided by TDOT and for missing inputs, level 2 (statewide) or level 3 (default) values were used.

Design Inputs

All pavements were analyzed as new constructions. Selected pavement design life was based on recommendations provided in the 2025 TDOT Pavement Design Guide (Table 3.3) [55]. Pavement reliability values used during analysis were 95% for Interstates and Principal Arterials and 90% for local streets and roads.

For analysis, layers were assumed to be of uniform material properties and pavement construction/maintenance procedures. Material layer properties were a combination of level 2 data (statewide) and level 3 (default) data, in case of missing information. Performance grade (PG) of binder used for asphalt mixtures were adopted according to the 2025 TDOT Pavement Design Guide. Generally, PG 76 -22 was adopted for urban/rural interstates (Roads with high traffic counts), PG 70 -22 was adopted for urban/rural principal arterials, and PG 64 -22 was

adopted for collectors and local roads, unless specific PG information for an asphalt binder used on a pavement was provided. Some of the pavement structure and material inputs for four stations, one from each region, are shown in Tables 3.4 to 3.7. Figure 4.52 shows the distribution of the 39 in-service pavement sections provided by TDOT.

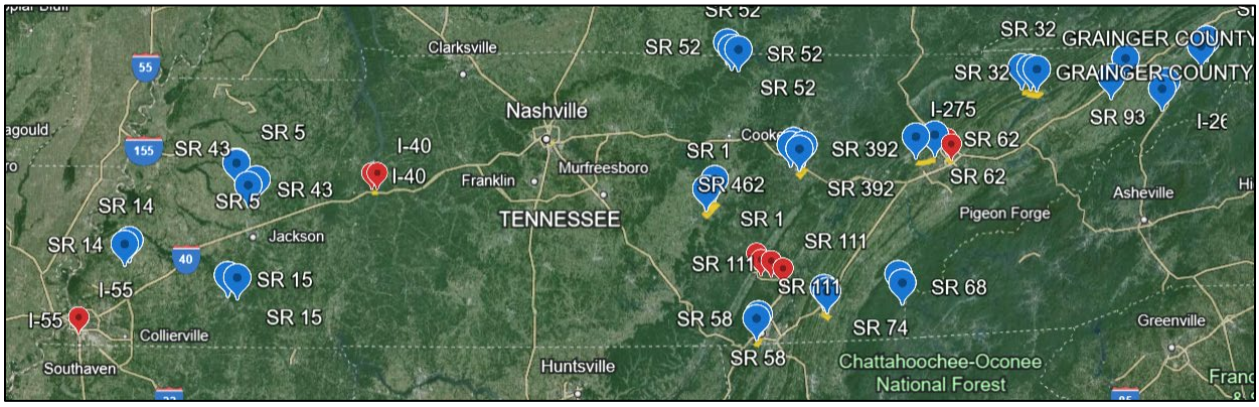

NOTE: Red pins- Concrete pavements Blue pins- Flexible pavements

FIGURE 4-52 Distribution of 39 in-service pavement sections provided by TDOT

Threshold values for pavement performance were applied as per recommendations in the Mechanistic-Empirical Pavement Design Guide [57], a summary of which is provided in Table 3.6. Distress calibration factors were applied as per recommendations by Gong et al., 2017 [56] for the state of Tennessee. However, calibration has not yet been done for AC thermal cracking, which is using a new prediction model on version 2.6.2.2. of the software. Traffic adjustment factors for vehicle class distribution and growth, monthly adjustment factors, and axles per truck were obtained and applied as per recommendations by Onyango et al., 2019 [59]. The statewide average linear growth factor of 1.34 % per year was applied as the truck growth factor for the state of Tennessee. These input data are provided in section 3.1 and Appendix A. AADTT was calculated based on 2023 base year traffic data provided.

Performances were run using MERRA climate data files existing in the software, together with those downloaded from the LTPP InfoPave website, with the latest climate data record being in December 2023. Water table depth information was obtained from sites closest to the pavement being analyzed from the National Water Information System Mapper (https://maps.waterdata.usgs.gov/mapper/index.html). Appendix A presents some of the input parameters used for analysis.

Results and Analysis

The AASHTOWare PMED software outputs pavement deterioration results in a manner that makes it easy to track in what year the pavement is expected to reach the distress threshold value that may warrant its maintenance. Figure 4.53 shows an example output indicating when the terminal IRI and total rut depth were reached for LTPP section 47-3108. It also indicates the value of the terminal distresses at the end of the analysis or design period.

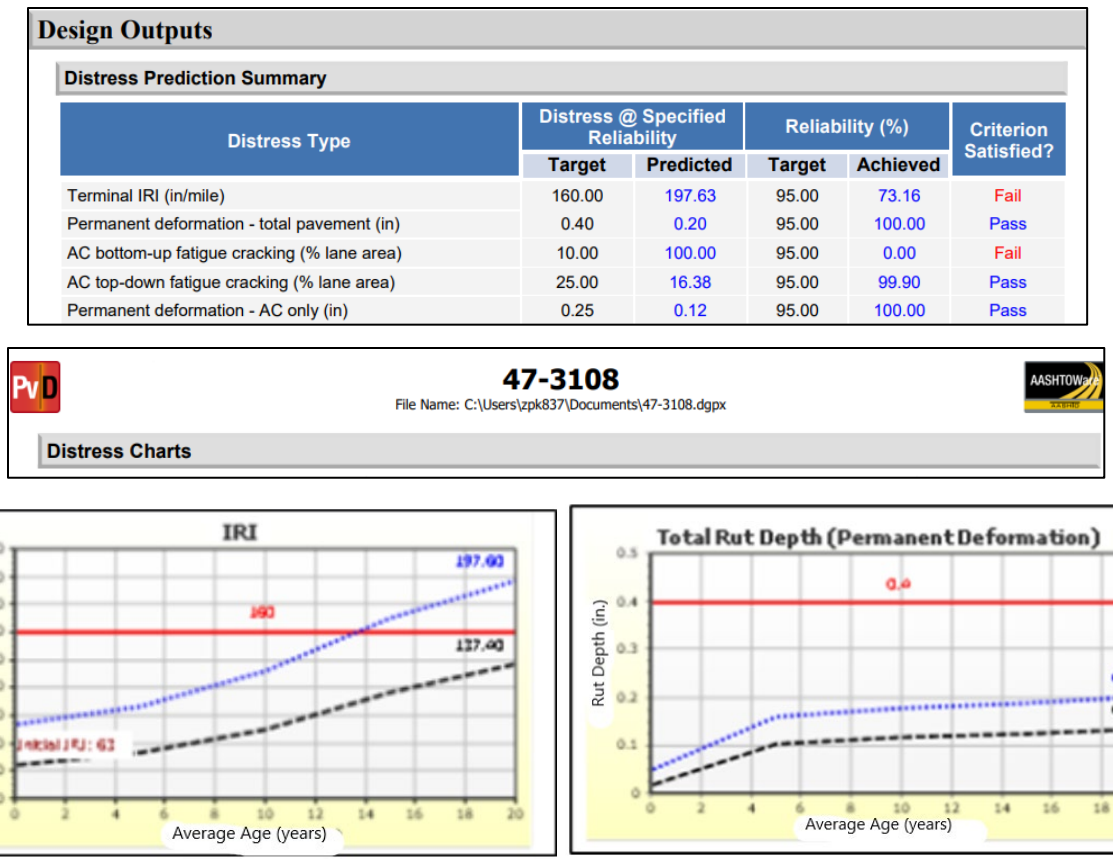

FIGURE 4-53 Predicted distresses for LTPP section 47-3108 (Red solid line: Threshold values Black broken lines: Values at 50% reliability. Blue broken lines: Values at 95% reliability)

Generally, the analyzed pavement sections exhibited satisfactory performance to the end of the expected service or design life with a failure below the set threshold for each distress. Tables 4.3 to 4.11 show the baseline performance analysis of the TDOT pavement sections across all four regions, using historical MERRA and NARR climate data files in Tennessee.

TABLE 4-3 Region 1 flexible pavement sections

Pavement Section	Climate scenarios	Terminal IRI (in/mile)	Total rutting (in)	AC bottom-up cracking (%)	AC top-down cracking (%)	AC rutting (in)
SR-62	Baseline	88.42	0.09	0.00	10.23	0.03
I-26	Baseline	78.98	0.09	0.00	12.96	0.03
SR-93	Baseline	85.70	0.07	0.00	6.01	0.02
SR-32	Baseline	121.55	0.15	2.21	16.07	0.08
SR-91	Baseline	80.67	0.05	0.00	4.69	0.02

TABLE 4-4 Region 1 composite pavement section

Pavement section	Climate scenarios	Terminal IRI (in/mile)	AC rutting (in)	AC bottom-up cracking (%)	AC top-down cracking (%)	JPCP transverse cracking (percent slabs)
I-275	Baseline	79.22	0.01	1.86	13.19	1.23

TABLE 4-5 Region 2 concrete pavement section

Pavement section	Climate scenarios	Terminal IRI (in/mile	Mean joint faulting (in)	JPCP transverse cracking (percent slabs)
SR-111 (Hamilton)	Baseline	132.56	0.12	5.12

TABLE 4-6 Region 2 Flexible pavement sections

Pavement Section	Climate scenarios	Terminal IRI (in/mile)	Total rutting (in)	AC bottom-up cracking (%)	AC top-down cracking (%)	AC rutting (in)
SR-74	Baseline	85.62	0.07	0.00	6.01	0.03
SR-52	Baseline	119.76	0.15	2.00	11.6	0.06
SR-462	Baseline	119.48	0.17	1.89	6.01	0.08
SR-392	Baseline	96.96	0.24	0.00	9.52	0.00
SR-58	Baseline	87.32	0.11	0.00	6.01	0.05
SR-68	Baseline	86.94	0.09	0.00	6.01	0.04
SR-111 (Sequatchie)	Baseline	122.41	0.14	0.00	15.25	0.07
SR-1	Baseline	93.75	0.17	0.00	12.6	0.09

TABLE 4-7 Region 3 flexible pavement sections

Pavement Section	Climate scenarios	Terminal IRI (in/mile)	Total rutting (in)	AC bottom-up cracking (%)	AC top-down cracking (%)	AC rutting (in)
SR-56 (1)	Baseline	91.35	0.16	0.00	6.01	0.00
SR-56 (2)	Baseline	89.13	0.10	0.00	6.01	0.04
SR-261	Baseline	89.04	0.11	0.08	6.01	0.03
SR-80	Baseline	88.10	0.10	0.00	6.01	0.03
SR-141 (Macon)	Baseline	87.41	0.08	0.14	6.01	0.02
SR-80	Baseline	87.33	0.08	0.00	6.01	0.02
SR-141 (Smith)	Baseline	88.68	0.13	0.00	6.01	0.00
SR-264	Baseline	92.39	0.18	0.00	6.01	0.00
SR-174	Baseline	88.82	0.10	0.00	6.01	0.03
SR-141 (Trousdale)	Baseline	83.29	0.11	0.00	4.69	0.03
SR-10 (Trousdale)	Baseline	86.95	0.08	0.00	6.01	0.02
SR-26	Baseline	88.60	0.10	0.00	6.01	0.03
SR-141 (Wilson)	Baseline	87.50	0.20	0.00	4.69	0.00

TABLE 4-8 Region 3 composite pavement section

Pavement section	Climate scenarios	Terminal IRI (in/mile)	AC rutting (in)	AC bottom-up cracking (%)	AC top-down cracking (%)	JPCP transverse cracking (percent slabs)
I-40 (Davidson)	Baseline	79.55	0.04	1.86	13.40	1.23

TABLE 4-9 Region 3 concrete pavement section

Pavement section	Climate scenarios	Terminal IRI (in/mile	Mean joint faulting (in)	JPCP transverse cracking (percent slabs)
SR-155	Baseline	207.93*	0.19*	3.53

Note: * The predicted values exceeded the distress threshold values at end of design life

TABLE 4-10 Region 4 flexible pavement sections

Pavement Section	Climate scenarios	Terminal IRI (in/mile)	Total rutting (in)	AC bottom-up cracking (%)	AC top-down cracking (%)	AC rutting (in)
I-40 (Benton)	Baseline 4	81.12	0.16	0.00	13.38	0.05
SR-5	Baseline 4	101.67	0.13	0.00	11.56	0.03
SR-15	Baseline	129.32	0.19	1.86	13.25	0.07
SR-43	Baseline	84.82	0.14	0.00	12.37	0.03
SR-14	Baseline	153.38	0.09	0.00	12.23	0.04

TABLE 4-11 Region 4 Composite pavement section

Pavement section	Climate scenarios	Terminal IRI (in/mile)	AC rutting (in)	AC bottom-up cracking (%)	AC top-down cracking (%)	JPCP transverse cracking (percent slabs)
I-55	Baseline	82.85	0.01	1.86	11.46	1.23

Results indicate that when using historical climate data files for analysis, all the in-service pavement sections within the four TDOT regions perform satisfactorily. This means that none of the distress threshold limits are exceeded during design life. The only exception is SR 155 in Region 3, Davidson County, that exceeded the threshold limits for Terminal IRI and mean joint faulting.

4.4.2 Comparison of Predicted Pavement Distresses using Historical Climate Data (Base Scenario) and Projected Climate Data

Climate projection has been a challenging task due to a lot of uncertainties, including human behavior in changing their environment. Many climate projection methods available cannot project future climate accurately, especially long-term projection. This is why pavement design uses historical climate data files for design purposes. This study used machine learning models to project the hourly MERRA climate data files to 20 years, from 2024 to 2044. These projected climate files were then used in AASHTOWare PMED, a pavement design software, to predict pavement distresses, which were then compared to those obtained using historical climate data files.

Moreover, machine learning climate data projection is a time-consuming undertaking. For instance, in this study, one station took over eight (8) hours to complete the prediction of all five climate data variables. Since there have not been many successful climate data projection models published, this research team opted to build climate projection models to fit the data. Furthermore, there was a challenge with AASHTOWare PMED. In 2025, PMED was updated to v3.0, which was not running like the previous models, and it took time to figure out the changes. Therefore, we have not been able to predict pavement distress using all the climate data points.

Seventeen (17) stations from Tennessee were analyzed and distresses were predicted before the AASHTOWare PMED upgrade to v3.0. All design parameters for each station were kept the same, and only climate data files were changed. Tables 4.11 to 4.17 show the predicted distresses using historical (baseline) and projected climate data files.

- Values in red indicate that there was an increase in pavement distress when projected climate data files were used.
- The PMED software underestimates JPCP transverse cracking and Alligator cracking (bottom-up fatigue cracking).

TABLE 4-12 Region 1 distresses using historical and projected climate data for flexible pavement sections

Pavement Section	Climate scenarios	Terminal IRI (in/mile)	Total rutting (in)	AC bottom-up cracking (%)	AC top-down cracking (%)	AC rutting (in)
SR-62 (Knox)	Baseline	123.09	0.18	2.53	15.27	0.08
	Projected	127.34	0.26	2.57	15.16	0.09
I-26 (Unicoi)	Baseline	120.75	0.11	1.9	16.25	0.04
	Projected	121.43	0.21	3.46	18.92	0.07
SR-93 (Greene)	Baseline	107.94	0.09	1.45	4.69	0.02
	Projected	110.00	0.14	3.49	5.32	0.02
SR-32 (Grainger)	Baseline	121.45	0.15	2.21	16.07	0.07
	Projected	122.49	0.17	2.47	17.49	0.09

TABLE 4-13 Region 1 distresses using historical and projected climate data for composite pavement sections

Pavement section	Climate scenarios	Terminal IRI (in/mile)	AC rutting (in)	AC bottom-up cracking (%)	AC top-down cracking (%)	JPCP transverse cracking (percent slabs)
I-275 (Knox)	Baseline	112.15	0.01	1.86	13.19	1.23
	Projected	112.49	0.01	1.86	13.41	1.23

TABLE 4-14 Region 2 distresses using historical and projected climate data for flexible pavement sections

Pavement Section	Climate scenarios	Terminal IRI (in/mile)	Total rutting (in)	AC bottom-up cracking (%)	AC top-down cracking (%)	AC rutting (in)
SR-52 (Clay)	Baseline	131.94	0.27	1.17	3.79	0
	Projected	132.49	0.36	1.17	12.26	0
SR-68 (Polk)	Baseline	127.35	0.08	1.17	3.79	0.03
	Projected	128.13	0.1	1.18	3.79	0.05
SR-111 (Sequatchie)	Baseline	132.11	0.26	1.17	3.79	0
	Projected	133.02	0.35	1.17	11.43	0

TABLE 4-15 Region 3 distresses using historical and projected climate data for flexible pavement sections

Pavement Section	Climate scenarios	Terminal IRI (in/mile)	Total rutting (in)	AC bottom-up cracking (%)	AC top-down cracking (%)	AC rutting (in)
SR-267 (Wilson)	Baseline	130.35	0.16	1.81	3.79	0.08
	Projected	137.46	0.2	36.33	10.28	0.1
SR-26 (Wilson)	Baseline	128.44	0.09	1.18	3.79	0.03
	Projected	128.45	0.12	1.98	6.82	0.04
SR 155 (Davidson)	Baseline	149.90	0.13	6.33	16.42	0.05
	Projected	152.00	0.15	34.42	16.47	0.07

TABLE 4-16 Region 3 distresses using historical and projected climate data for composite pavement sections

Pavement section	Climate scenarios	Terminal IRI (in/mile)	AC rutting (in)	AC bottom-up cracking (%)	AC top-down cracking (%)	JPCP transverse cracking (percent slabs)
I-40 (Davidson)	Baseline	113.37	0.04	1.86	13.40	1.23
	Projected	113.97	0.06	1.86	13.43	1.23

TABLE 4-17 Region 4 distresses using historical and projected climate data for flexible pavement sections

Pavement Section	Climate scenarios	Terminal IRI (in/mile)	Total rutting (in)	AC bottom-up cracking (%)	AC top-down cracking (%)	AC rutting (in)
I-40 (Benton)	Baseline	158.42	0.07	23.09	16.44	0.15
	Projected	163.00	0.09	52.42	16.47	0.17

TABLE 4-18 Region 4 distresses using historical and projected climate data for flexible composite pavement sections

Pavement section	Climate scenarios	Terminal IRI (in/mile)	AC rutting (in)	AC bottom-up cracking (%)	AC top-down cracking (%)	JPCP transverse cracking (percent slabs)
I-55 (Shelby)	Baseline	118.50	0.12	1.86	13.4	1.23
	Projected	118.72	0.21	1.86	13.43	1.23

The predicted distresses using historical and projected climate data files were statistically analyzed to evaluate any significant changes caused by the projected climate changes. Figures 4.54 to 4.58 show the plots of distress comparison.

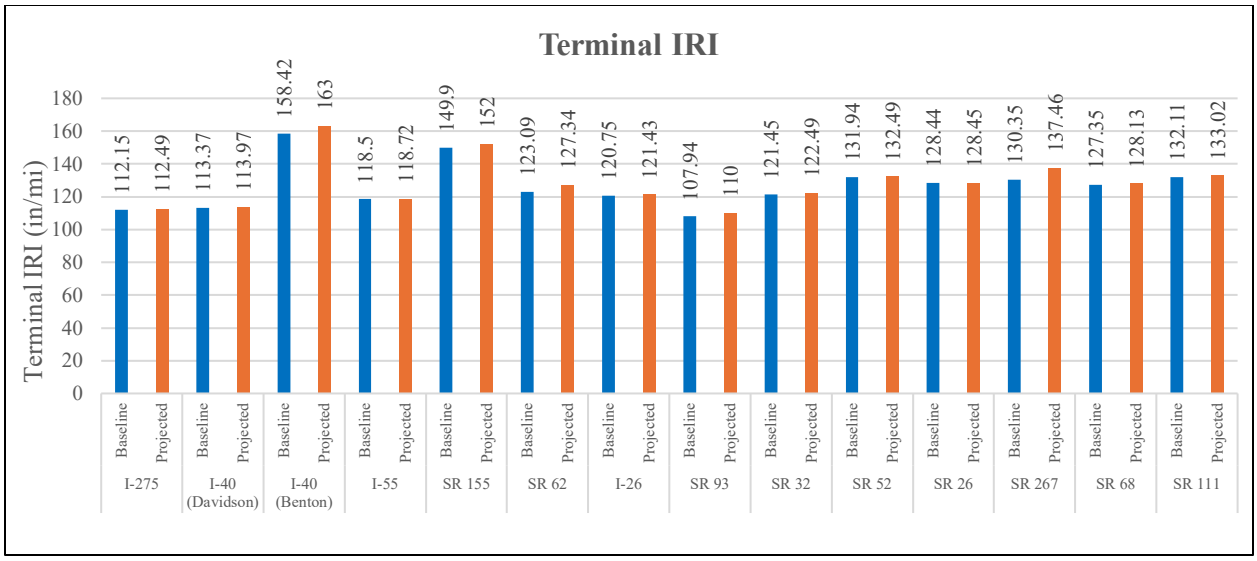

FIGURE 4-54 Comparison of Terminal IRI between baseline and projected climate data

From Figure 4.54 there is an average of 1.7 % increase in terminal IRI with projected climate data compared to baseline scenario for flexible pavements. A t-test for the mean difference was conducted at 95% confidence level. The null hypothesis H_0: $\mu D = 0$ (meaning that the difference between the means is not statistically significant): and alternative hypothesis H1: $\mu D \neq 0$ (meaning that the difference between the means is statistically significant). The decision rule is: Reject H_0 if $t > t_{n-1}$ or if $t < -t_{n-1}$; otherwise, do not reject H_0. The t-test indicated that the difference between the predicted terminal IRI means is not statistically significant. Meaning the projected climate data increases the terminal IRI but it is not statistically significantly different from the historical data, and the terminal IRI is still below the threshold at the end of the analysis period.

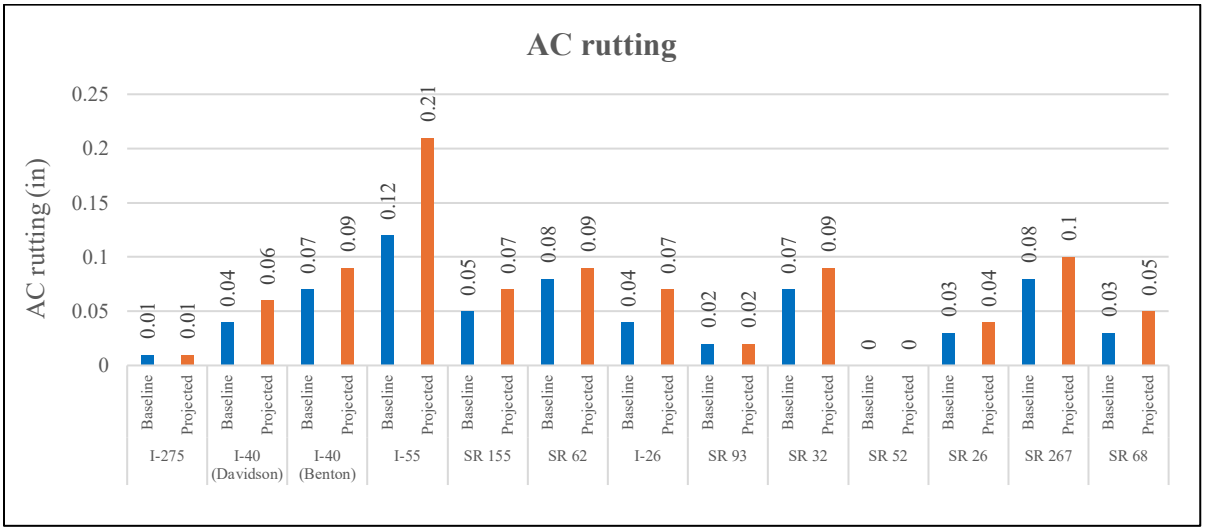

FIGURE 4-55 Comparison of AC rutting between baseline and projected climate data

From the analysis, AC rutting projected using climate data files showed an average increase of 27% as compared to historical climate data files (Figure 4.55). Like the terminal IRI, using the t-test at 95% confidence level, the difference between the predicted AC rutting means

is not statistically significant. Meaning higher AC rutting values with projected climate data is not statistically different from that with historical climate data. However, the increased AC rutting values are still below the threshold values.

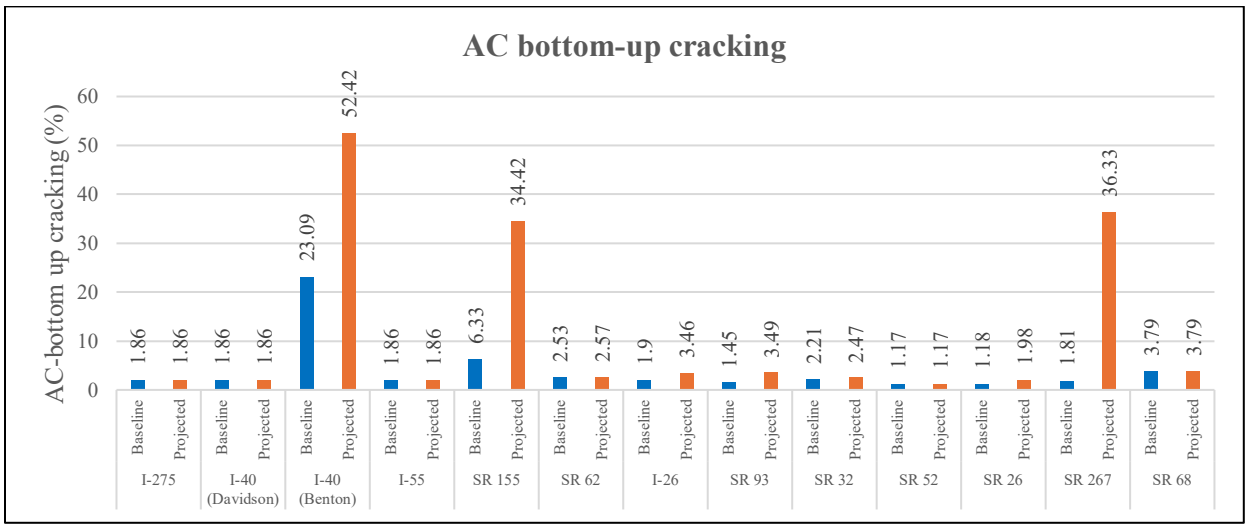

FIGURE 4-56 Comparison of AC bottom-up cracking between baseline and projected climate data

The AC bottom-up cracking (fatigue cracking) model is not calibrated, and its predictions (Figure 4.56) are not reliable when the validation test was performed. Three predictions showed extremely high cracking values. On average, the increase in bottom-up cracking is 219% because of the three extremely high cracking values, which is unrealistic. Excluding the three extreme values, the percent increase in distresses falls to 37%. The projected distress means difference is not statistically significantly different at 95% confidence level.

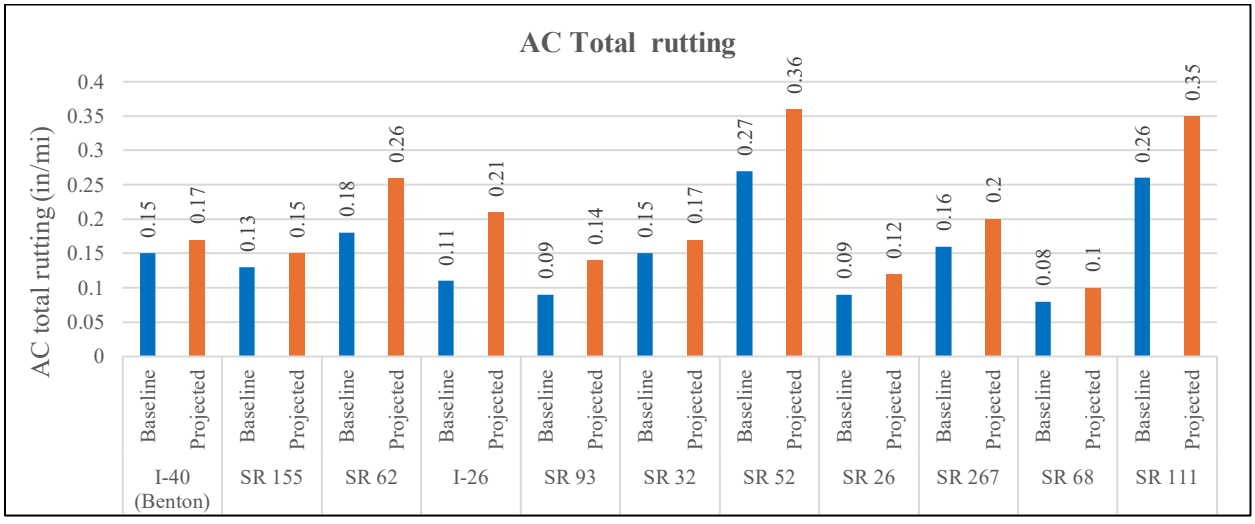

FIGURE 4-57 Comparison of AC total rutting between baseline and projected climate data

AC total rutting had an average increase of 36% with projected climate data files compared to historical climate data. Although the increase on rutting is seen on predicted distresses using projected climate data files, the distress means difference is not statistically significantly different at 95% confidence level. According to TDOT rating for state route rutting,

the predicted distresses at the end of the analysis period are at good to fair rating (< 0.2 good, 0.2 – 0.4 fair and >0.4 poor).

Only three sections were evaluated for jointed plain concrete pavement (JCPC). No change in distresses was observed between the historical and projected climate data files.

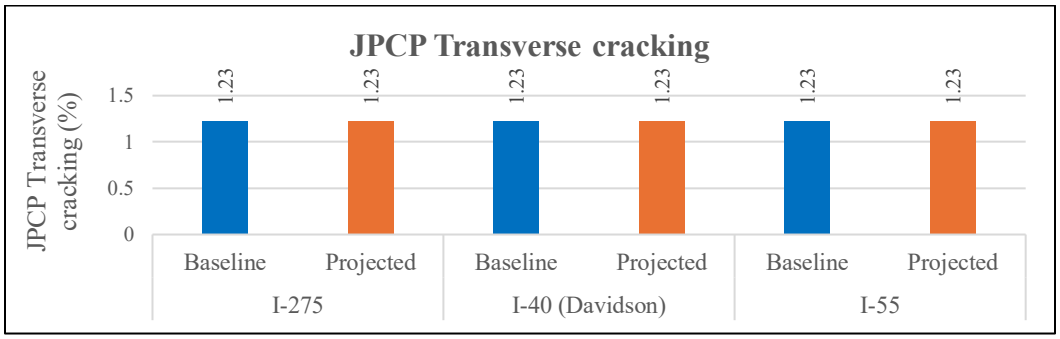

FIGURE 4-58 Comparison of JCPC transverse cracking between baseline and projected climate data

4.4.3 Section Summary

- Considering the historical data visualization, the Tennessee climate has been fluctuating with no specific trends. The machine learning projected climate data followed a similar trend, although a slight increase in temperature over the years was observed.
- The historical and projected climate data was used to predict distresses, and a statistical comparative analysis was performed to evaluate the differences observed.
- From the results, there was an increase in predicted distress values using projected climate data. The average increase in predicted distresses was 1.7% for terminal IRI, 36% for total rutting, 37% for bottom-up cracking, 29% for top-down cracking, and 27% for AC rutting. Although the increase is observed, statistical analysis showed that the difference is not statistically significant. Furthermore, at the end of the analysis period, the thresholds were not exceeded.
- For most of the pavement sections analyzed, the increase on distresses was observed, but the difference of means was not statistically significant, and the increase did not exceed the distress thresholds at the end of the analysis period (Figures 4.54 to 4.57).
- According to the visualization of historical climate data files, instances of extreme weather events in recent years may not have been captured on the climate data input files (Figures 4.21 and 4.22). Consequently, the machine learning algorithm may have not fully captured the climate inputs increase with high accuracy. As a result, the projected climate data does not deviate significantly from the historical records, leading to only minimal increases in predicted pavement distresses (Tables 4.12 to 4.18).
- In addition, the PMED software, like many pavement design methods, does not rely solely on extreme climate values when predicting pavement distresses. Instead, it processes the hourly climatic data from the input files by averaging the values, which are then used to estimate pavement performance over the specified design life. This averaging approach may also contribute to the minimal increases observed in projected pavement distresses.
- Few rigid pavements sections were analyzed, and the predicted distress increase with projected climate data files were not statistically significant.

Challenges:

- The climate projection took longer than expected since there are no climate projection models or methods that are readily available. The team had to use different models (LSTM, XGBoost, and NeuralProphet) to train the historical data. Of the three, NeuralProphet had a better response for long term projection, although it was not able to accurately capture the extreme climate data. After training the data set, projection of climate data took over 8 hours using super computers at UTC for each station. This delayed the project completion.
- PMED software was updated to version 3.0 in 2025. The new version (3.0 ran very differently from the previous version 2.6.2.2 and repeatedly generated errors, which the team initially believed were caused by the projected climate data. Extensive consultations with AASHTOWare PMED personnel and multiple modifications were required to adapt the projected climate data files to meet the software's input requirements.
- These challenges significantly delayed project progress, and before the analysis could be completed, the software license expired and was not renewed due to lack of funding. This led to distress prediction of only 17 stations with projected climate data.

4.5 Pavement Maintenance Recommendations

Pavement maintenance data was availed by TDOT for the four regions. Big data analytics methods were used to analyze the maintenance data given. The dataset used for this analysis is comprised of 121,541 pavement segments across four TDOT regions. Both numerical and categorical characteristics are among the factors chosen for analysis, with an emphasis on how they might affect ride quality and pavement roughness.

4.5.1 Structure of the Data

The data is comprised of 121,541 total observations, 19 total variables, and the key numerical variables include: IRI values (hr_iri_rt, hr_iri_lt, hr_hc_iri), Rut depths (hr_rut_rt, hr_rut_lt, hr_rutmaxl), Slope, PSI, speed, and segment mileage. Missing data is found in the hr_hc_iri column, where 26,606 values (approximately 22%) are missing.

4.5.2 Descriptive Statistic of Key Variables

Table 4.19 shows the descriptive statistics of key variables. From the table, the average IRI values (84 in./mi. for the right path and 77 in./mi. for the left) suggest fair ride quality, but high maximum values indicate the presence of severely deteriorated segments or outliers. The average Present Serviceability Index (PSI) is approximately 3.35, which is close to the acceptable condition criterion for many pavement systems. Although rutting numbers are generally low, unusual extreme numbers (such as 29.99 in) may indicate irregularities in the measurement or data entry. Most of the segments in the slope data are flat (median = 0%), but some have extreme gradients, indicating a very high variance.

4.5.3 Correlation Analysis of Pavement Condition Variables

The linear relationships (Figure 4.59) between the important pavement performance factors were assessed using a correlation analysis. The factors that have a strong correlation with pavement serviceability and ride quality were identified by the correlation matrix.

Variables associated with the IRI showed strong positive connections with one another (Figure 4.59). For instance, there is a 0.91 correlation between high-confidence IRI and right-wheel path roughness. Similarly, there is a 0.86 correlation between the roughness of the left

and right wheel paths, indicating symmetrical pavement behavior. There are significant negative correlations between the Present Serviceability Index and IRI values: -0.82 for the right wheel, -0.81 for the left wheel, and -0.91 for the high confidence. According to this, the serviceability index decreases as roughness increases.

TABLE 4-19 Descriptive statistics of key variables

Variable	Description	Mean	Std Dev	Min	25%	Median	75%	Max
hr_iri_rt	Roughness (Right IRI) [in/mi]	84.16	45.71	0.00	53.10	73.00	102.90	814.30
hr_iri_lt	Roughness (Left IRI) [in/mi]	77.16	40.58	0.00	50.50	67.30	92.40	851.60
hr_rut_rt	Rut Depth (Right) [in]	0.106	0.187	0.00	0.05	0.09	0.14	29.99
hr_rut_lt	Rut Depth (Left) [in]	0.157	0.359	0.00	0.07	0.11	0.16	4.15
hr_rutmaxl	Max Rut Depth (Left) [in]	0.317	0.414	0.00	0.01	0.23	0.38	7.32
hr_slope	Roadway Slope [%]	1.52	12.06	-19.00	0.00	0.00	0.00	99.00
hr_psi	Serviceability Index (PSI)	3.35	0.68	0.11	2.98	3.44	3.78	10.00
hr_speed	Speed [mph]	47.15	19.55	0.00	41.00	52.00	59.00	93.00
hr_hc_iri	High-Confidence IRI [in/mi]	63.09	36.56	0.00	40.50	55.80	78.00	697.00

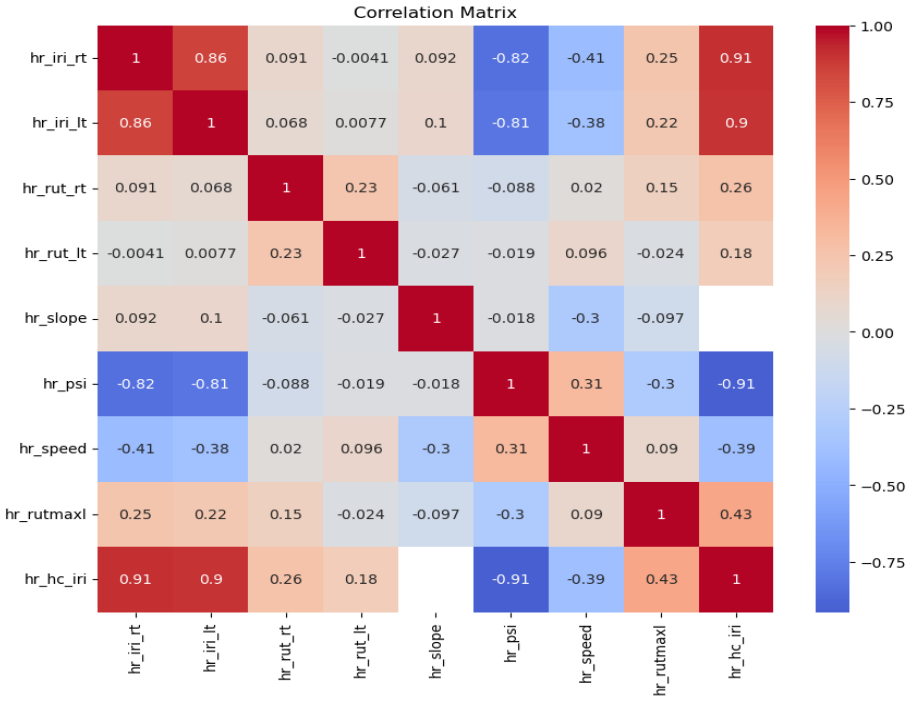

FIGURE 4-59 Correlation Matrix of pavement condition variables

4.5.4 Regression Analysis: Modeling Pavement Serviceability Index

A further analysis was carried out using an Ordinary Least Squares (OLS) regression model, developed to quantify how specific pavement surface features affect the Present Serviceability Index (PSI). The independent variables included in the model were: International Roughness Index (Right Wheel Path), Rut Depth (Right Wheel Path), and Roadway Slope. The

regression model (Figure 4.60) showed a strong match, accounting for roughly 68.3% of the variance in PSI (R^2 = 0.683). Every predictor variable had a p-value of less than 0.001, indicating statistical significance. The model coefficients are as explained below:

Intercept (`const`) = 4.3852: This is the baseline PSI when all predictors are zero.

`hr_iri_rt` = –0.0123: Each 1 in/mi increase in IRI reduces PSI by approximately 0.0123, highlighting the strong negative relationship between roughness and serviceability.

`hr_rut_rt` = –0.0345: Each inch of rutting reduces PSI by 0.0345, showing a modest negative impact.

`hr_slope` = +0.0032: A small positive coefficient suggests slightly higher PSI values in segments with more slope.

OLS Regression Results

Dep. Variable:	hr_psi	R-squared:	0.683
Model:	OLS	Adj. R-squared:	0.683
Method:	Least Squares	F-statistic:	8.711e+04
Date:	Sat, 28 Jun 2025	Prob (F-statistic):	0.00
Time:	08:35:52	Log-Likelihood:	-55851.
No. Observations:	121541	AIC:	1.117e+05
Df Residuals:	121537	BIC:	1.117e+05
Df Model:	3		
Covariance Type:	nonrobust		

	coef	std err	t	P>|t|	[0.025	0.975]
const	4.3852	0.002	1870.587	0.000	4.381	4.390
hr_iri_rt	-0.0123	2.43e-05	-508.051	0.000	-0.012	-0.012
hr_rut_rt	-0.0345	0.006	-5.832	0.000	-0.046	-0.023
hr_slope	0.0032	9.17e-05	35.390	0.000	0.003	0.003

Omnibus:	137686.778	Durbin-Watson:	1.620
Prob(Omnibus):	0.000	Jarque-Bera (JB):	16862093.662
Skew:	5.858	Prob(JB):	0.00
Kurtosis:	59.501	Cond. No.	518.

FIGURE 4-60 OLS regression analysis results

4.5.5 Pavement Condition Comparison by Region

Boxplots were used to compare the Present Serviceability Index (PSI) and right-wheel path roughness (IRI) across the four regions to evaluate regional differences in pavement quality (Figure 4.61).

From Figure 4.62, the median IRI values cluster between 70 and 90 in./mi., indicating a rather uniform distribution across regions (Figure 4.61a). With a greater number of extreme outliers and a broader interquartile range, Region 3 stands out, suggesting higher variability and rougher segments in some areas. Additionally, compared to Regions 1 and 2, Region 4 displays a marginally higher median and upper quartile, indicating more widespread roughness in that area.

Additionally, PSI values showed Regions 1 and 2 had the greatest median serviceability scores (around 3.5), suggesting generally better pavement conditions (Figure 4.61b). Like the roughness shown in the IRI distribution, Region 3 exhibits greater variation with a wider spread

and more low-end outliers. In general, Region 4 road segments have lower serviceability, as indicated by its lowest median and most noticeable low-end outliers.

While the overall differences are not drastic, the results suggest that Region 4 has the worst condition of the four regions and both Region 3 and Region 4 may require more targeted pavement maintenance due to greater roughness and lower serviceability in several segments.

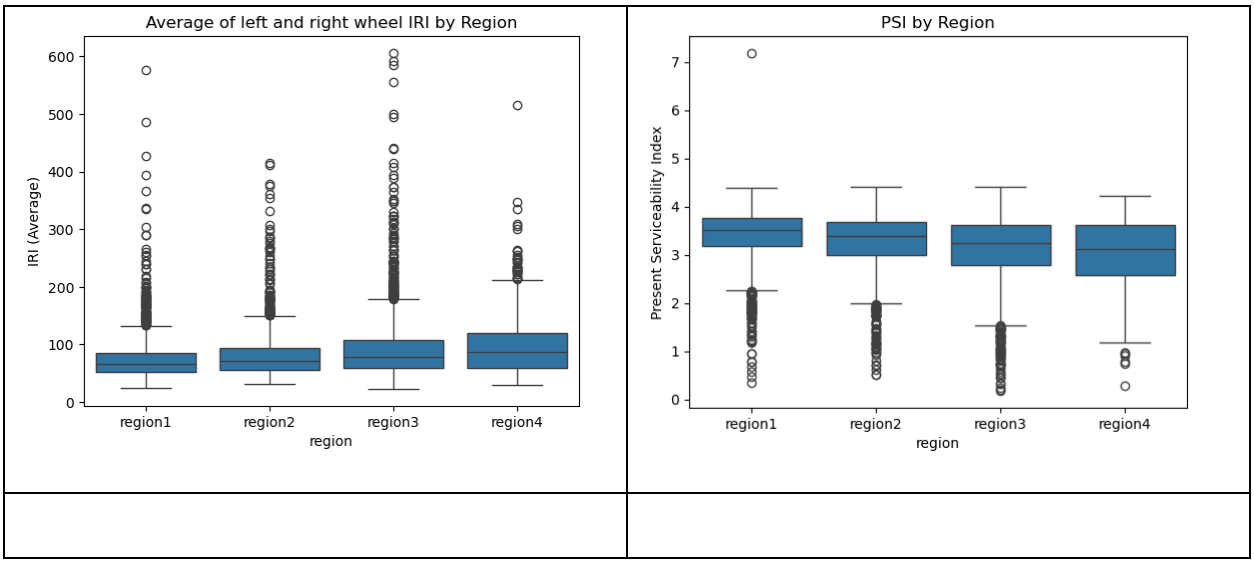

(a) (b)

FIGURE 4-61 Pavement condition analysis by region

4.5.6 Analysis of Pavement Distresses

The scatter plot (Figure 4.61) shows a significant inverse association between pavement serviceability (PSI) and right-wheel path roughness (IRI). Figure 4.61 shows that PSI decreases with increase with IRI, confirming that pavement section serviceability decreases with pavement roughness, among other factors. A nonlinear deterioration in serviceability with increasing roughness, particularly beyond 150 in./mi., is suggested by the curve-like pattern.

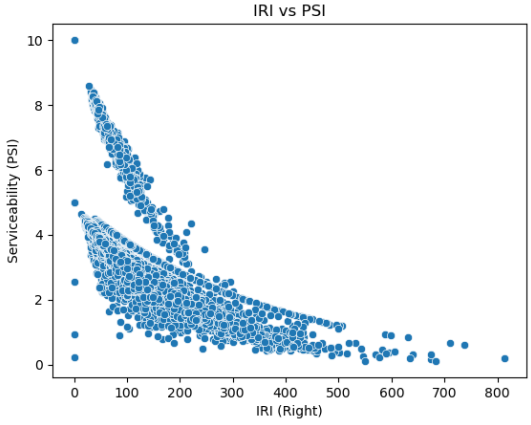

FIGURE 4-62 A scatter plot of IRI versus PSI

Further analysis was performed on the distresses where the state averages were calculated with respect to year 1 to year 30, for the three variables: IRI, rutting, and PSI. Generally, all three variables had averages below the trigger values, except year 7 for PSI and year 10 for rutting, which could be a data anomaly. (Figure 4.63).

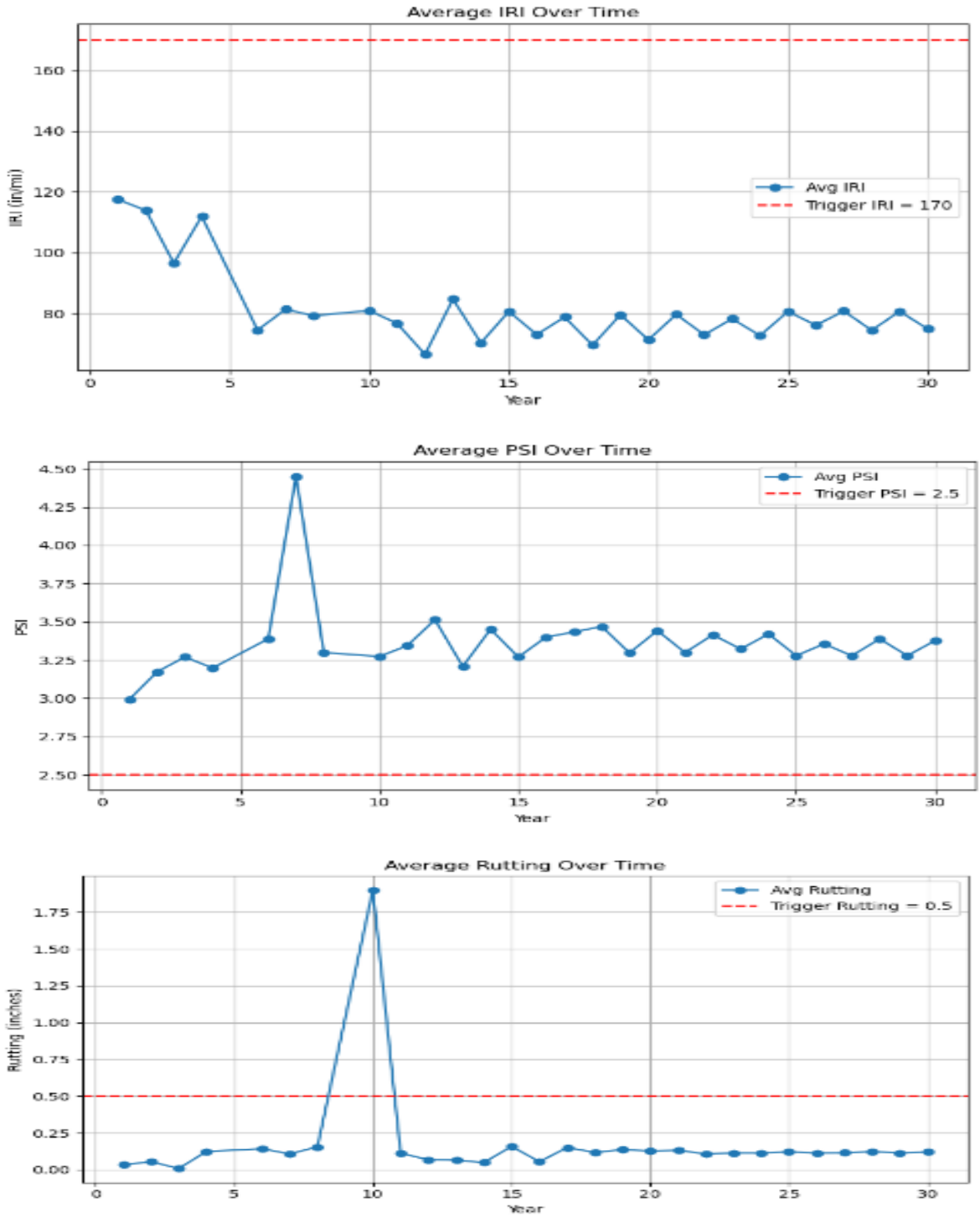

FIGURE 4-63 State averages for IRI, PSI and rutting

4.5.7 Section Summary

- The analysis of maintenance data for the state of Tennessee used more than 120,000 road segments to offer a thorough assessment of pavement conditions across the TDOT regions. The results showed that the most important element influencing pavement serviceability was IRI, which has a substantial negative association with PSI. This association was validated by the regression model, which accounted for more than 68% of the variation in PSI. Overall, the analysis supports using IRI and PSI as reliable indicators for prioritizing pavement management strategies and identifying segments requiring immediate attention.
- The predicted distresses using projected climate data showed an increase in the predicted distresses compared to historical data, although the increase did not reach or exceed the distresses thresholds. This calls for closer monitoring of climate change, bearing in mind the expected increase in distresses caused by climate change, among other factors.
- The research team planned to use PMED software to evaluate feasible maintenance strategies, if the distress increase was statistically significant.
- According to the maintenance data, TDOT is doing well with pavement maintenance having an average PSI of 3.35. Sections with higher IRI and lower PSI, especially in Regions 3 and 4, should be identified and maintenance planned as needed, which TDOT is already doing.
- Region 3 showed higher variability and segments with higher IRI values in some areas, and Region 4 displayed a marginally higher median and upper quartile, which indicated more widespread roughness in that area.
- On the IRI distribution, Region 3 exhibited greater variation with a wider spread and more low-end outliers. In general, Region 4 road segments have lower serviceability, as indicated by its lowest median and most noticeable low-end outliers.
- While the overall differences were not drastic, the results suggest that Region 3 and Region 4 may require more targeted pavement maintenance due to greater roughness and lower serviceability in several segments.

4.6 Chapter Summary

Chapter 4 presents results and data analysis, including data visualization, prediction model validation, climate data files projection, pavement performance analysis using both historical and projected climate data, and pavement maintenance. The following can be drawn from the results analysis:

1. The data visualization indicated that the historical data does not exhibit a specific trend that clearly describes the data for all five climate variables. The patterns were consistent over the years with peak values of temperature and precipitation occurring in different years for the four TDOT regions.
2. A further analysis with annual average temperature and precipitation indicated that both temperature and precipitation did not show a particular/definite trend. The last few years, 2016 to 2023, showed slightly elevated temperatures for all four regions, but the temperatures were consistent with the maximum annual average temperatures recorded in previous years. Peak temperatures were 98.06^{o}F in year 1988, 107.24^{o}F in 2012, 109.04^{o}F in 2012, and 110.12^{o}F in 2007, for Regions 1, 2, 3, and 4, respectively. Peak precipitations were 1.08 in./hr. in year 2022, 1.14 in./hr. in 1989, 1.28 in./hr. in 2023, and 1.46 in./hr. in 1994, for Regions 1, 2, 3, and 4, respectively. Regions 1 and 3 had peak precipitations in 2022 and 2023,

respectively, but they are not higher than the overall peak precipitation of 1.46 in/hr. in 1994. This observation may suggest a slight change in climate patterns; however, there is no definitive conclusion.

3. The validation of distress prediction models in PMED software indicated that IRI model predicted values are not statistically different from the measured values when using local coefficients for flexible pavements and default coefficients for rigid pavements. For total rutting, the differences between measured and predicted distress values were statistically significant, when both local (statewide) and global calibration coefficients were applied. Both default and local coefficients underestimated alligator cracking. Transverse cracking for rigid pavements was underestimated by the prediction model. This means that only IRI local (for flexible) and global (for rigid) coefficients predicted values statistically close to measured values.
4. Climate data projection utilized machine learning models to project the historical MERRA climate data for all five-climate data variables. The climate data was projected for twenty years (2024 – 2044), using NeuralProphet and LSTM machine learning models, whereas the XGBoost model did not produce predictions closely aligned with the historical values. The projected climate data was employed to predict pavement distresses and were then compared to pavement distresses predicted using historical climate data.
5. A better climate data projection model was obtained using a hybrid of Variational Autoencoder (VAE) with LSTM layers, in which the LSTM encoder is responsible for learning the sequential climate data (daily, monthly, and yearly cycles). Then, the decoder helped with reconstructing the values while keeping critical weather patterns. The hybrid model was able to capture the annual extremes better than the NeuralProphet. However, access to the PMED software was restricted as the software license expired and not renewed by the project sponsor. Since the project was ending, there was no budget for the PMED license renewal, hence distress predictions were not performed. However, it is believed that evaluating distress would have provided a better understanding of performance of the climate projection models.
6. A comparative analysis of distress between baseline and projected climate data scenarios was performed. The distress results indicated an increase in distresses with projected climate data files. However, the distress increase was not statistically significant and was below the thresholds at the end of the analysis period. While such findings suggest close monitoring of climate change impact on the pavement, no immediate changes to current standards is recommended. Furthermore, historical climate data can still be used to design pavements.
7. The analysis of the maintenance data provided by TDOT data indicated that IRI is more negatively correlated with PSI by 68%, meaning that PSI decreases with increase in IRI. The data also shows that most of the roads have PSI of about 3.35, which is an acceptable condition, but maintenance planning is still recommended to maintain the pavement in good condition. According to regional comparisons, Regions 1 and 2 had higher mean PSI and IRI compared to Regions 3 and 4. Region 4 had a lower overall performance, which indicated the need for focused maintenance, while Region 3 had more lower end outliers compared to other Regions. Identifying the problem sections and making strategic plans accordingly is recommended.
8. The projected climate indicated an increase in distresses, although it was not statistically significant. Likewise, the distresses did not exceed the threshold during the analysis period.

Although climate change was not captured by the hourly predictions, the projected weather patterns indicate increased critical weather parameters in recent years. As shown in Figure 4.64, the number of annual climate disasters for Tennessee increased from one event in 1980 to 11 events in 2023. Although the hourly climate data did not show a dramatic increase, it is evident from literature that weather and climate disaster events are becoming more frequent. Figure 4.64 shows a significant increase of severe storms and tropical cyclones in recent years in Tennessee. This requires a closer evaluation of events and strategically planning for pavement maintenance [11].

Some maintenance strategies may include:

I. Increasing PG binder grade in areas expecting higher temperatures. Higher temperatures soften asphalt when it is subjected to repeated traffic loading, becoming susceptible to rutting. On the other hand, lower temperatures make asphalt brittle, making it susceptible to thermal cracking. Increasing the performance grade of asphalt to withstand these extremes is a potential solution to overcoming distresses. One PG binder grade change is recommended for higher temperature (example from PG 64 -22 to PG 70 -22), while two PG binder grade changes are recommended for both temperature and high traffic (example from PG 64 -22 to PG 76 -22).

II. Severe storms, accompanied by heavy rainfall can lead to flooding, causing asphalt degradation, stripping, and portholes among other distresses. According to results from a study performed after Hurricane Katrina in Louisiana, rigid pavements were found to have less damage as compared to flexible pavements that were inundated during flooding. As a result, the use of rigid pavements in areas prone to flooding is recommended [14]. Likewise, subgrade stabilization may help and strengthen the subgrade to minimize effects of submerged subgrade

III. Drainage plays a critical role in the performance of pavements. In cases of high rainfall intensity, the key is to get water off pavements as fast as possible. This can be achieved in multiple ways:
    - Clearing out debris from drainage features in order to allow for efficient flow of water to prevent ponding and flooding of pavements
    - Increasing the capacity of water conveyance channels, such as culverts, to accommodate increased rainfall amounts
    - Incorporating more green infrastructure, such as bioswales and rain gardens, to reduce the quantity of water pooling or flooding in streets.

IV. Well compacted treated subgrades have a high modulus of elasticity, which have been proven to perform better under flooding events.

V. Open graded friction course (OGFC) pavements could be a problem when rainfall exceeds the holding capacity of the void spaces. The longer water stays in the voids, the more likely it may result in other problems like stripping and degradation due to freezing and thawing, which can compromise the structural integrity. Avoiding OGFC pavements in flood prone areas could be helpful to keep the pavement structure integrity.

VI. The installation of digital warning infrastructure on flood-prone sections is recommended to alert first responders and inform road users of closures and alternative safe routes, helping to prevent exposure to severe storms or flooding, hence saving lives.

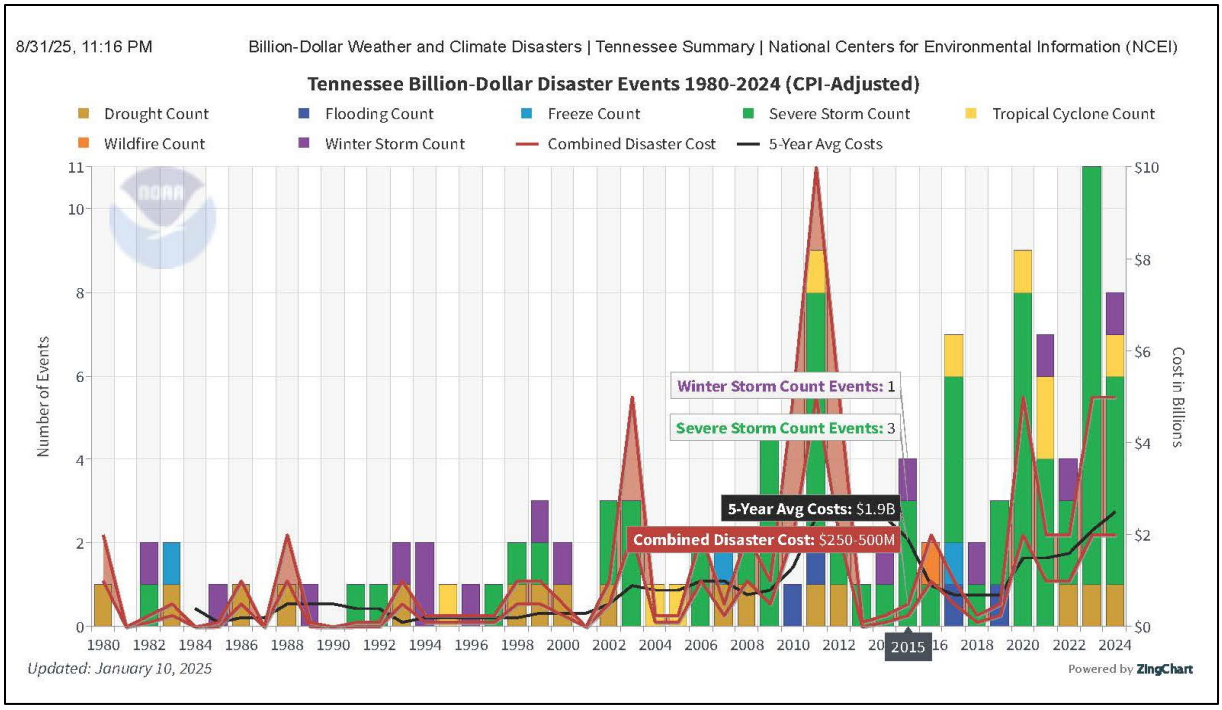

Figure 4-64 Billion-Dollar weather and climate disaster events for Tennessee in 1980 to 2024 **[11]**.

Chapter 5 Conclusion

This research study evaluated the effects of climate shifts on Tennessee pavements. The study analyzed selected pavement sections in Tennessee provided by TDOT. Two scenarios were evaluated for this study: the baseline scenario that used the historical climate data, and the projected climate data scenario that used 20-year machine learning projected climate data files. For each case, pavement distresses were predicted using AASHTOWare PMED software v2.6.2.2, with all variables held constant except the climate data files. A statistical comparative analysis was performed to assess the effect of climate change on pavement infrastructure.

Machine learning methods were used to predict future climate data inputs. Although the machine learning approach for climate data prediction was rigorous and time-consuming, it was chosen because it allowed the use of historical data to project future climate while formatting the data files to be compatible with the PMED software used for distress prediction. The North American Regional Climate Change Assessment Program (NARCCAP) developed methods to forecast temperature and rainfall for the US and Canada. These methods are promising as an attempt to quantify the future climate, but for this research the method needed downscaling of data to fit local conditions and formatting for PMED software climate data input. The downscaling methods are active research areas and require appropriate expertise to implement, hence it was not considered. Machine learning was a better approach since UTC has expertise in the Computer Science Department, and it is a fast-growing method for data processing and projections. Machine learning methods successfully projected future climate data inputs for 20 years from 2024 to 2044, which were used for pavement distress prediction.

Climate data visualization was performed to capture trends of climate data inputs over the years (1982 to 2023) and draw inferences. Hourly data was used for visualization of all five climate inputs, temperature, precipitation, wind speed, percent sunshine, and humidity. The results indicated that there was no clear trend on all the climate inputs. Temperature and humidity values showed a slight variation across all four regions, whereas percent sunshine remained nearly consistent in all four regions throughout the analysis period. Hourly precipitation for Region 1 was generally lower throughout the analysis period compared to other regions. Regions 3 and 4 showed a slightly higher hourly precipitation in recent years. Region 3 experienced the highest wind speeds, up to 20 mph, while Regions 1, 2, and 4 had wind speeds of less than 10 mph. Analysis was further performed using annual averages of temperature and precipitation to provide an in-depth understanding of the historical climate data trends. The results indicated no clear trend for both temperature and precipitation. Temperature visualization showed an increase in annual average temperatures from 2016 to 2023, being consistent with recorded maximum average annual temperatures. The ranges in 2016 to 2023 were from 57°F to 58.5°F for Region 1 (recorded minimum 53.5°F and maximum 58.5°F); 58°F to 60°F for Region 2 (recorded minimum 55°F and maximum 59.5°F); 58.5°F to 60.5°F for Region 3 (recorded minimum 55.5°F and maximum 60.5°F); and 59°F to 61°F for Region 4 (recorded minimum 57°F and maximum 61.5°F). Precipitation had no trend, but for Regions 3 and 4 it showed a slight increase in precipitation but did not exceed the annual average maximums recorded previously.

The distress prediction models on PMED software were validated using LTPP sections in Tennessee that had measured distress values available. Tennessee calibrated its prediction model coefficients using PMED version 2.2, and this project used version 2.6.2.2. Most of the distress prediction model coefficients have changed and improved. The thermal cracking prediction model for asphalt pavements is completely new and not calibrated for Tennessee. Validation of the prediction models gave an indication of reliability in the results. Three models were validated for flexible pavements (terminal IRI, alligator cracking, and total rutting) and two for rigid pavements (terminal IRI and transverse cracking), using local calibrated and global (software default) coefficients. On flexible pavements, the difference between predicted and measured values for IRI were not statistically significant when using local coefficients but were statistically significantly different when using global coefficients. Alligator cracking and total rutting were statistically significantly different with both local and global coefficients. Rigid pavements had a predicted terminal IRI that was not statistically significantly different with measured values using local coefficients, while the transverse cracking model was statistically significantly different from measured values. This shows that only terminal IRI predicted values were close to measured values and emphasizes the importance of local calibration of distress prediction models.

The comparative analysis of distresses predicted using historical and projected climate data files was performed using 39 pavement sections provided by TDOT, scattered over all 4 TDOT regions. Using t-test statistical method at 95 % confidence level, the analysis compared distresses predicted using historical and machine learning projected climate data. The results showed an increase in predicted distresses using projected climate data as follows: 1.7% for terminal IRI, 36% for total rutting, 37% for bottom-up cracking, 29% for top-down cracking, and 27% for AC rutting. Although the increase was observed, statistical analysis showed that the difference between distresses predicted using historical and projected climate data files is not statistically significant. Furthermore, the distresses at the end of the design/analysis period did not exceed the design thresholds. This could be attributed to the fact that projected climate used historical data and from the visualization there is no trend that shows a significant increase in climate data inputs in recent years, hence the projected data was trained in the same way.

Maintenance data was provided by TDOT for all four regions. From the data it is implied that TDOT has a great pavement management system since the average PSI for the state is 3.35, which is good. A strong negative correlation (68%) between PSI and IRI was observed: PSI decreases with increase in IRI. Further analysis indicated that Regions 1 and 2 had better performance with an average PSI of about 3.5. On the IRI distribution, Region 3 exhibited greater variation with a wider spread and more low-end outliers. In general, Region 4 road segments had lower serviceability, as indicated by its lowest median and most noticeable low-end outliers. While the overall differences were not drastic, the results suggested that Region 3 and Region 4 may require more targeted pavement maintenance due to greater roughness and lower serviceability in several segments.

The maintenance data indicated that TDOT has a good pavement management system, with regular data collection and maintenance strategies using pavement condition index. According to this study, the effect of climate shifts on Tennessee pavements is minimum and does not show immediate need to change design inputs on pavement infrastructure in Tennessee. However, evidence showed an increase in the number of climate and weather events

in Tennessee from one event in 1980 to 11 events in 2023, with the prevailing event being a severe storm. It is recommended for TDOT to identify areas that are prone to flooding and create evacuation routes in case of events, place instrumentation in the affected routes to alert first responders in case of severe storms, and post messages to road users to use alternative routes. TDOT should consider using concrete pavements on stubborn sections that are prone to severe flooding, since studies have indicated that concrete pavements perform better than flexible pavements in similar conditions. It is also recommended to stabilize the subgrade.

5.1 Benefits and Policy Implementation

The benefits of this research include:

1. The findings from this study indicated that there is an increase in distresses predicted using projected climate data files as compared to historical climate data, although the difference was not statistically significant and thresholds were not reached at the end of the analysis period. It is recommended to monitor for sustained change in climate inputs and weather events then change design parameters when triggered by actual climate input changes. This will enable TDOT to use more proactive design inputs, when needed, for efficient pavement design. Design inputs that could be changed when triggered include increasing binder PG by one grade in response to temperature change. When designing pavement sections prone to flooding or severe storms use poor to very poor drainage coefficients on AASHTO Guide for Design of Pavement Structures 1993, or if using PMED software reduce layer moduli by a certain percent to account for modulus loss on submerged pavement sections. Furthermore, provide stable pavement infrastructures like signs to account for strong winds.
2. There is no need for immediate change of design and maintenance parameters. Therefore, no immediate policy implementation changes are recommended.
3. From the results of this study, historical climate data can still be used successfully to design pavement infrastructures.
4. To quantify the capacity building needed to manage effects of climate change, DOTs should establish the status of present infrastructure against the current climate and predict the status of a future infrastructure under expected climate change. Moreover, TDOT should evaluate and document pavement infrastructure health after major weather events to quantify the damage. This will give a clear direction regarding design needs depending on the frequency of events and the amount of damage recorded.

5.2 Challenges and Limitations

Pavement analysis relied on data that was provided by TDOT or obtained from the LTPP database. The team assumed the data to be satisfactory for this analysis. The historical climate data (MERRA) are collected and managed by NASA. The accuracy of the data is established to be high and reliable. AASHTO has recommended using this data for pavement design and analysis. The team did not collect the data but cleaned the data to eliminate outliers and used the data as obtained, therefore, may not be conversant with errors on data collection and processing. Data cleaning was performed before using for analysis. The AASHTOWare PMED software was used for prediction of pavement distresses. As the project started the software was version 2.6.2.2, and at the end of the project the version was 3.0. The change of versions during the project created some issues with the distress prediction, including new distress prediction models, new

prediction coefficients, or different methods of running the data. This could be a source of error for data analyzed using different software versions. Other limitations include:

- Many of the MERRA climate stations adopted for this study were not situated at the precise location of the pavement being analyzed, even though they were the closest possible stations. Consequently, minor variations in climatic parameters could result in discrepancies in the predicted pavement distresses.
- Water table depth values incorporated in this study were obtained exclusively from active sites. However, given that some of these sites were considerably far from the location of the pavement under analysis, there is a significant possibility that the value may not accurately reflect the water table depth at the pavement's location. This could possibly be cause for discrepancies in the predicted distresses.
- The version of the PMED software used in this research study (version 2.6.2.2) had not yet been recalibrated to suit Tennessee conditions at the time of analysis. Subsequent investigations using a calibrated software version are expected to produce more accurate and reliable results. Nevertheless, predicted IRI values can be considered reliable based on the findings presented by M. Otieno in her thesis study [26].
- Climate data projection took a longer time than expected to get the models that correctly predicted the data. The NeuralProphet model worked well but could not correctly capture the extremes. In the end, a hybrid model was developed that captured temperatures and the extremes better, but this could not be used in distress prediction because the PMED license expired and was not renewed.
- After many trials, a hybrid model based on a Variational Autoencoder (VAE) with LSTM layers was developed. This model gave more promising results when compared to other models for long-term hourly temperature predictions from 2024 to 2044. But due to PMED software license issues, the projected results with this model were not tested.
- The analysis of the projected climate data was performed on 17 pavement sections using v2.6.2.2. The new PMED v3.0 had a lot of problems in predicting distress. After several consultations with AASHTOWare PMED personnel, the software worked, but it was close to the end of its licensure, which was not renewed by the project sponsor. Some of the projected data was not used to predict distresses.

5.3 Recommendations

Resilience in the design and maintenance of pavement infrastructure in Tennessee needs to be tailored to the most imminent climate threat in each area. According to this study, there is an increase in predicted distresses using projected climate data, but the difference from historical data is not statistically significant, and predicted distresses do not exceed the thresholds at the end of the design/analysis period. Even though there is no evidence of significant increase in climate data inputs from projected climate data, there is an indication of an increased number of events in recent years (Figure 4.64), which need to be closely monitored. Possible recommendations include:

- The projected climate inputs did not show statistically significant difference from historical climate input in terms of predicted distresses. Furthermore, the reported increase in the

number of severe weather occurrences (Figure 4.64) [11] is not clearly reflected in the MERRA climate data. The overall highest temperature in the state was in 2007 (110.12°F) and overall highest precipitation was in 1994 (2.05 in./hr.). Although Regions 1 and 3 had peak precipitation in 2022 (1.08 in./hr.) and 2023 (1.28 in./hr.), respectively, it did not exceed the state overall peak precipitation in 1994. This indicates that although the frequency of weather events has increased in recent years, the climate inputs have not exceeded the highest recorded values for the state. Therefore, designing for the long-term continuous effects of climate is more practical than isolating and considering extremes weather events only. However, the extreme weather events can be used to provide the design inputs for the given recurrence period. Therefore, historical data can still be used to design resilient pavement infrastructure.

- The validation of prediction models revealed that only IRI predicts distresses that are close to measured values for both flexible and rigid pavements. Other predicted distresses like fatigue cracking and rutting for flexible pavements and transvers cracking for rigid pavements were statistically significantly different from measured values at 95% confidence level. Given frequent revisions and enhancements of the PMED software, methods of making the local calibration or model validation procedure easier, such as automating the process, are recommended for local agencies looking to adopt the software. Currently, Tennessee may need to calibrate all models for PMED v3 and then keep the calibrated models and reject all future PMED changes if calibration/validation automation will be a challenge.
- Pavement design uses historical climate data because of complications and lack of available methods to project future climate inputs. For this study, the climate data projection used the NeuralProphet machine learning model on the yearly, weekly, and daily patterns, running it for 500 epochs for 2024–2044. However, the data suggested a gradual year-by-year increase in temperature. From the results, since the difference in distresses were not statistically significant, the use of historical climate data for pavement design can continue until the climate projection methods are perfected. With AI and machine learning, this future is not too far away. The hybrid model based on a Variational Autoencoder (VAE) with LSTM layers seems promising.
- From maintenance data provided by TDOT, Region 4 displayed the highest IRI compared to other regions, with marginally higher median and upper quartile, indicating more widespread roughness. Region 3 showed higher IRI variation in some areas and a wider spread and more low-end outliers. Sections with higher IRI and lower PSI, especially in Regions 3 and 4, should be identified and maintenance planned as needed, which TDOT is already doing. While the overall differences are not drastic, the results suggest that Region 3 and Region 4 may require more targeted pavement maintenance due to greater roughness and lower serviceability in several segments.

5.4 Deliverables

This study delivers a final report with research objectives, methodology used, results analysis, findings, and recommendations. Other deliverables are the manuscripts prepared, presented, and published as listed below. Three more publications are in the pipeline.

1. An outline of TDOT's existing pavement design and maintenance practices, material characterization, and recommendations.
2. Projected climate data files.
3. M. D. A. Otieno, "Validating the Empirical Distress Prediction Models Within the AASHTOWare Pavement Mechanistic-Empirical Design, using Tennessee Pavement Performance Data from the Long-Term Pavement Performance Database," Master's Thesis, University of Tennessee at Chattanooga, 2024.
4. M. Otieno, J. Bathi, M. Onyango. "Enhancing Stormwater Management: Climate Data Sources and Methodologies for Informed Decision-Making." World Environmental and Water Resources Congress, 2024. Milwaukee, Wisconsin, May, 2024 https://ascelibrary.org/doi/abs/10.1061/9780784485477.105
5. J. Bathi, M. Otieno, M. Onyango, J. Owino, I. Fomunung. "Climate Change and Pavement Performance: An Overview of Current Status and Research Approaches." World Environmental and Water Resources Congress, 2023. Henderson, Nevada, May, 2023. https://ascelibrary.org/doi/10.1061/9780784484852.071
6. A. Amiri, Y. Liang, M. Onyango. "Pioneering Climate Forecasting in Tennessee with LSTM-ANN Machine Learning Model". IEEE 21st International Conference on Smart Communities: Improving Quality of Life using AI, Robotics and IoT. Boca Raton, FL, USA. December 2023. https://ieeexplore.ieee.org/document/10374680 .

References

[1] Y. Qiao, A. R. Dawson, T. Parry, G. Flintsch, and W. Wang, "Flexible pavements and climate change: A comprehensive review and implications," *Sustainability,* vol. 12, no. 3, p. 1057, 2020.

[2] S. Sen, H. Li, and L. Khazanovich, "Effect of climate change and urban heat islands on the deterioration of concrete roads," *Results in Engineering,* vol. 16, p. 100736, 2022.

[3] W. Brink, H. Von Quintus, and L. F. Osborne Jr, "Updates to hourly climate data for use in AASHTOWare pavement mechanistic–empirical design," *Transportation Research Record,* vol. 2640, no. 1, pp. 11-20, 2017.

[4] N. Humphrey, "Potential impacts of climate change on US transportation," *TR news,* vol. 256, no. May, pp. 21-24, 2008.

[5] V. Masson-Delmotte *et al.*, "Climate change 2021: the physical science basis," *Contribution of working group I to the sixth assessment report of the intergovernmental panel on climate change,* vol. 2, no. 1, p. 2391, 2021.

[6] A. M. Stoner, J. S. Daniel, J. M. Jacobs, K. Hayhoe, and I. Scott-Fleming, "Quantifying the impact of climate change on flexible pavement performance and lifetime in the United States," *Transportation Research Record,* vol. 2673, no. 1, pp. 110-122, 2019.

[7] P. P. Gudipudi, B. S. Underwood, and A. Zalghout, "Impact of climate change on pavement structural performance in the United States," *Transportation Research Part D: Transport and Environment,* vol. 57, pp. 172-184, 2017.

[8] W. Meagher, J. S. Daniel, J. Jacobs, and E. Linder, "Method for evaluating implications of climate change for design and performance of flexible pavements," *Transportation research record,* vol. 2305, no. 1, pp. 111-120, 2012.

[9] K. E. Trenberth, "Changes in precipitation with climate change," *Climate research,* vol. 47, no. 1-2, pp. 123-138, 2011.

[10] Y. Qiao, A. Dawson, T. Parry, and G. F. Flintsch, "Quantifying the effect of climate change on the deterioration of a flexible pavement," in *Proceedings of the international conferences on the bearing capacity of roads, railways and airfields*, 2013, pp. 555-563.

[11] Adam B. Smith, "2023: A historic year of U.S. billion-dollar weather and climate disasters," vol. 2024, ed, January 8, 2024.

[12] R. M. Ashley, D. J. Balmforth, A. J. Saul, and J. Blanskby, "Flooding in the future–predicting climate change, risks and responses in urban areas," *Water Science and Technology,* vol. 52, no. 5, pp. 265-273, 2005.

[13] J. S. Kikstra *et al.*, "The IPCC Sixth Assessment Report WGIII climate assessment of mitigation pathways: from emissions to global temperatures," *Geoscientific Model Development,* vol. 15, no. 24, pp. 9075-9109, 2022.

[14] K. Gaspard, M. Martinez, Z. Zhang, and Z. Wu, "Impact of Hurricane Katrina on roadways in the New Orleans Area : technical assistance report," (in English), Tech Report 2007. [Online]. Available: https://rosap.ntl.bts.gov/view/dot/22259.

[15] Y. Qiao, G. W. Flintsch, A. R. Dawson, and T. Parry, "Examining effects of climatic factors on flexible pavement performance and service life," *Transportation research record,* vol. 2349, no. 1, pp. 100-107, 2013.

[16] K. Msechu, M. Onyango, W. Wu, and S. Udeh, "Sensitivity analysis of AASHTOWare PMED to climatic inputs and depth of water table," in *Advances in Materials and Pavement Performance Prediction II*: CRC Press, 2020, pp. 68-72.

[17] H. T. Yu, L. Khazanovich, M. I. Darter, and A. Ardani, "Analysis of concrete pavement responses to temperature and wheel loads measured from intrumented slabs," *Transportation Research Record,* vol. 1639, no. 1, pp. 94-101, 1998.

[18] J. Bathi, M. Otieno, M. Onyango, I. Fomunung, and J. Owino, "Climate Change and Pavement Performance: An Overview of Current Status and Research Approaches," in *World Environmental and Water Resources Congress 2023*, 2023, pp. 755-766.

[19] R. Li, C. W. Schwartz, and B. Forman, "Sensitivity of predicted pavement performance to climate characteristics," in *Airfield and Highway Pavement 2013: Sustainable and Efficient Pavements*, 2013, pp. 760-771.

[20] Y. Qiao, "Flexible Pavements and Climate Change. Impact of Climate Change on the Performance, Maintenance, and Life-cycle Costs of Flexible Pavements.," Department of Civil Engineering, The University of Nottingham, 2015.

[21] M. U. Khan, M. Mesbah, L. Ferreira, and D. J. Williams, "Estimating pavement's flood resilience," *Journal of Transportation Engineering, Part B: Pavements,* vol. 143, no. 3, p. 04017009, 2017.

[22] J. Powell. "CRCP roadways proved resilient after Hurricane Harvey – and states are taking note." https://www.equipmentworld.com/roadbuilding/article/14969093/crcp-roadways-proved-resilient-after-hurricane-harvey-and-states-are-taking-note?utm_source=daily&utm_medium=email&utm_content=05-10-2018&utm_campaign=Equipment+World&ust_id=7d2bc74cefb0415f270b9a30b57b461d (accessed June 25, 2024).

[23] X. Yang, Z. You, J. Hiller, and D. Watkins, "Sensitivity of flexible pavement design to Michigan's climatic inputs using pavement ME design," *International Journal of Pavement Engineering,* vol. 18, no. 7, pp. 622-632, 2017.

[24] M. Onyango, J. Owino, W. Wu, and K. Msechu, "MEPDG Climate Data Input for the State of Tennessee," Tennessee Department of Transportation, 2022.

[25] L. Khazanovich *et al.*, "Design and construction guidelines for thermally insulated concrete pavements," 2013.

[26] M. D. A. Otieno, "Validating the Empirical Distress Prediction Models Within the AASHTOWare Pavement Mechanistic-Empirical Design, using Tennessee Pavement Performance Data from the Long Term Pavement Performance Database," MS Civil Engineering, Civil and Chemical Engineering, University of Tennessee at Chattanooga, 2024.

[27] C. E. Zapata and W. N. Houston, *Calibration and validation of the enhanced integrated climatic model for pavement design*. Transportation Research Board, 2008.

[28] "North American Regional Reanalysis (NARR)." [Online]. Available: https://www.ncei.noaa.gov/products/weather-climate-models/north-american-regional.

[29] A. D. Kennedy, X. Dong, B. Xi, S. Xie, Y. Zhang, and J. Chen, "A Comparison of MERRA and NARR Reanalyses with the DOE ARM SGP Data," *Journal of Climate,* Research Article vol. 24, no. 17, pp. 4541-4557, 01 Sep 2011 2011, doi: 10.1175/2011jcli3978.1.

[30] G. E. D. I. M. E. BY F EDOR M ESINGER , E UGENIA K ALNAY, K ENNETH M ITCHELL , P ERRY C. S HAFRAN , *et al.*, "NORTH AMERICAN REGIONAL REANALYSIS," 2005. [Online]. Available: Challenge | OpenSky. (n.d.). https://opensky.ucar.edu/islandora/object/articles:10210.

[31] a. M. E. . Rogers, "NORTH AMERICAN REGIONAL REANALYSIS," 2004. [Online]. Available: https://www.e-education.psu.edu/meteo810/sites/www.e-education.psu.edu.meteo810/files/Images/Lesson5/narr_bams.pdf.

[32] J. G. Guidotti, September 3, 2013 1976. [Online]. Available: Guidotti, J. The National Aeronautics and Space Administration (NASA)/Goddard Space Flight Center (GSFC) sounding-rocket program. 1976]. June 1, 1976.
[33] R. K. Pachauri and A. Reisinger, *Climate change 2007: Synthesis report. Contribution of working groups I, II and III to the fourth assessment report of the Intergovernmental Panel on Climate Change*. IPCC, 2007.
[34] N. Nakicenovic *et al.*, "Special report on emissions scenarios," 2000.
[35] R. H. Moss *et al.*, "Towards new scenarios for analysis of emissions, climate change, impacts, and response strategies," 2008.
[36] D. P. Van Vuuren *et al.*, "The representative concentration pathways: an overview," *Climatic change,* vol. 109, pp. 5-31, 2011.
[37] North American Regional Climate Change Assessment Program. "About NARCCAP." https://www.narccap.ucar.edu/about/index.html (accessed May, 1, 2024).
[38] S. M. Piryonesi and T. El-Diraby, "Climate change impact on infrastructure: A machine learning solution for predicting pavement condition index," *Construction & building materials,* vol. 306, p. 124905, 2021, doi: 10.1016/j.conbuildmat.2021.124905.
[39] S.-J. Park and D.-K. Lee, "Prediction of coastal flooding risk under climate change impacts in South Korea using machine learning algorithms," *Environmental Research Letters,* vol. 15, no. 9, p. 094052, 2020.
[40] [Online]. Available: https://en.wikipedia.org/wiki/History_of_numerical_weather_prediction.
[41] I. Price *et al.*, "Probabilistic weather forecasting with machine learning," *Nature,* vol. 637, no. 8044, pp. 84-90, 2025/01/01 2025, doi: 10.1038/s41586-024-08252-9.
[42] L. M. a. C. Gillis, "History of Numerical weather predictions," 2013. [Online]. Available: https://www.vos.noaa.gov/MWL/dec_07/weatherprediction.shtml.
[43] A. Darwin, "Better Forecasting with NeuralProphet," 2023. [Online]. Available: https://www.journeyfurther.com/articles/better-forecasting-with-neuralprophet.
[44] O. Triebe, "NeuralProphet:Explainable Forecasting at scale," 2021. [Online]. Available: arXiv:2111.15397
[45] "Long Short Term Memory." https://www.geeksforgeeks.org/deep-learning-introduction-to-long-short-term-memory/ (accessed.
[46] "Long Short term Memory," in *Long Short Term Memory*, ed, 2022.
[47] M. Ghislieri, Cerone, G.L., Knaflitz, M. , "LSTM Recurrent Neural Network " 2021. [Online]. Available: Ghislieri, M., Cerone, G.L., Knaflitz, M. et al. Long short-term memory (LSTM) recurrent neural network for muscle activity detection. J NeuroEngineering Rehabil 18, 153 (2021). https://doi.org/10.1186/s12984-021-00945-w.
[48] "XGBoost," in *XGBoost*, ed, 2014.
[49] C. G. Tianqi Chen, "XGBoost: A Scalable Tree Boosting System," 2016. [Online]. Available: https://dl.acm.org/doi/pdf/10.1145/2939672.2939785.
[50] A. Hachcham, "XGBoos: Everythig You Need to Know," ed, 2024.
[51] "Transformer (deep learning architecture)," 25 August 2019. [Online]. Available: Wikipedia contributors. (2025, June 19). Transformer (deep learning architecture). Wikipedia. https://en.wikipedia.org/wiki/Transformer_(deep_learning_architecture).
[52] H. S. Amjad Issa, Mohammad Ghanim, "Predicting pavement condition index using artificial neural networks approach," 2021. [Online]. Available: Issa, A., Samaneh, H., & Ghanim, M. (2021). Predicting pavement condition index using artificial neural networks approach. Ain Shams Engineering Journal, 13(1), 101490. https://doi.org/10.1016/j.asej.2021.04.033.

[53] R. Oyediji, D. Lu, and S. L. Tighe, "Impact of flooding and inundation on concrete pavement performance," *International Journal of Pavement Engineering,* vol. 22, no. 11, pp. 1363-1375, 2021.
[54] M. D. Meyer, M. Flood, C. Dorney, K. Leonard, R. Hyman, and J. Smith, "Climate change and the highway system: Impacts and adaptation approaches," *Task,* vol. 2, pp. 20-83, 2010.
[55] Tennessee Department of Transportation Materials and Test Division, *PAVEMENT DESIGN GUIDE*. May 2025.
[56] H. Gong, B. Huang, X. Shu, and S. Udeh, "Local calibration of the fatigue cracking models in the mechanistic-empirical pavement design guide for Tennessee," *Road Materials and Pavement Design,* vol. 18, no. sup3, pp. 130-138, 2017.
[57] American Association of State Highway and Transportation Officials, *Mechanistic Empirical Pavement Design Guide: A Manual of Practice*, Third ed. United States of America, 2020.
[58] C. Zhou, B. Huang, X. Shu, and Q. Dong, "Validating MEPDG with Tennessee pavement performance data," *Journal of Transportation Engineering,* vol. 139, no. 3, pp. 306-312, 2013.
[59] M. Onyango, J. Owino, I. Fomunung, and W. Wu, "Traffic Data Input for Mechanistic Empirical Pavement Design Guide (MEPDG) for Tennessee," Tennessee Department of Transportation, 2019.
[60] U.S. Department of Transportation Federal Highway Administration. LTPP InfoPave [Online] Available: https://infopave.fhwa.dot.gov/
[61] "The application of NeuralProphet," 2023. [Online]. Available: https://www.researchgate.net/publication/373146220_The_application_of_Neural_Prophet_Time_Series_in_predicting_rice_stock_at_Rice_Stores.
[62] "NeuralProphet for weather prediction." [Online]. Available: https://towardsdatascience.com/in-depth-understanding-of-neuralprophet-through-a-complete-example-2474f675bc96/.

Appendices

APPENDIX A: Pavement Design Input Parameters

Table A1: Local calibration coefficients for flexible pavements [56]

136 *H. Gong* et al.

Table 2. Summarisation of the local calibration coefficients.

Model	C_1	C_2	C_3
Alligator cracking	1.023	0.045	6000
Longitudinal cracking	6.44	0.27	204.54
Rutting	$\beta_{r1} = 0.111$	$\beta_{BS} = 0.196$	$\beta_{SG} = 0.722$
IRI (national defaults)	SF = 0.015; Total cracking = 0.400; TC = 0.0080; RD = 40.0		

Note: The rutting model was calibrated by Zhou et al. (2013).

Table A2: Design criteria or threshold values recommended for use in judging the acceptability of a trial design [57]

Table 7-1. Design Criteria or Threshold Values Recommended for Use in Judging the Acceptability of a Trial Design

Pavement Type	Performance Criteria	Threshold Value at End of Design Life
AC pavement and overlays	Alligator cracking (AC bottom-up cracking)	Interstate: 10% lane area Primary: 20% lane area Secondary: 35% lane area
	Total rut depth (permanent deformation in wheel paths)	Interstate: 0.40 in. Primary: 0.50 in. Others (<45 mph): 0.65 in.
	Transverse cracking length (thermal cracks)	Interstate: 500 ft/mi Primary: 700 ft/mi Secondary: 700 ft/mi
	IRI (smoothness)	Interstate: 160 in./mi Primary: 200 in./mi Secondary: 200 in./m
JPCP new, CPR, and overlays	Mean joint faulting	Interstate: 0.15 in. Primary: 0.20 in. Secondary: 0.25 in.
	Percent transverse slab cracking	Interstate: 10% Primary: 15% Secondary: 20%
	IRI (smoothness)	Interstate: 160 in./mi Primary: 200 in./mi Secondary: 200 in./mi

Tabel A3: Number of Axles per Truck [59]

Table 4. 9: Number of Axles per Truck

Vehicle Class	Single	Tandem	Tridem	Quad
4	1.43	0.57	0	0
5	2.16	0.02	0	0
6	1.02	0.99	0	0
7	1.26	0.2	0.63	0.15
8	2.62	0.49	0	0
9	1.27	1.86	0	0
10	1.09	1.15	0.79	0.05
11	4.99	0	0	0
12	3.99	1	0	0
13	1.59	1.26	0.69	0.31

Tabel A4: Leve l 2 Vehicle Distribution Values [59]

Month	Class 4	Class 5	Class 6	Class 7	Class 8	Class 9	Class 10	Class 11	Class 12	Class 13
January	0.94	0.99	0.77	0.6	0.79	0.93	0.78	0.72	0.77	0.58
February	0.96	1.05	0.84	0.64	0.87	1.03	0.87	0.82	0.83	0.73
March	1.08	1.04	0.95	0.82	1.03	1.07	1.13	0.86	0.93	1.07
April	1.04	1.02	1.01	0.95	1.1	1.04	0.94	0.84	0.96	1.05
May	0.93	0.96	1.02	1.01	1.05	0.99	0.98	0.85	0.98	1.02
June	0.93	0.96	1.11	1.11	1.05	1.01	1.01	0.97	0.97	1.08
July	0.94	0.88	1	1.19	1.02	0.92	1.13	1.04	0.97	0.98
August	0.93	0.92	1.1	1.27	1.09	0.99	1.06	1.05	0.97	1.17
September	0.99	0.96	1.19	1.02	1.02	1.05	1.25	1.27	1.1	1.12
October	1.11	1.06	1.17	1.24	1.1	1.06	0.99	1.22	1.17	1.15
November	1.07	1.07	0.98	1.19	1	0.98	0.94	1.14	1.17	1.03
December	1.08	1.09	0.86	0.96	0.88	0.93	0.92	1.22	1.18	1.02

Table A5: List of Tennessee pavement sections by Region

	REGION 1			
SN	**Road**	**Functional class**	**Pavement type-Lane mile analyzed**	**County (County no)**
1	I-275	11- Urban Interstate	Composite- LM 0.71-0.94	Knox (47)
2	SR 62	14- Urban Principal Arterial	Flexible- LM 1.69-6.96	Knox (47)
3	I-26	11- Urban Interstate	Flexible- LM 2.19-5.81	Unicoi (86)
4	SR 93	06- Rural Minor Arterial	Flexible- LM 8.00-18.18	Greene (30)
5	SR 32	02- Rural Principal Arterial	Flexible- LM 5.83-7.25	Grainger (29)
6	SR 91	07- Rural Major Collector	Flexible- LM 12.82-16.00	Carter (10)
	REGION 2			
7	SR 74	16- Urban Minor Arterial	Flexible- LM 11-11.96	Bradley (06)
8	SR 52	02- Rural Principal Arterial	Flexible- LM 20.58-23.47	Clay (14)
9	SR 462	16- Urban Minor Arterial	Flexible- LM 0.00-2.05	Cumberland (18)
10	SR 392	16- Urban Minor Arterial	Flexible- LM 2.79-5.79	Cumberland (18)
11	SR 111	02- Rural Principal Arterial	Concrete- LM 0.90-1.05	Hamilton (33)
12	SR 58	16- Urban Minor Arterial	Flexible- LM 1.53-2.12	Hamilton (33)
13	SR 68	06- Rural Minor Arterial	Flexible- LM 0.00-4.83	Polk (70)
14	SR 111	02- Rural Principal Arterial	Flexible- LM 4.33-7.59	Sequatchie (77)
15	SR 1	02- Rural Principal Arterial	Flexible- LM 18.5-20.00	Warren (89)

	REGION 3			
16	I-40	11- Urban Interstate	Composite- LM 20.56-21.37	Davidson (19)
17	SR 155	12- Urban Freeway	Concrete- LM 16.81-16.86	Davidson (19)
18	SR 56	06- Rural Minor Arterial	Flexible- LM 11.90-12.00	Macon (56)
19	SR 56	07- Rural Major Collector	Flexible- LM 5.90-6.05	Macon (56)
20	SR 261	07- Rural Major Collector	Flexible- LM 2.16-2.43	Macon (56)
21	SR 10	07- Rural Major Collector	Flexible- LM 7.57-7.61	Macon (56)
22	SR 80	06- Rural Minor Arterial	Flexible- LM 0.00-0.40	Macon (56)
23	SR 141	07- Rural Major Collector	Flexible- LM 4.90-5.53	Macon (56)
24	SR 80	06- Rural Minor Arterial	Flexible- LM 6.80-7.20	Smith (80)
25	SR 141	07- Rural Major Collector	Flexible- LM 5.30	Smith (80)
26	SR 264	07- Rural Major Collector	Flexible- LM 12.20	Smith (80)
27	SR 174	07- Rural Major Collector	Flexible- LM 34.78-34.85	Sumner (83)
28	SR 141	07- Rural Major Collector	Flexible- LM 2.60	Trousdale (85)
29	SR 10	06- Rural Minor Arterial	Flexible- LM 11.80	Trousdale (85)
30	SR 26	16- Urban Minor Arterial	Flexible- LM 7.00	Wilson (95)
31	SR 265	16- Urban Minor Arterial	Flexible- LM 0.30	Wilson (95)
32	SR 141	07- Rural Major Collector	Flexible- LM 17.30-17.35	Wilson (95)
33	SR 267	07- Rural Major Collector	Flexible- LM 9.50-10.50	Wilson (95)
	REGION 4			
34	I-40	01- Rural Interstate	Flexible- LM 7.20-8.10	Benton (03)
35	SR 5	02- Rural Principal Arterial	Flexible- LM 7.70-7.82	Gibson (27)
36	SR 15	02- Rural Principal Arterial	Flexible- LM 15.08-18.16	Hardeman (35)
37	SR 43	02- Rural Principal Arterial	Flexible- LM 0.00-0.25	Madison (57)
38	I-55	11- Urban Interstate	Composite- LM 3.10-3.21	Shelby (79)
39	SR 14	02- Rural Principal Arterial	Flexible- LM 2.27-4.06	Tipton (84)

APPENDIX B: Data Visualization for Historical Climate Data Files

The following figures show the visualization of climate data for different MERRA stations. Color codes: Blue- Temperature, Green- Wind speed, Orange- Percent Sunshine, Red- Precipitation, Purple- Humidity. The number below each plot is the station that was analyses.

Region 1

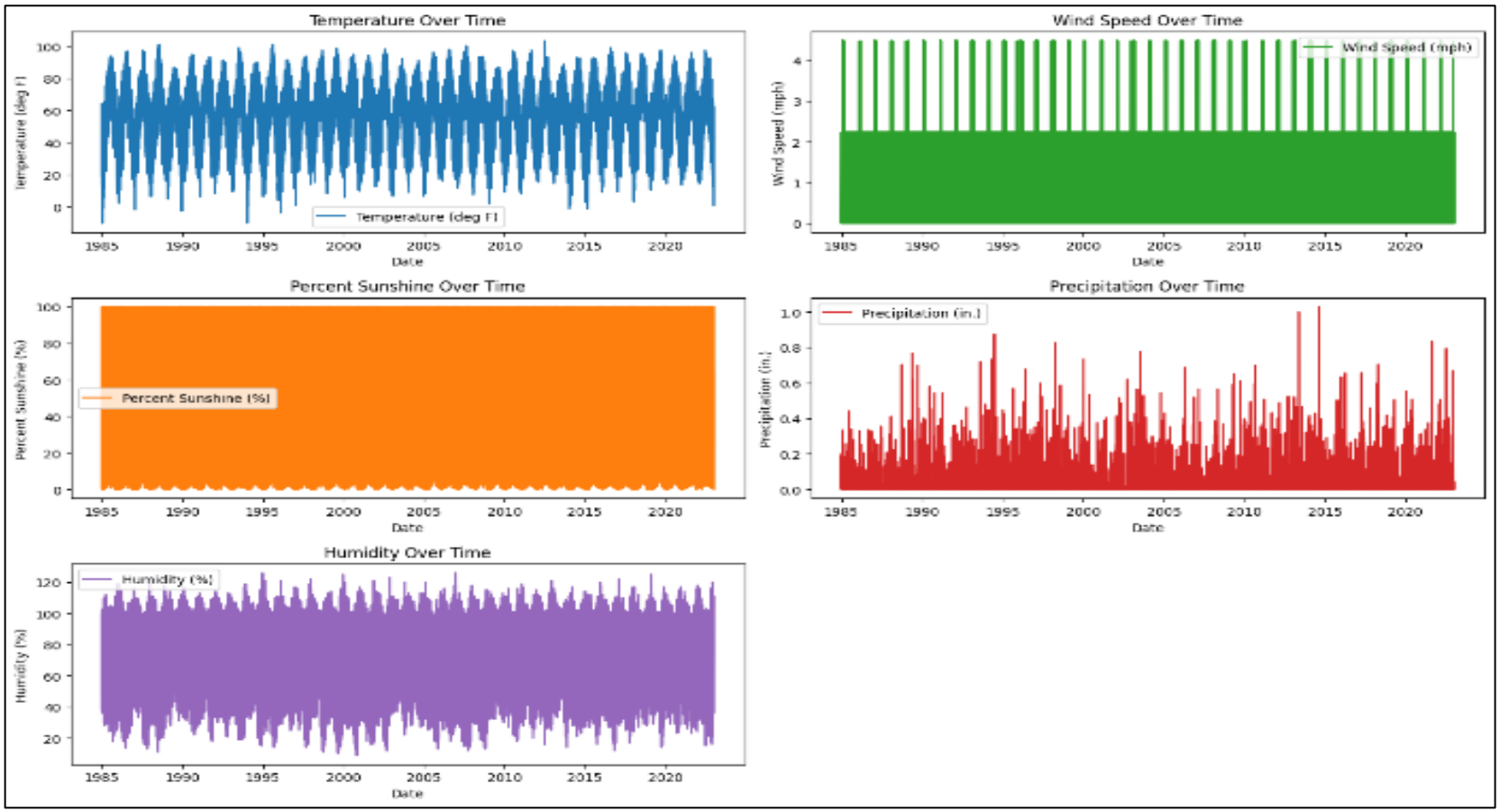

Station 140124

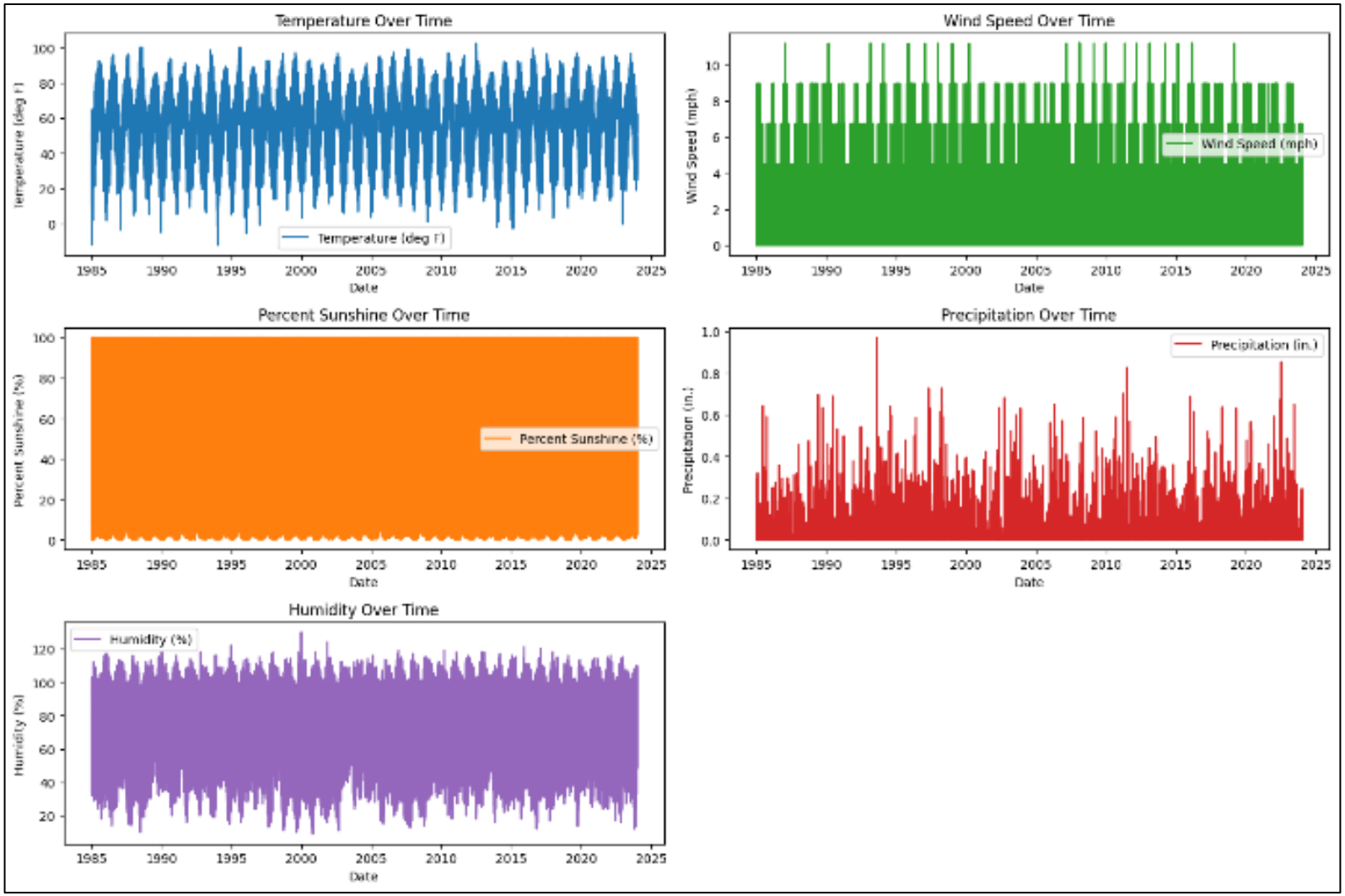

Station 140125

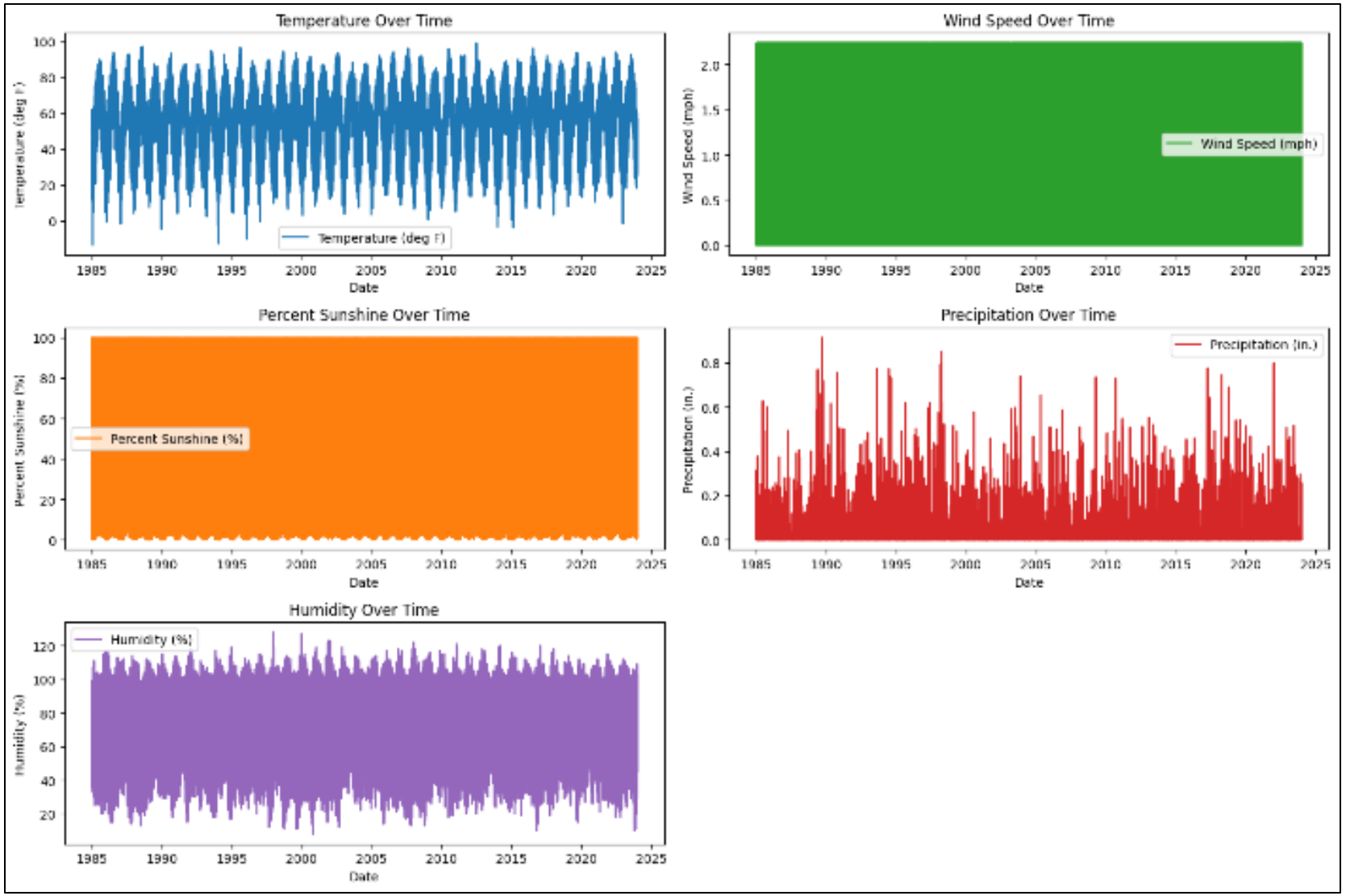

Station 139549

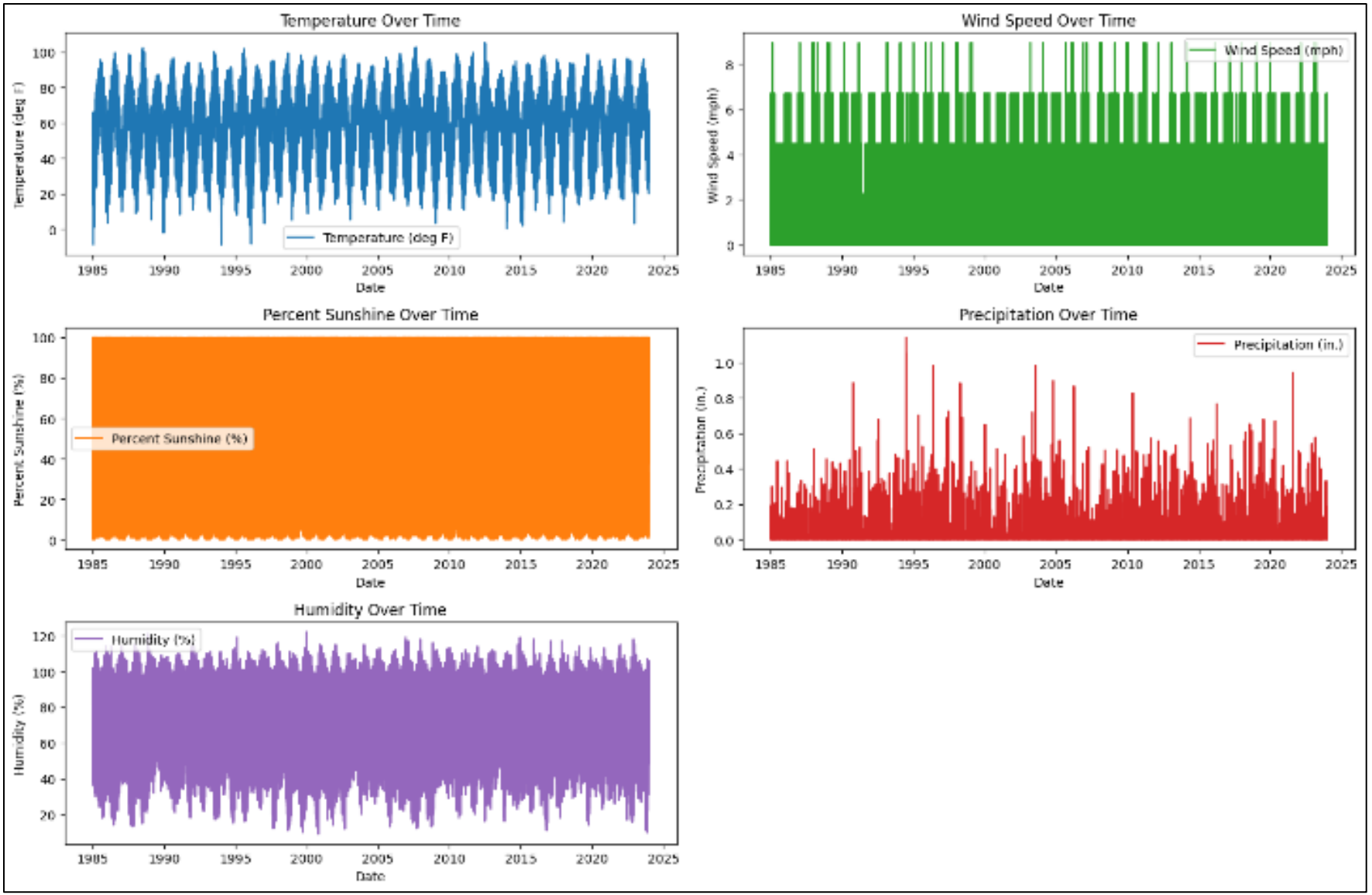

Staton 139547

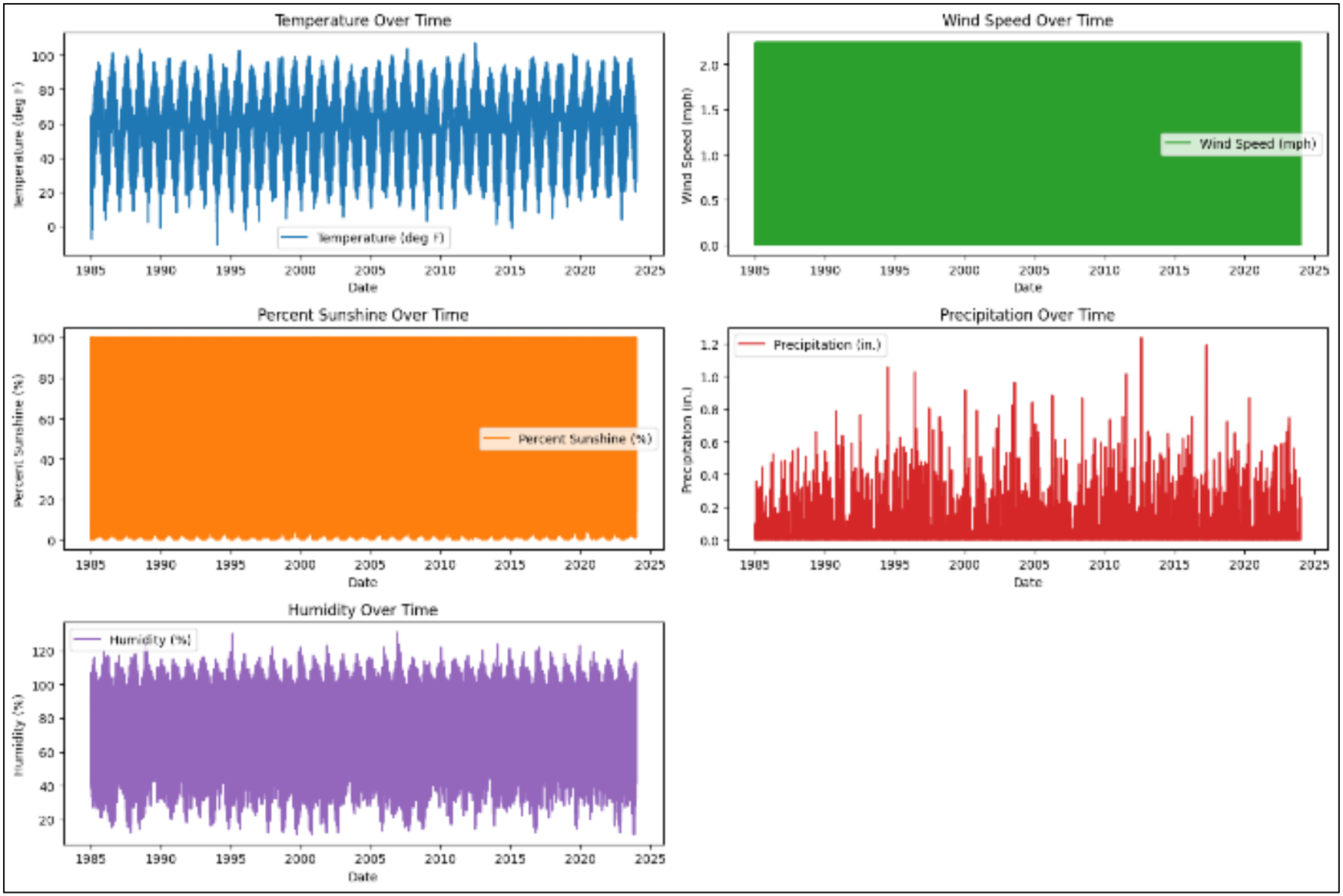

Station 139546

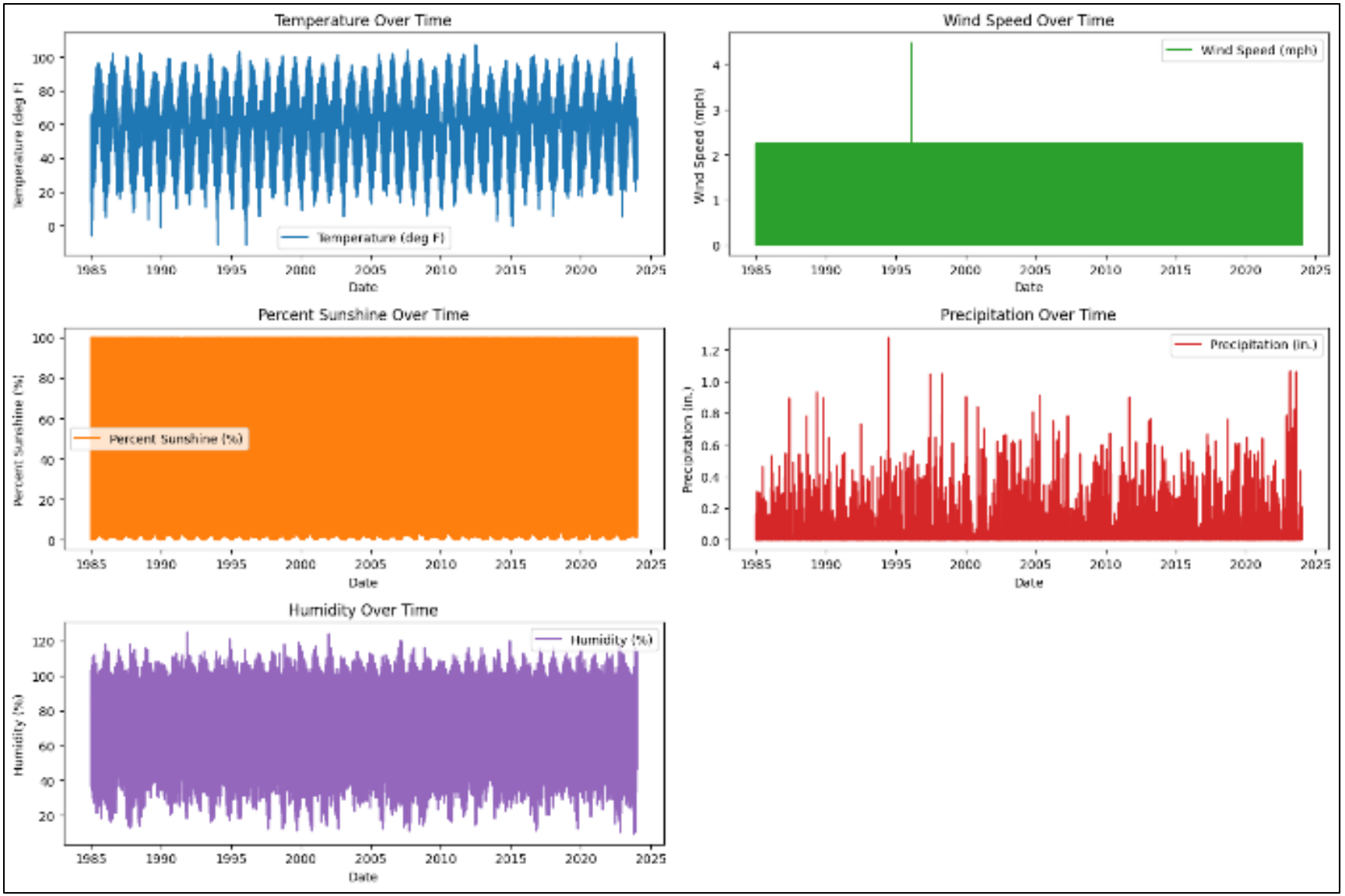

Station 138970

The following figures show the visualization of climate data for different MERRA and NARR stations. Color codes: Blue- Temperature, Green- Wind speed, Orange- Percent Sunshine, Red- Precipitation, Purple- Humidity. The number below each plot is the station that was analyses.

Region 2

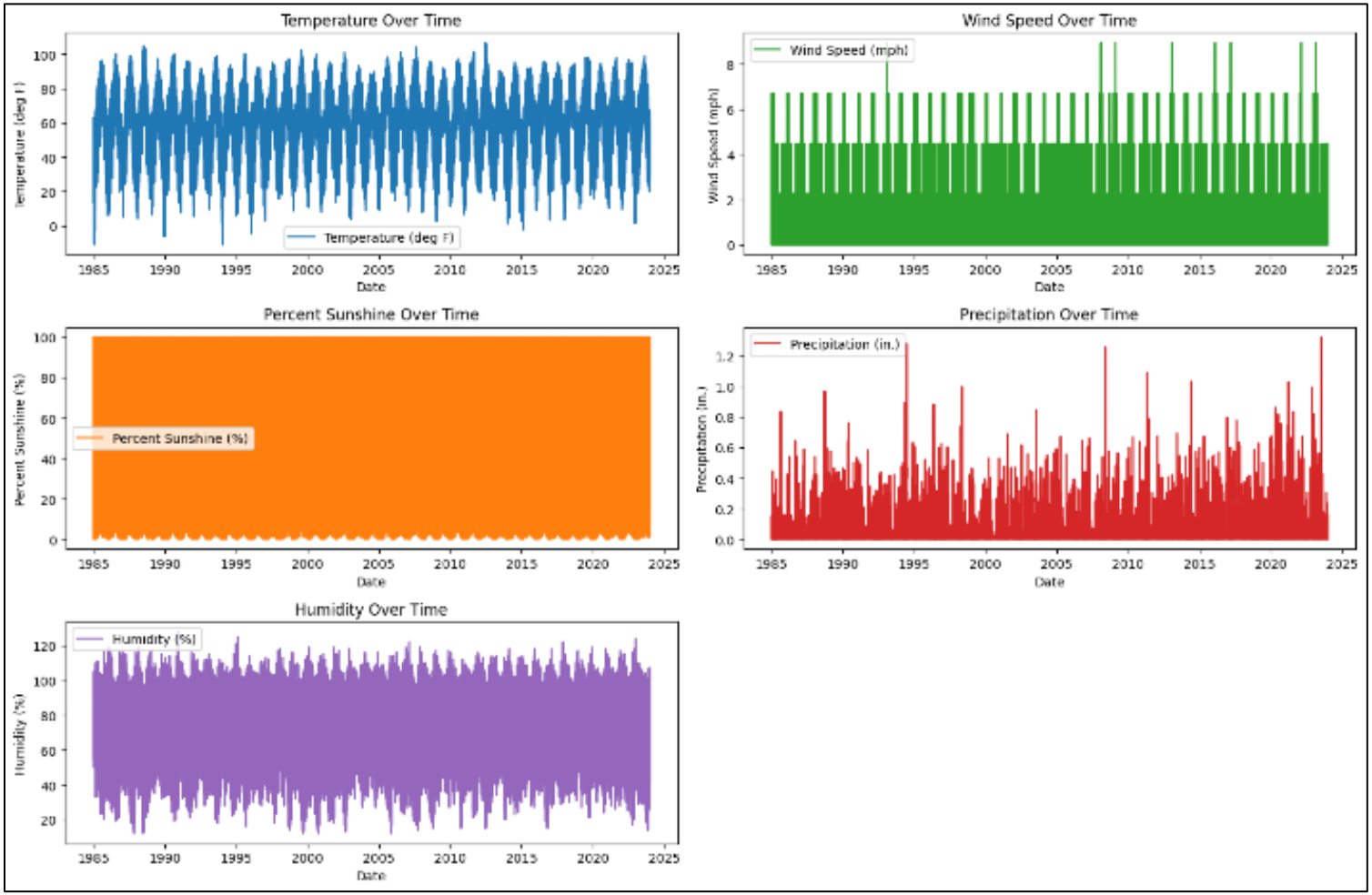

Station 140120

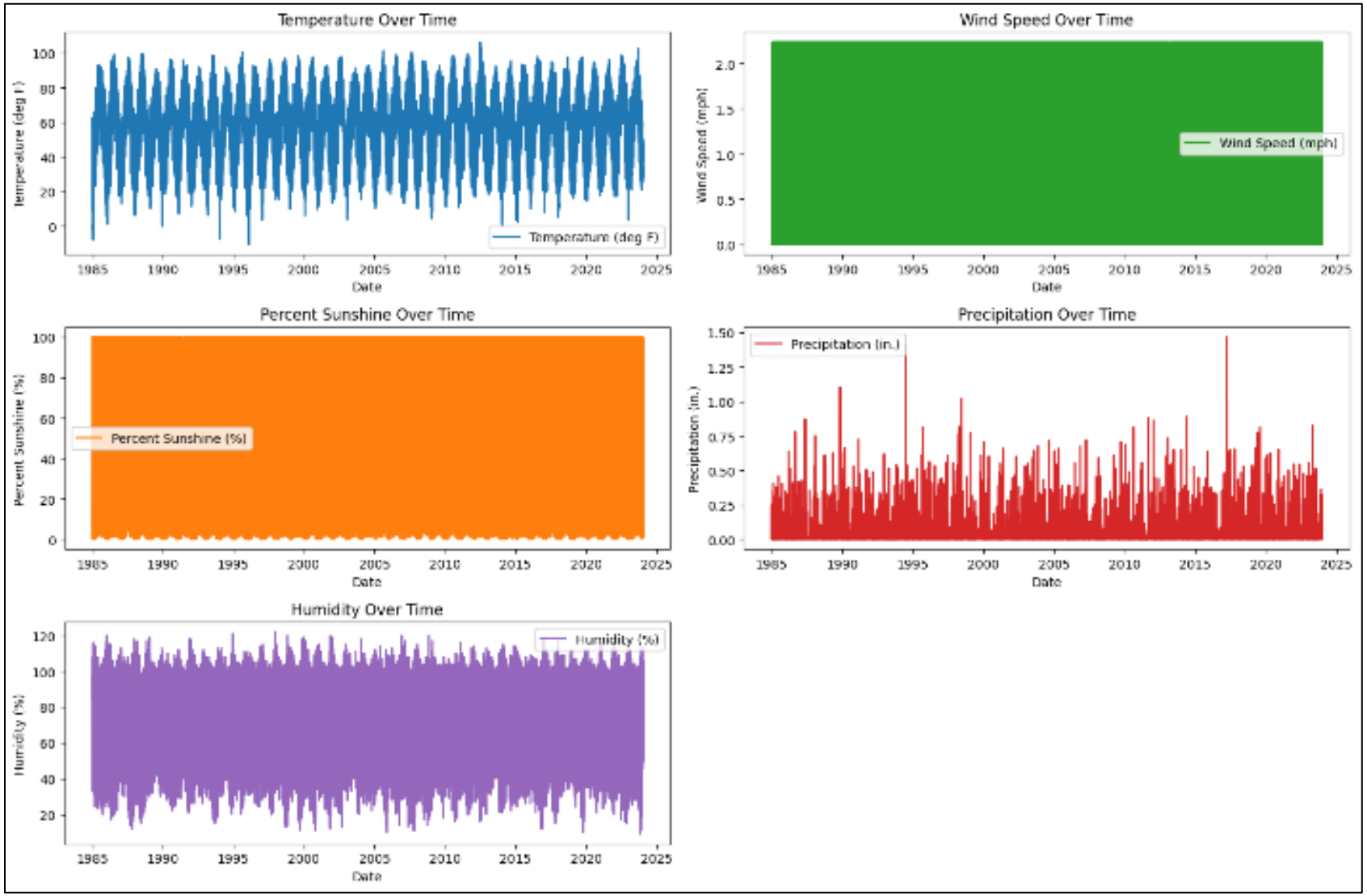

Station 138394

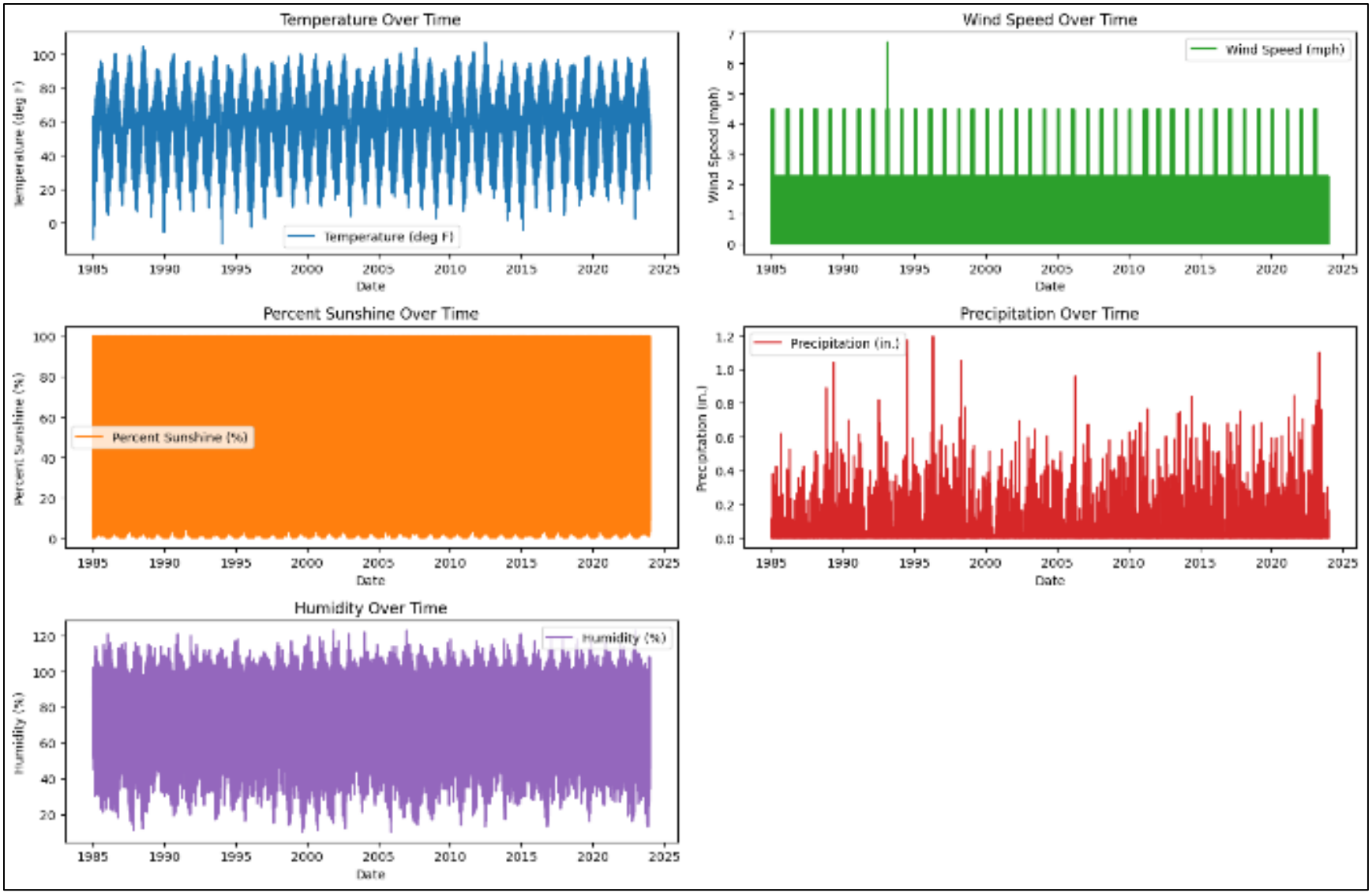

Station 139544

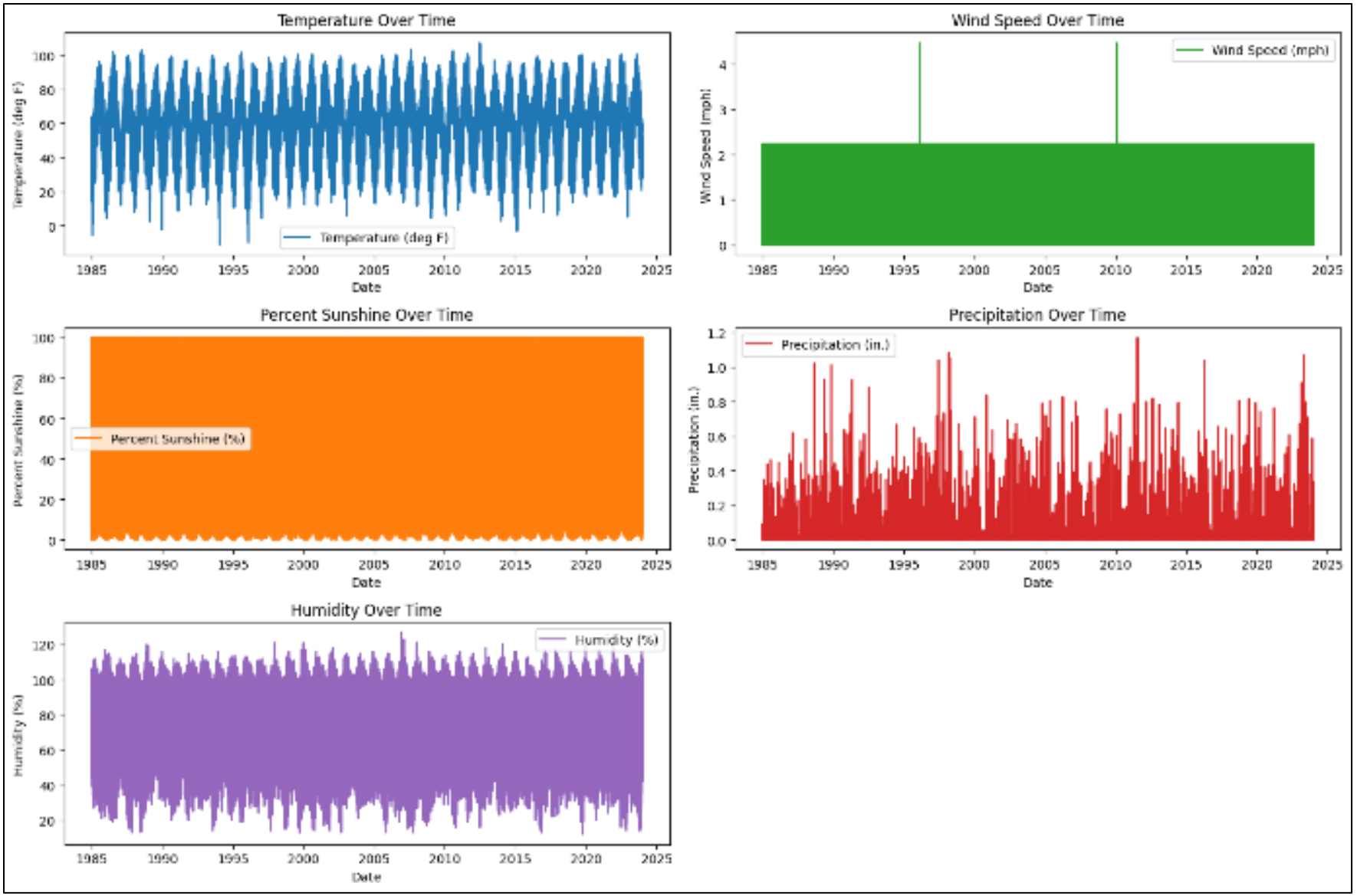

Station 138969

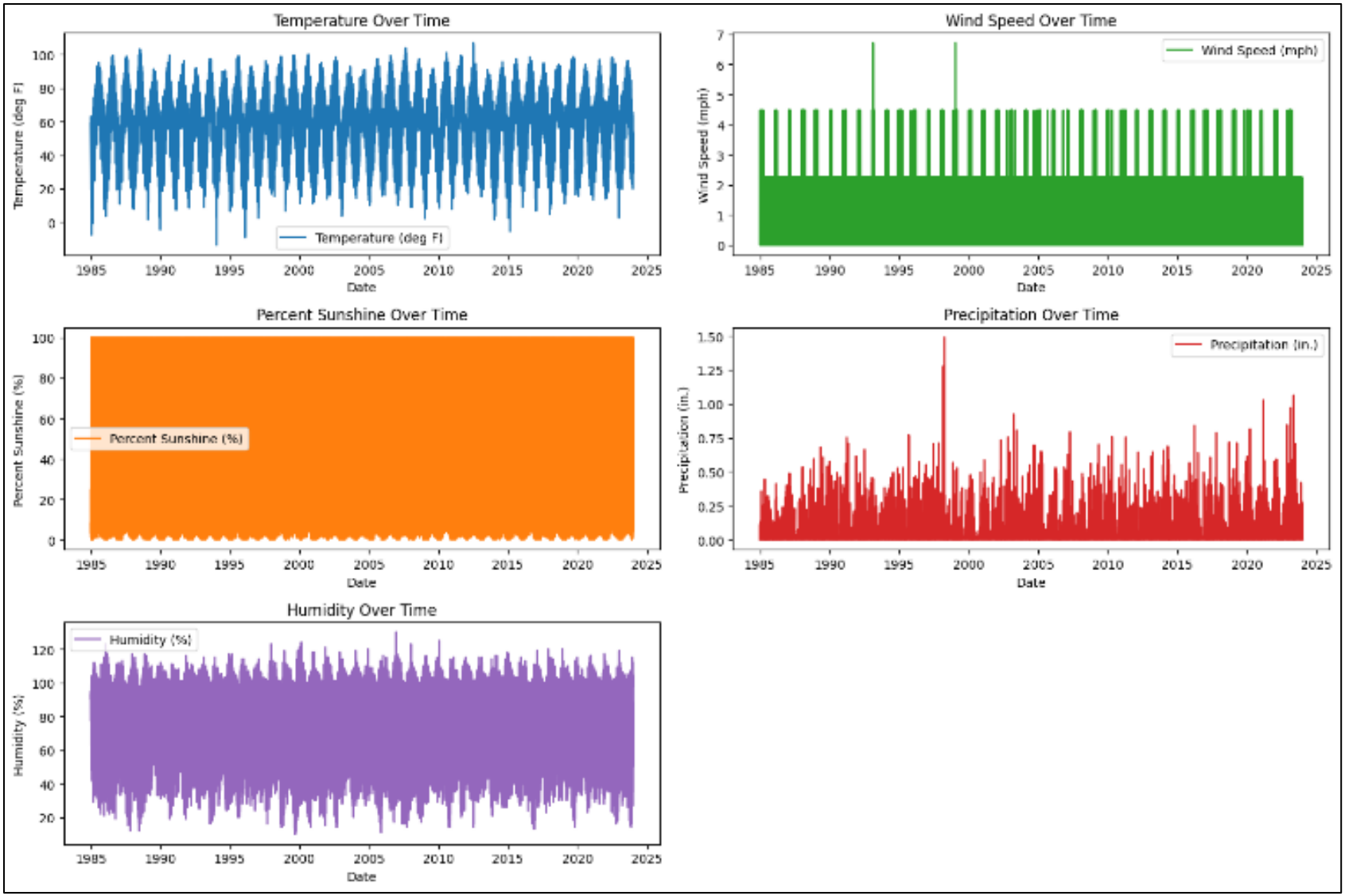

Station 138968

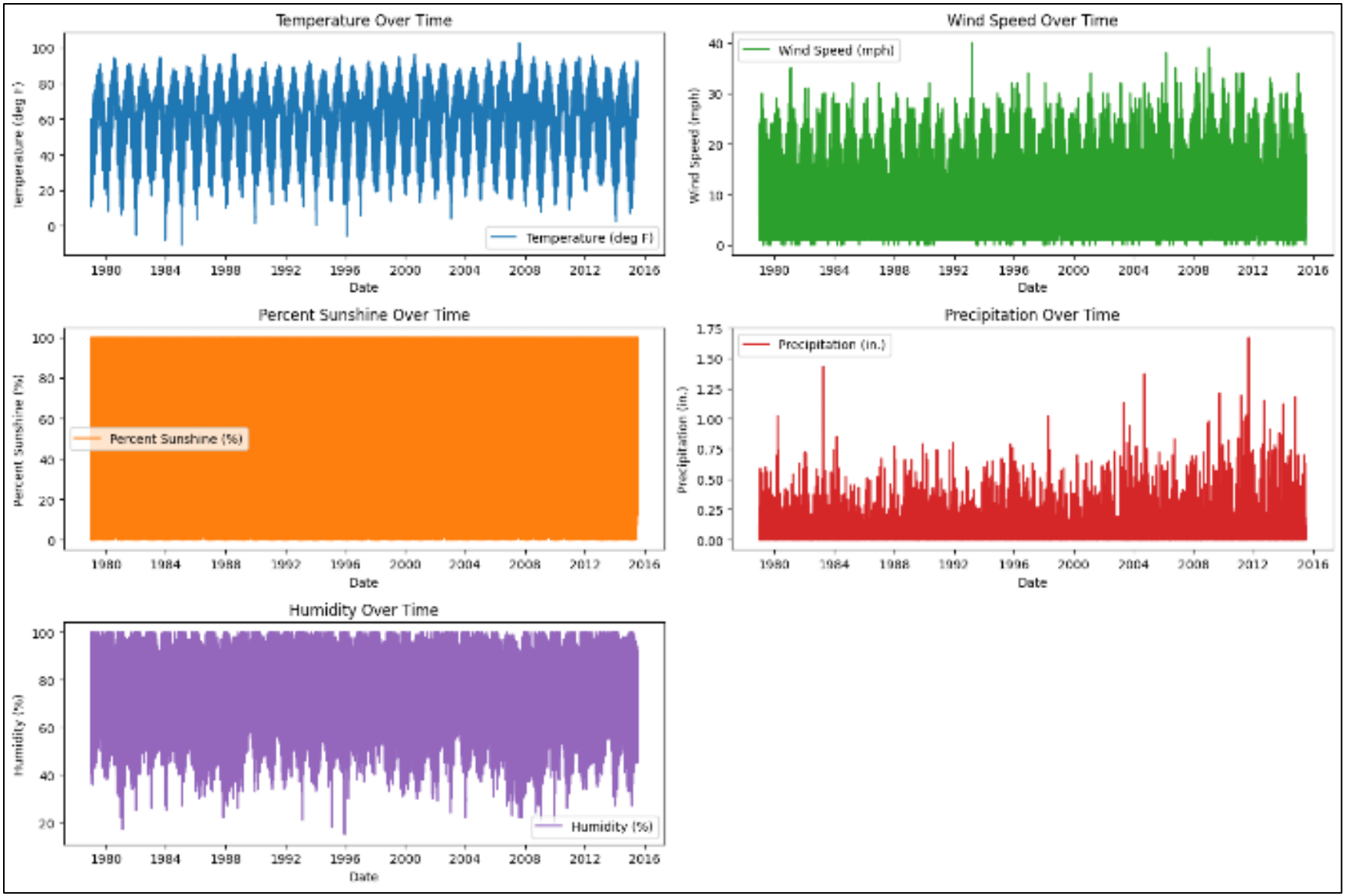

Station 13882 (NAAR data file)

The following figures show the visualization of climate data for different MERRA and NARR stations. Color codes: Blue- Temperature, Green- Wind speed, Orange- Percent Sunshine, Red- Precipitation, Purple- Humidity. The number below each plot is the station that was analyses.

Region 3

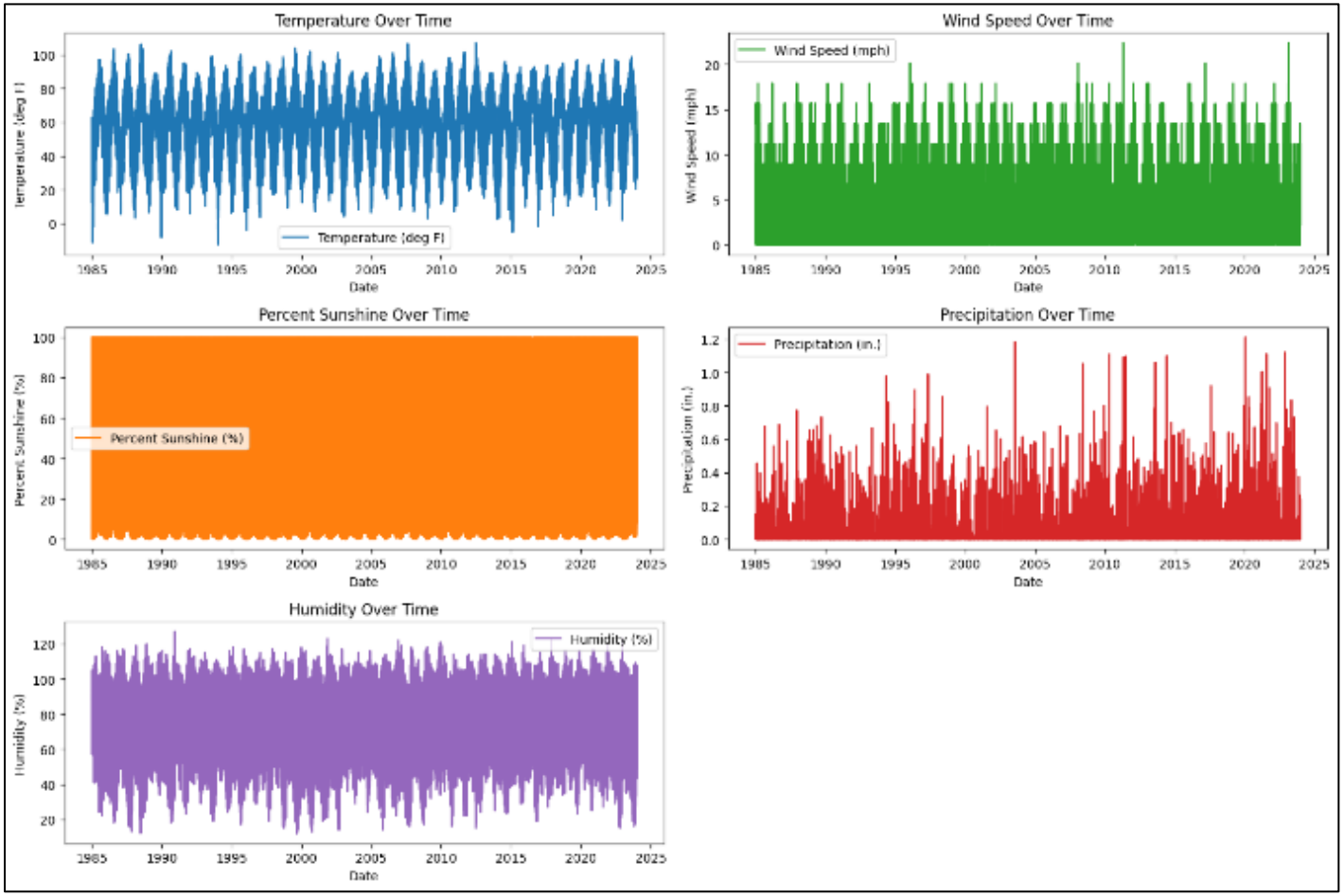

Station 140119

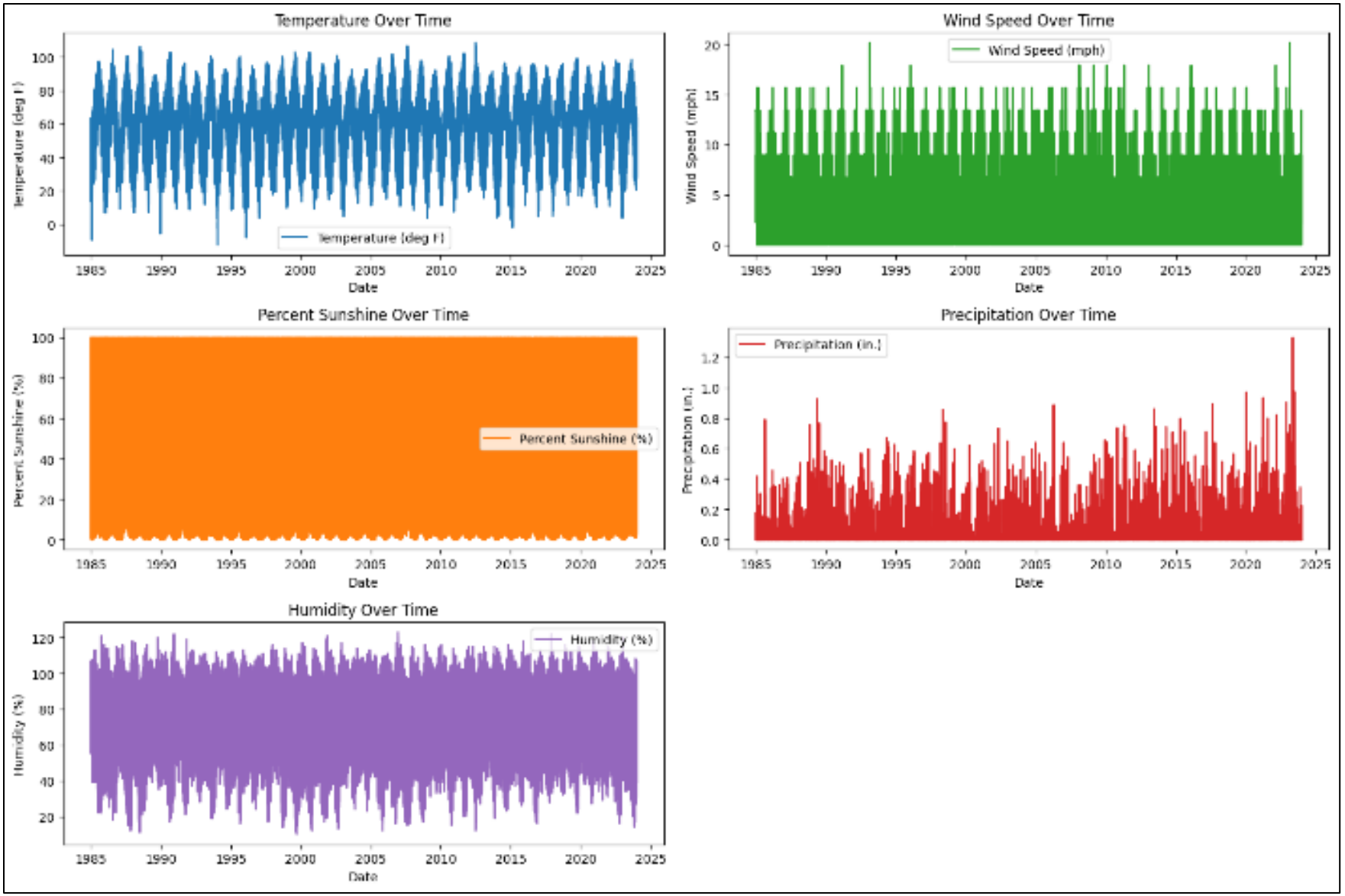

Station 139543

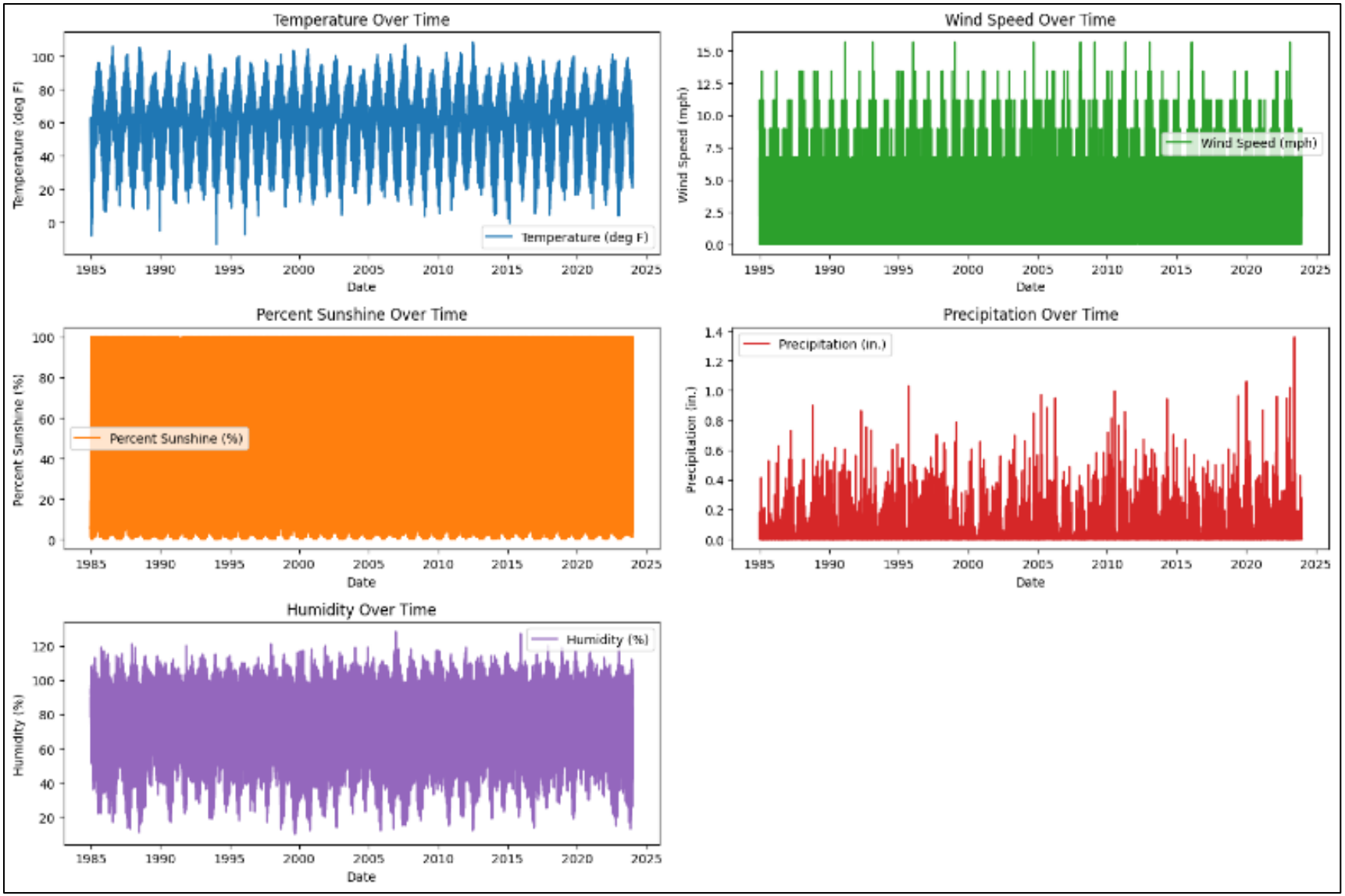

Station 138966

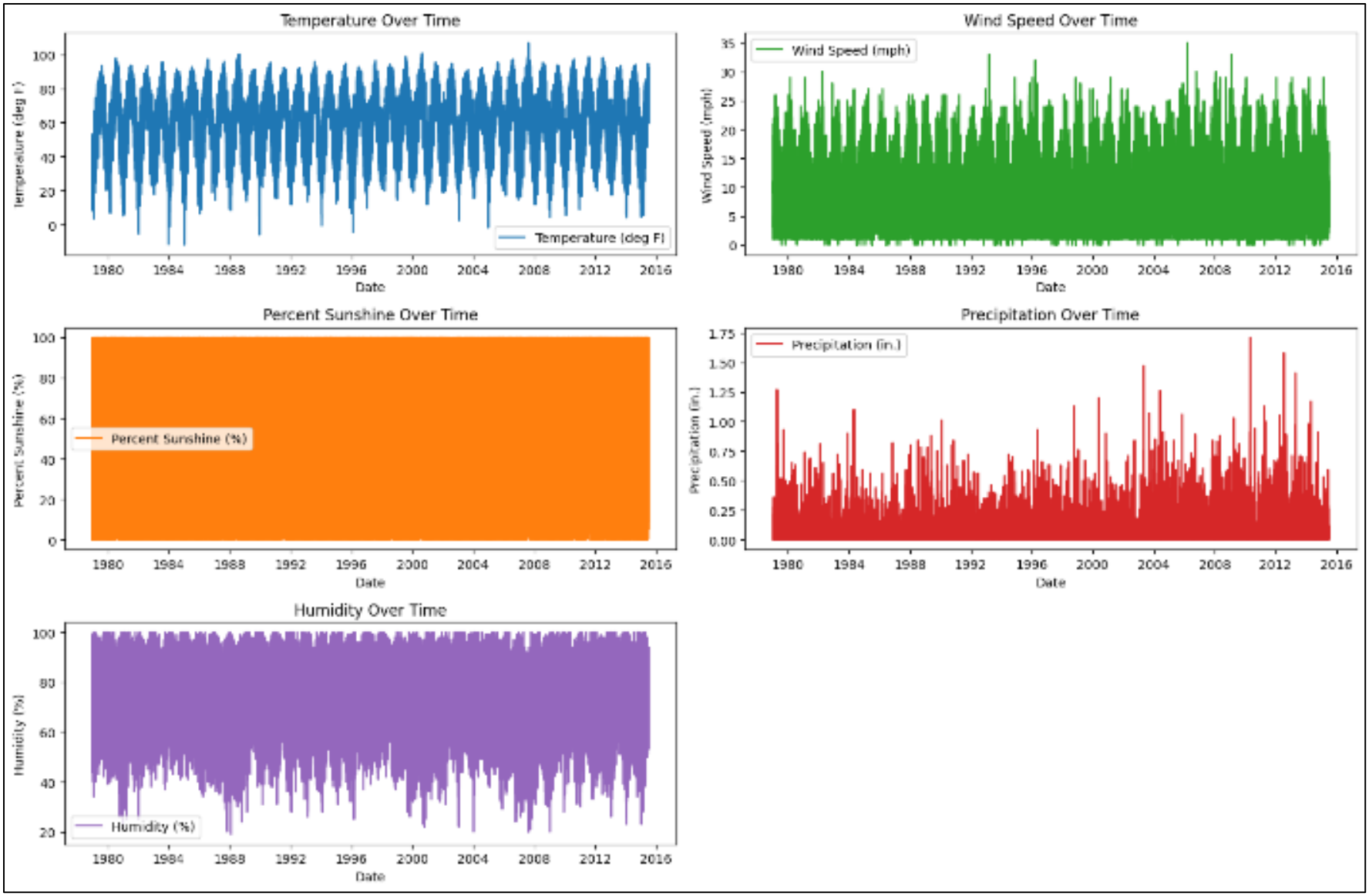

Station 13897 (NAAR data file)

The following figures show the visualization of climate data for different MERRA and NARR stations. Color codes: Blue- Temperature, Green- Wind speed, Orange- Percent Sunshine, Red- Precipitation, Purple- Humidity. The number below each plot is the station that was analyses.

Region 4

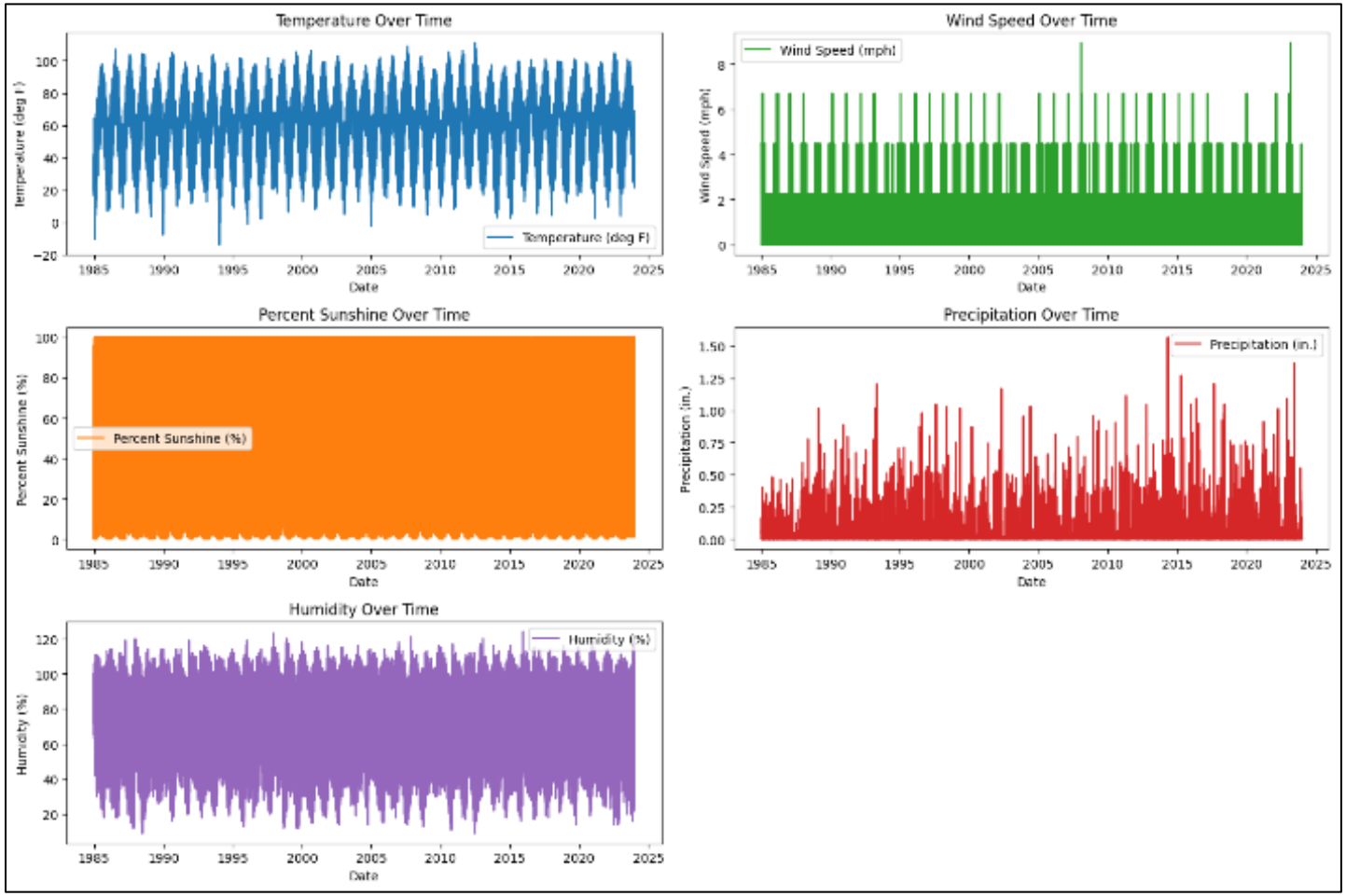

Station 139540

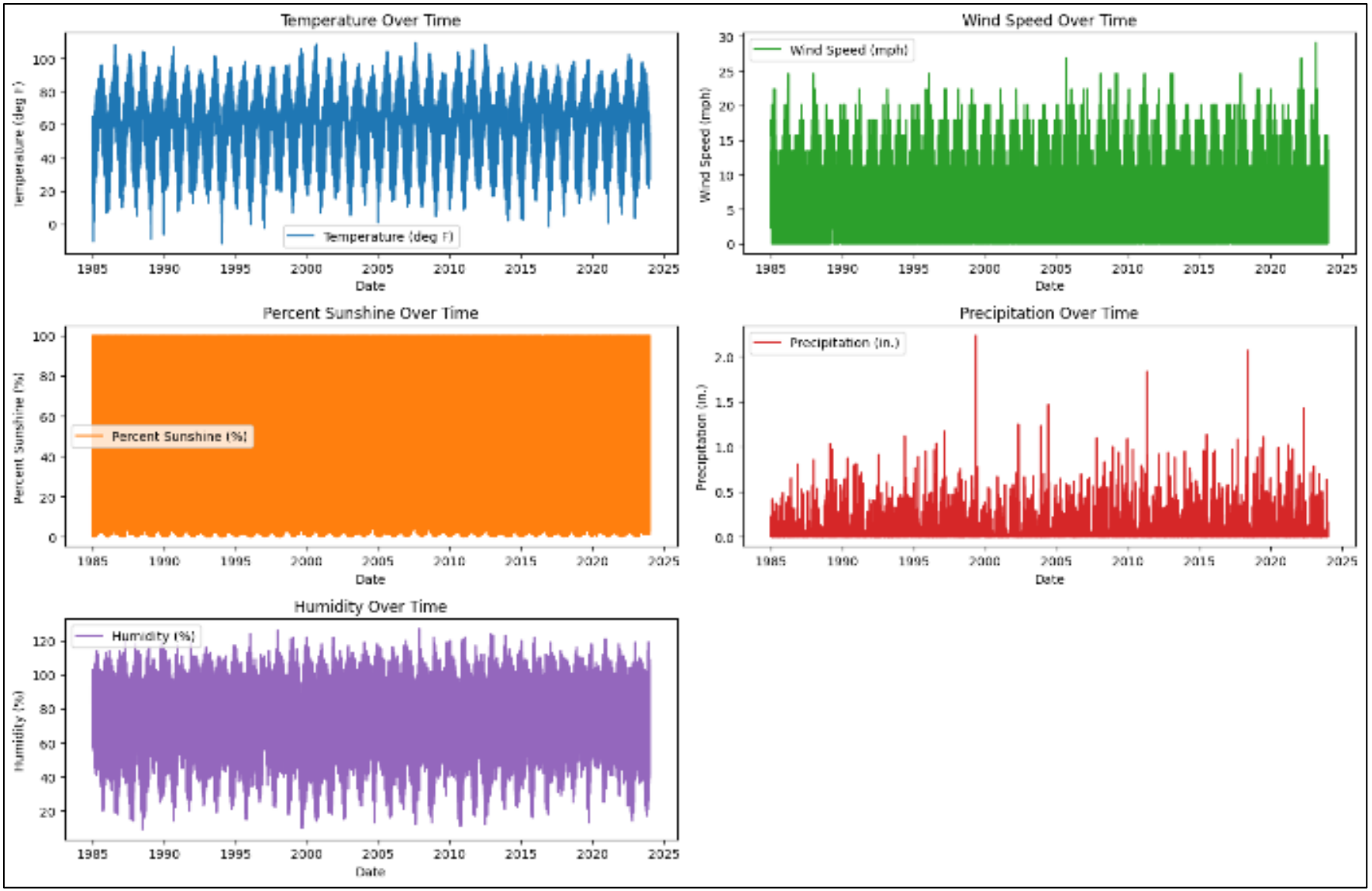

Station 139539

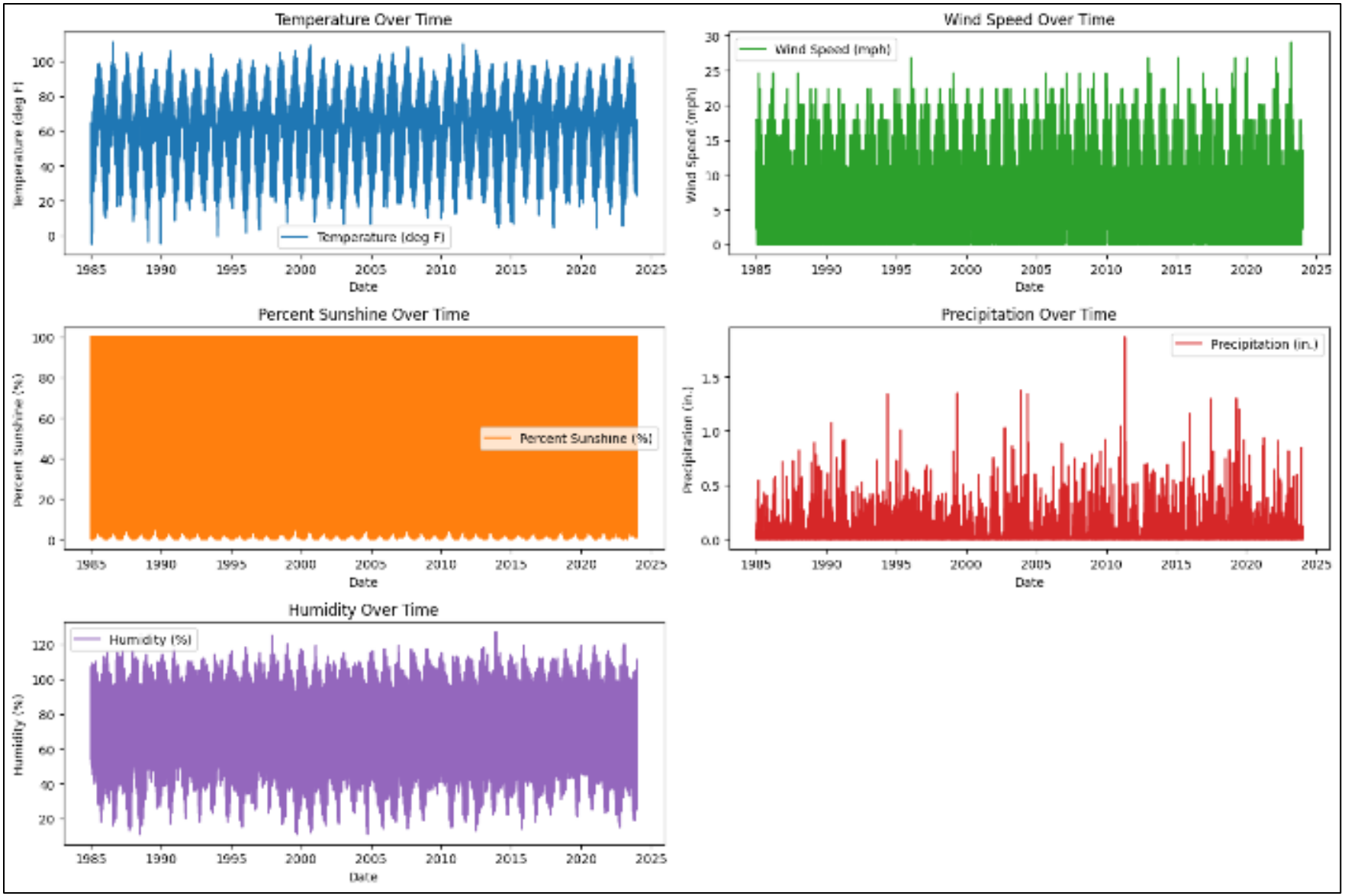
Temperature Over Time
Temperature (deg F)
Date
Wind Speed Over Time
Wind Speed (mph)
Date
Percent Sunshine Over Time
Percent Sunshine (%)
Date
Precipitation Over Time
Precipitation (in.)
Date
Humidity Over Time
Humidity (%)
Date

Station 138961

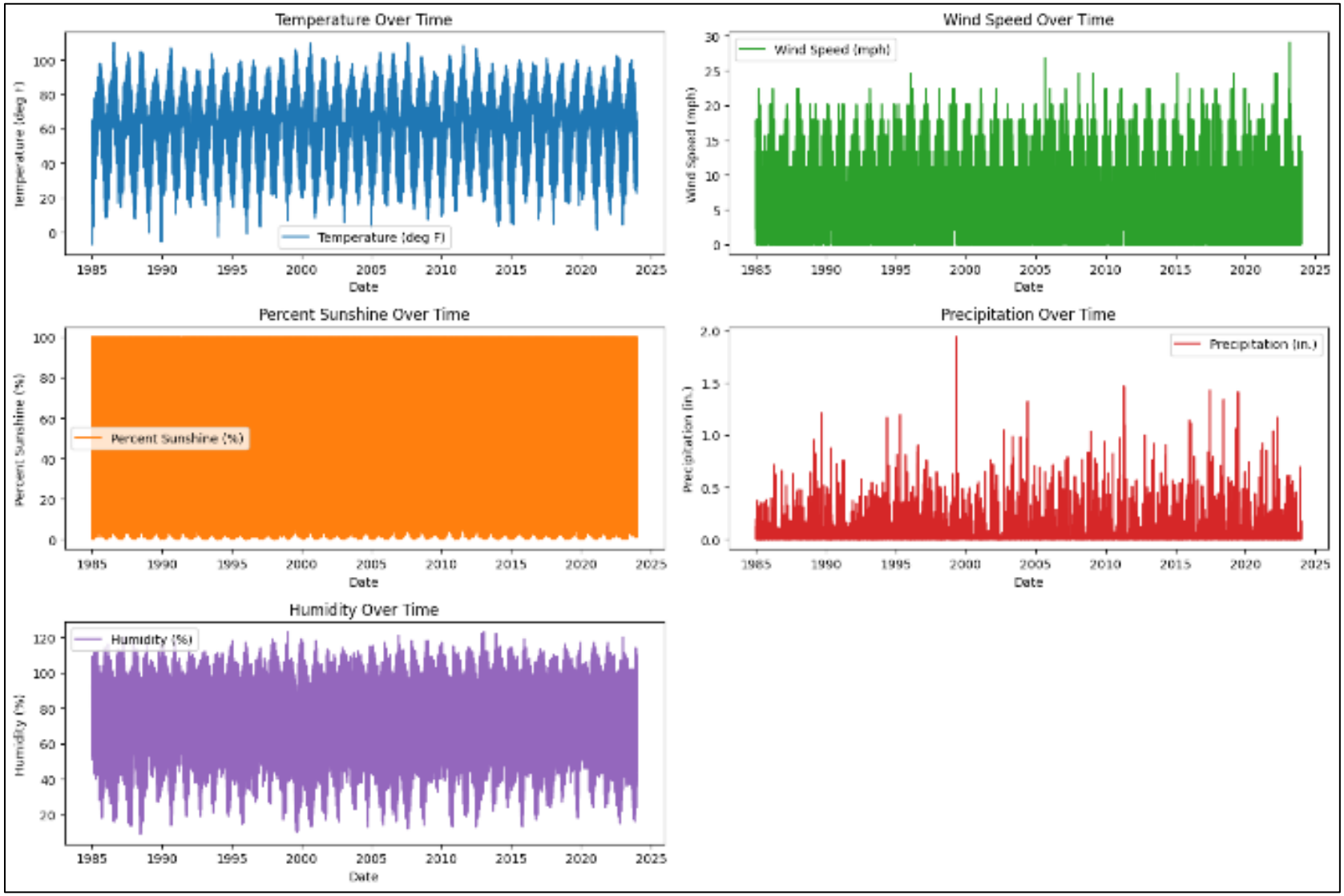

Station 138962

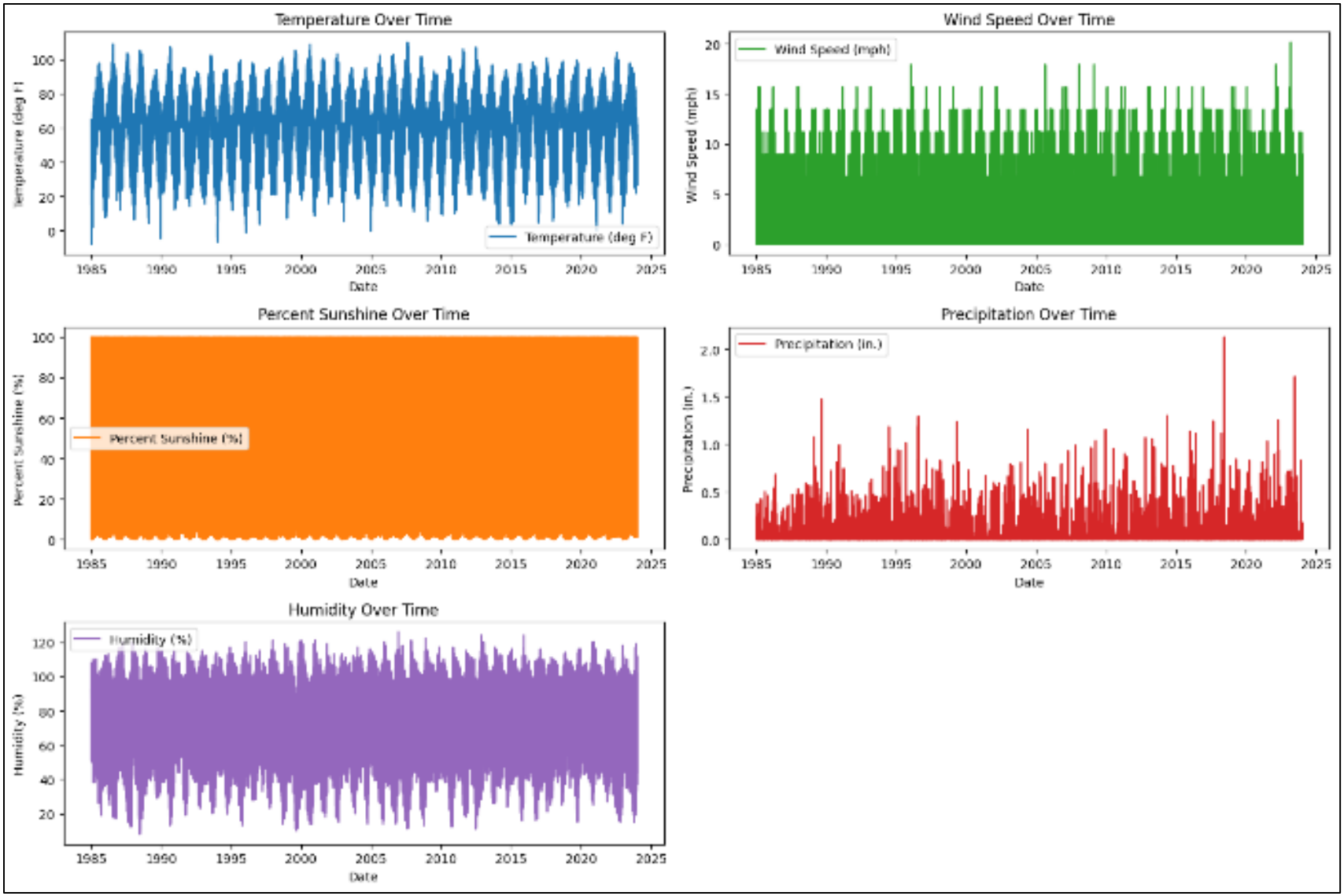

Station 138963

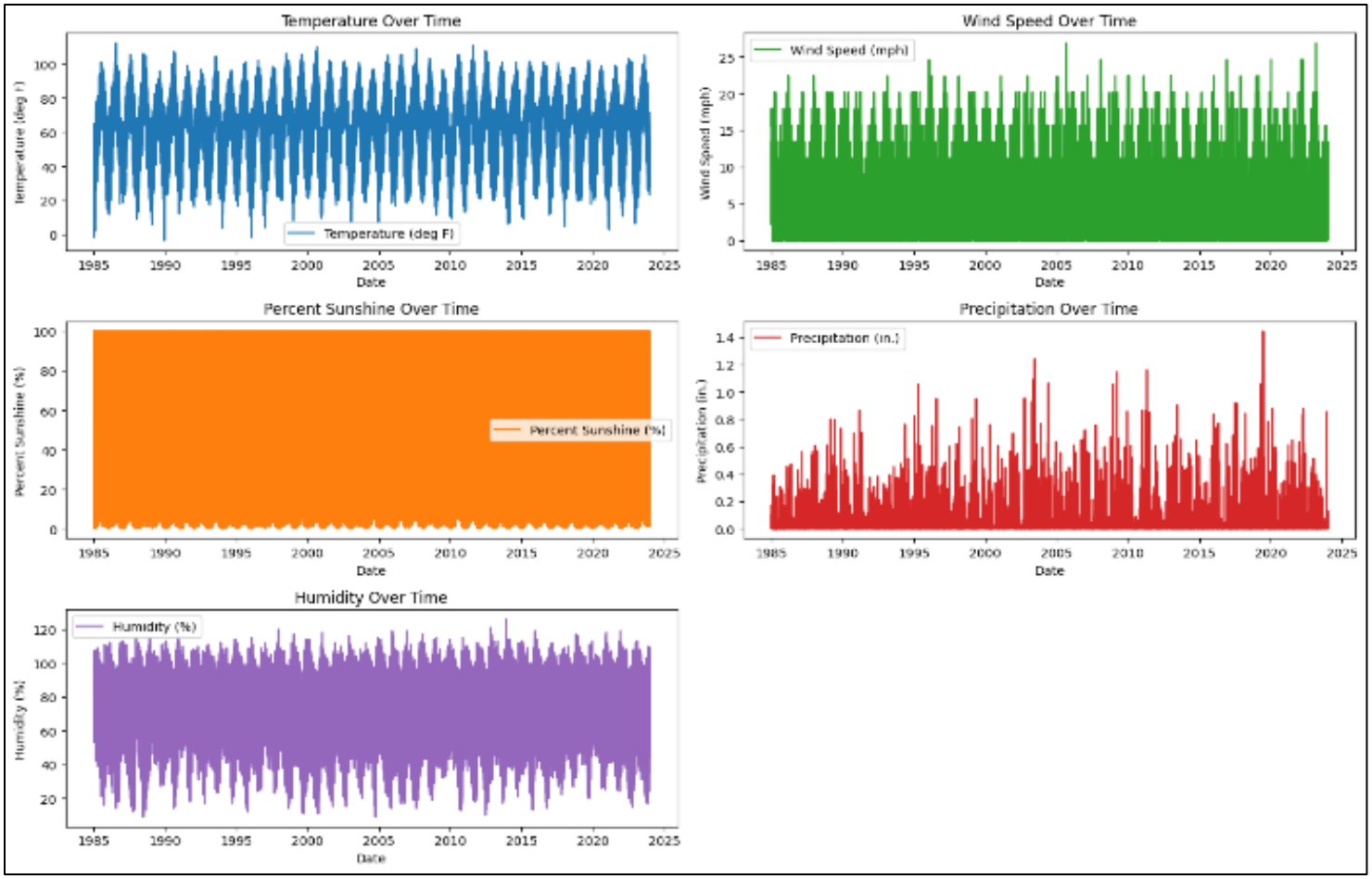

Station 138385

From the trends it is clearly seen that no particular trend is inherent for all climate stations, but trends appear to not be significantly changing with time. The trends for average annual temperature and precipitation were further analyzed for each region to see if a particular trend can be drawn. Graphs below present individual sites and regions and state averages for temperature and precipitation.

A2.1: Temperature: File 1 to file 6 are different stations in that region

Region 1

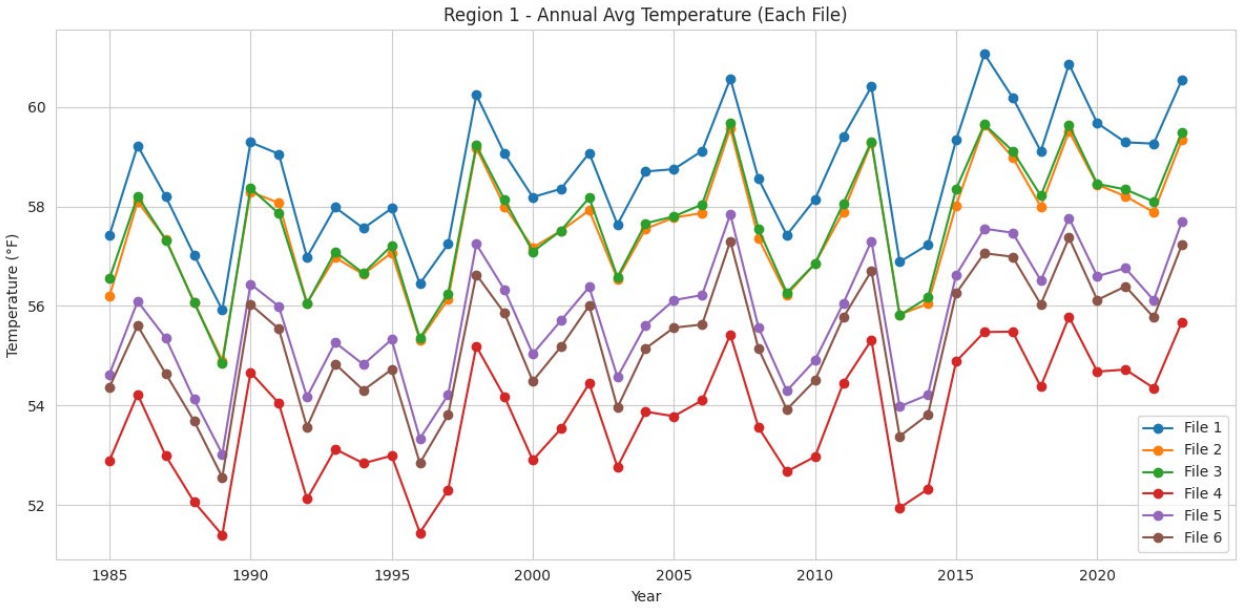

Annual Average Temperatures of each site in Region 1

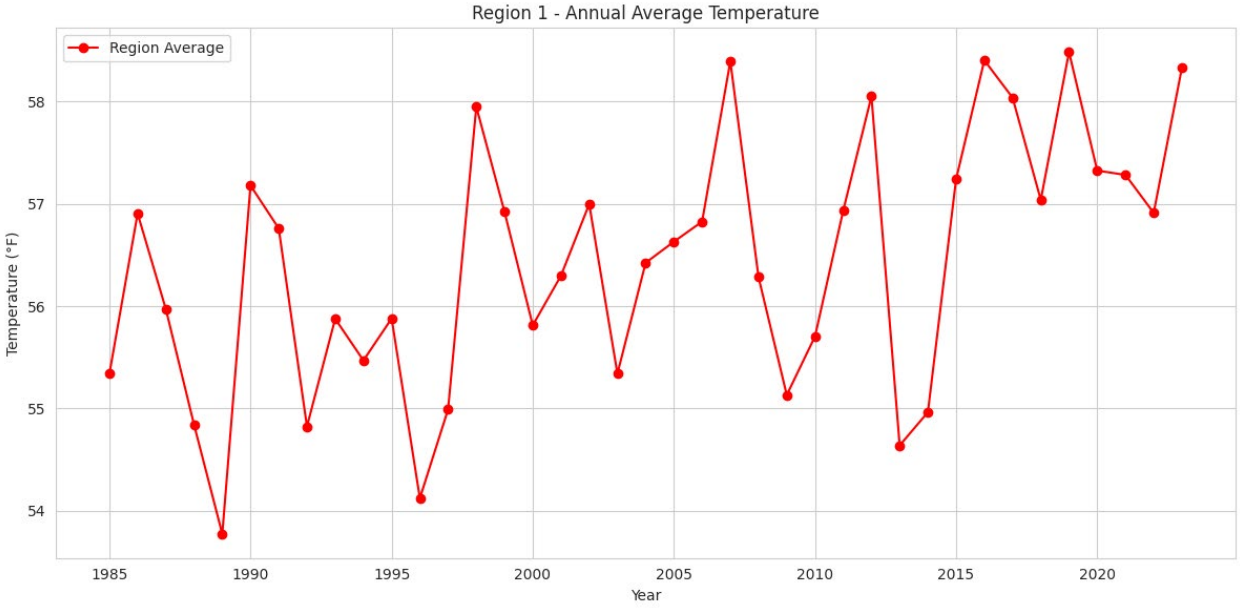

Annual Average Temperatures from all sites in Region 1

Region 2

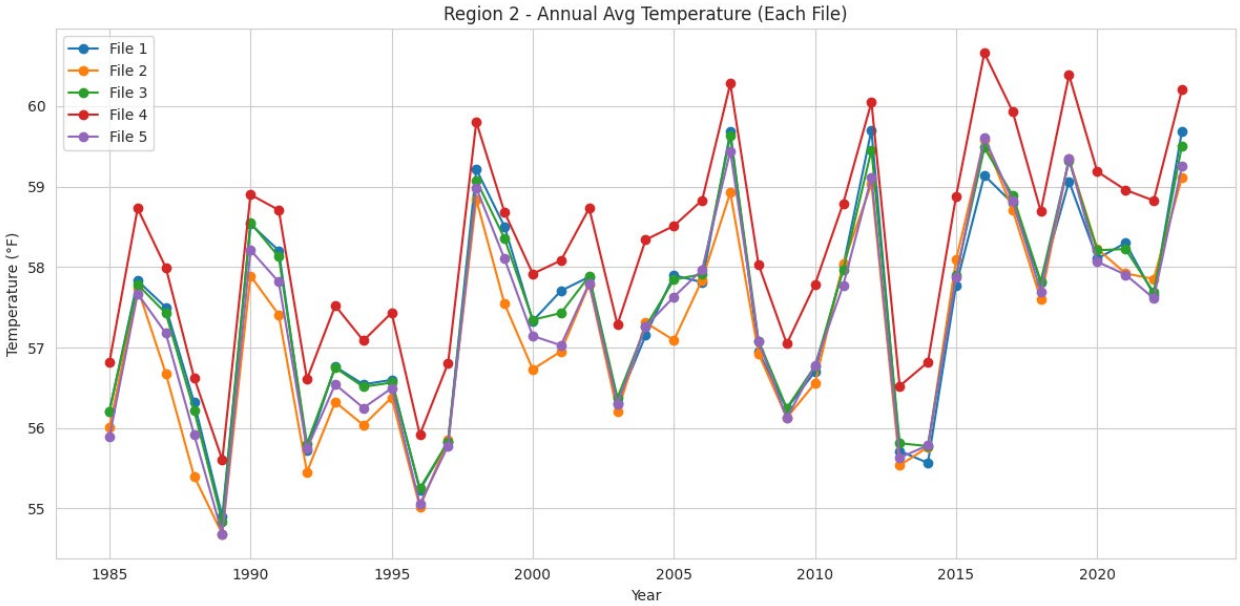

Annual Average Temperatures of each site in Region 2

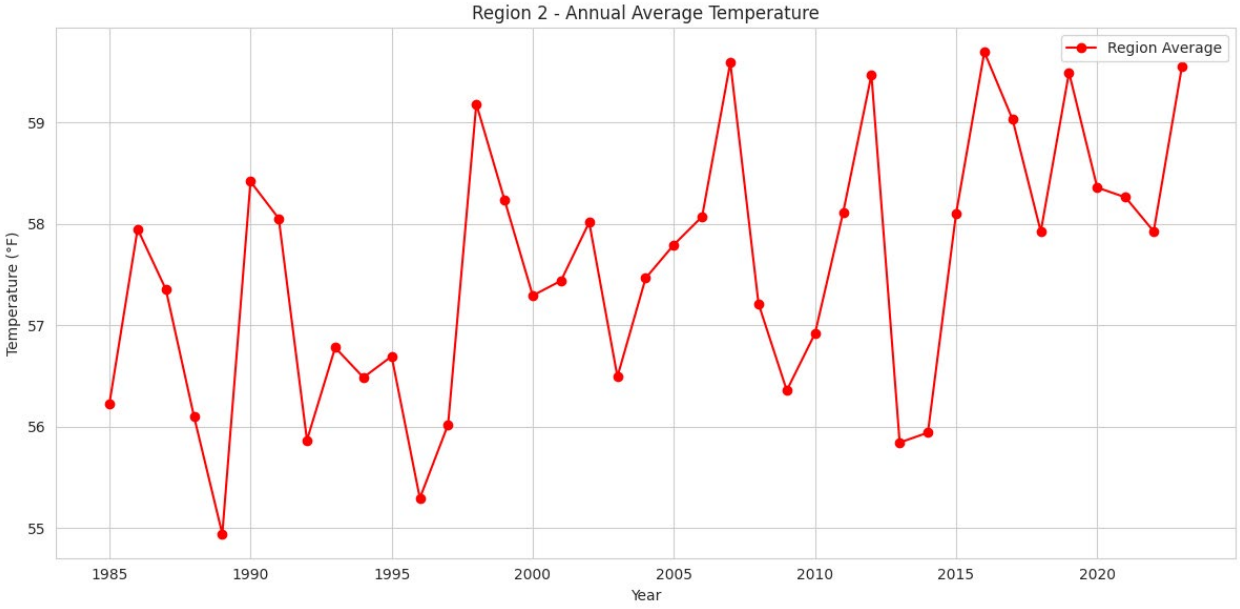

Annual Average Temperatures from all sites in Region 2

Region 3

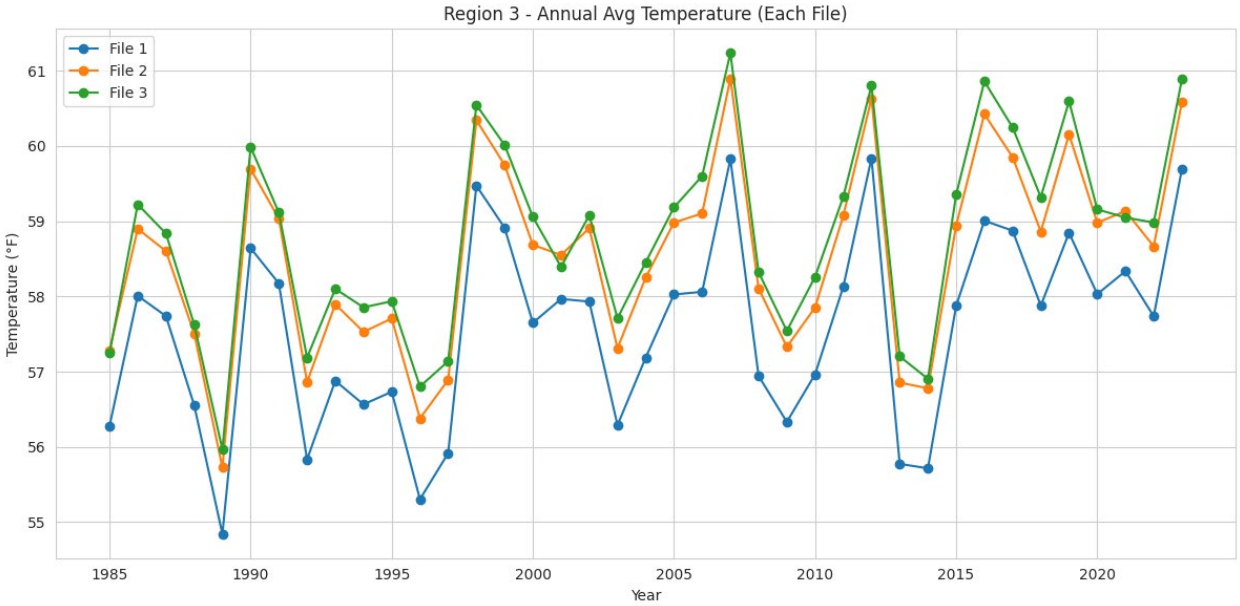

Annual Average Temperatures of each site in Region 3

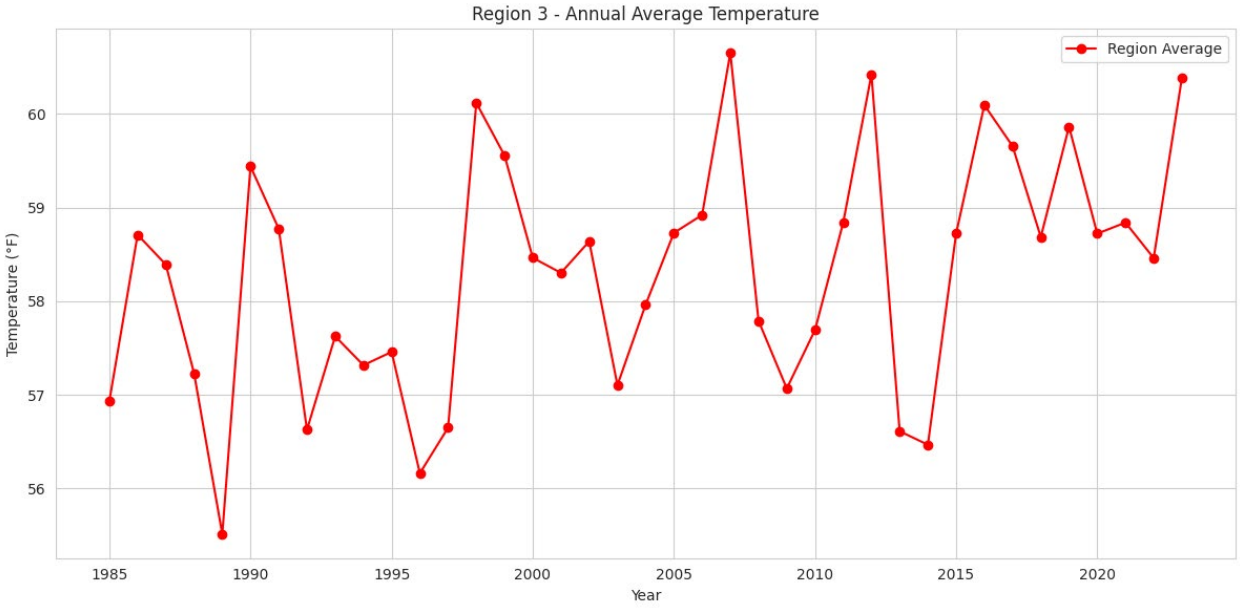

Annual Average Temperatures from all sites in Region 3

Region 4

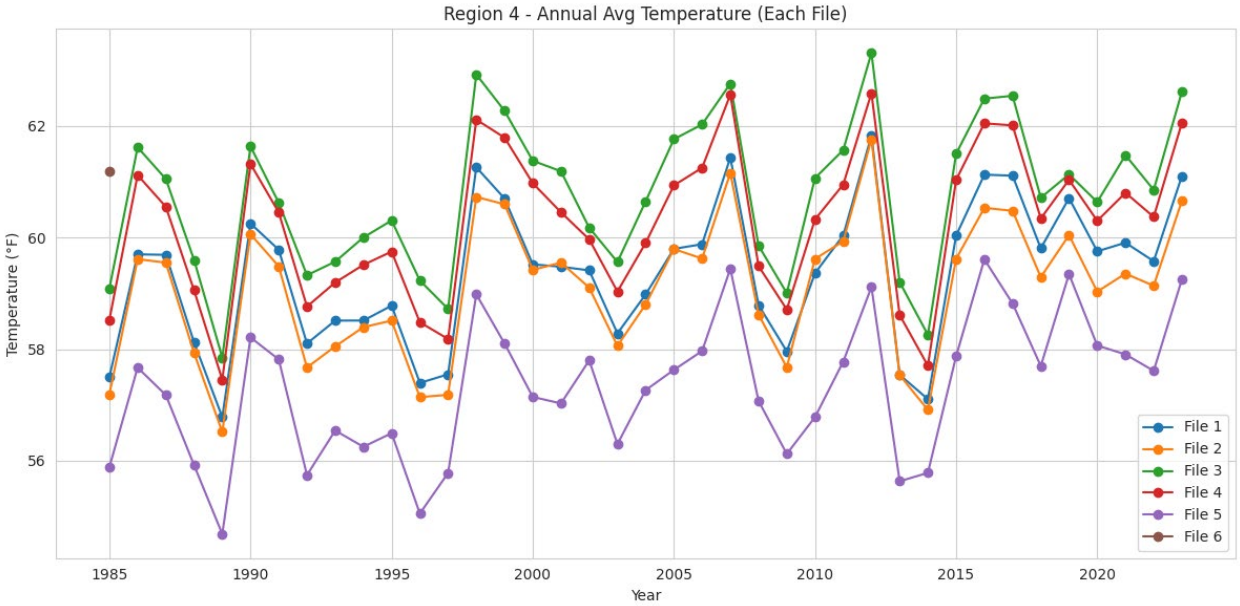

Annual Average Temperatures of each site in Region 4

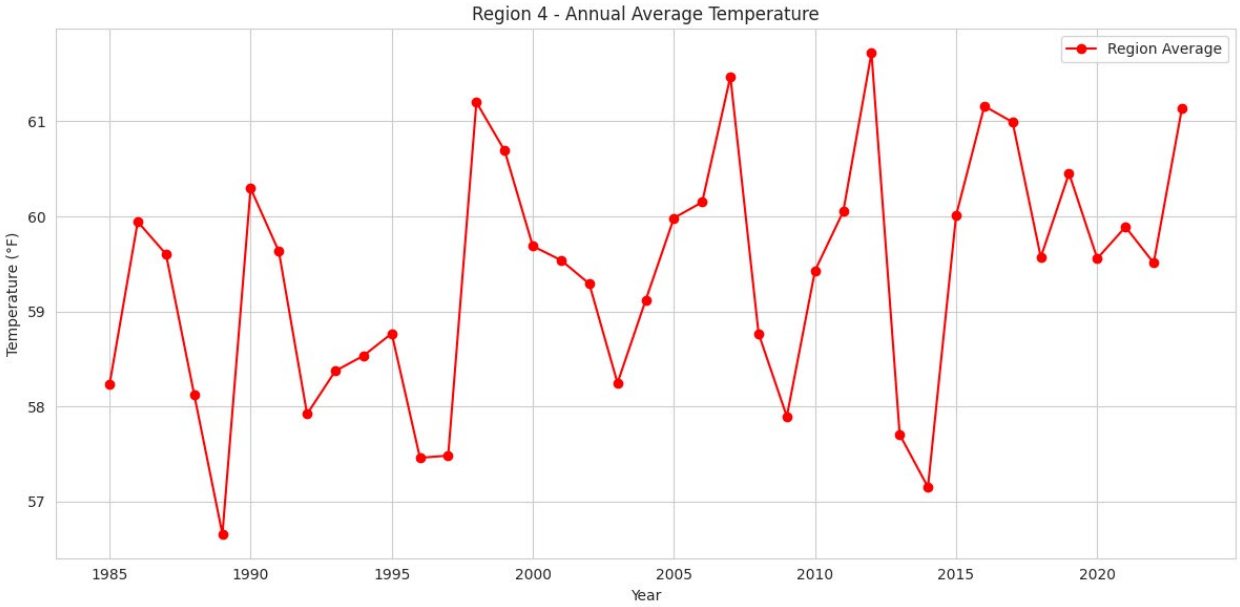

Annual Average Temperatures from all sites in Region 4

All Four (4) regions Annual Average Temperatures

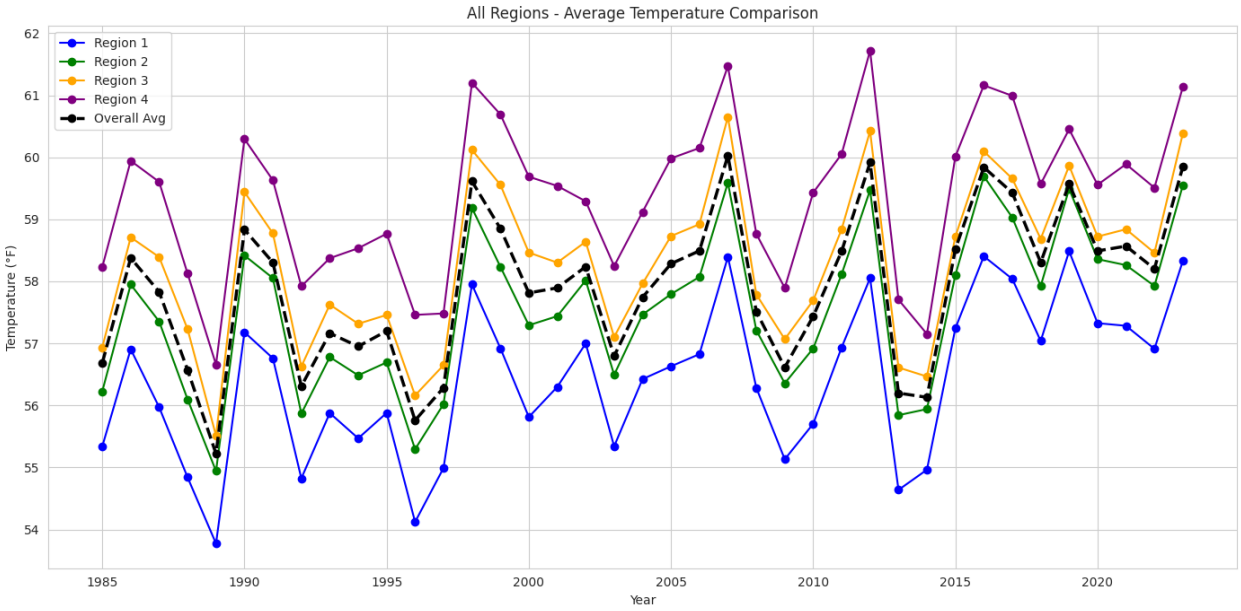

A2.2: Precipitation: File 1 to file 6 are different stations in that region

Region1

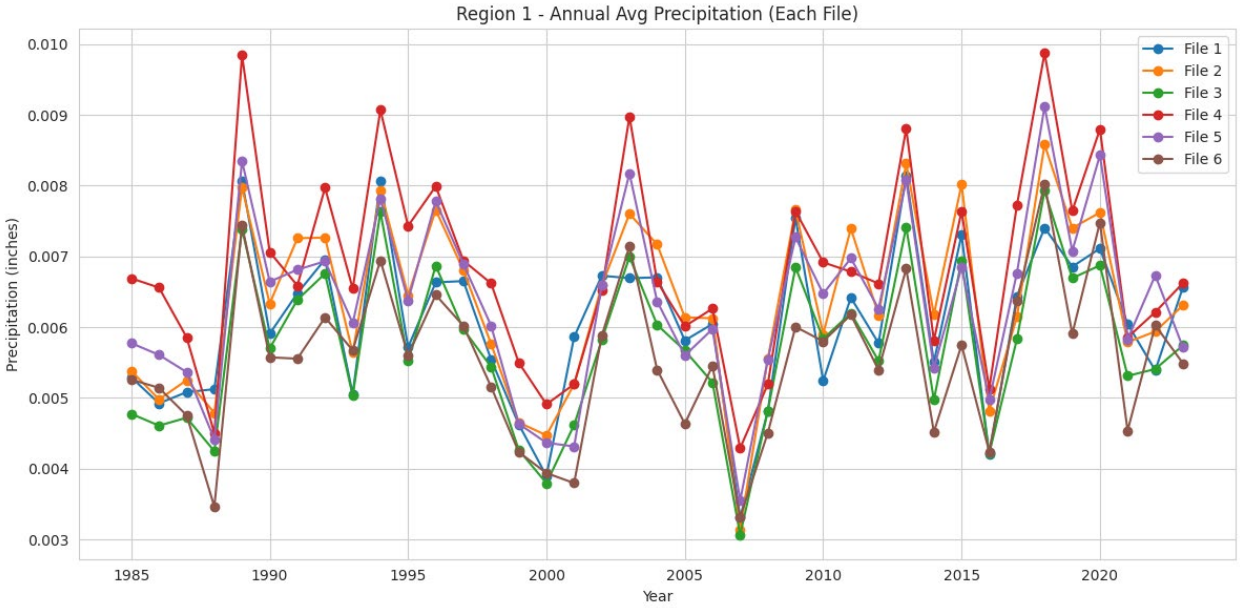

Annual Average Precipitation of each site in Region 1

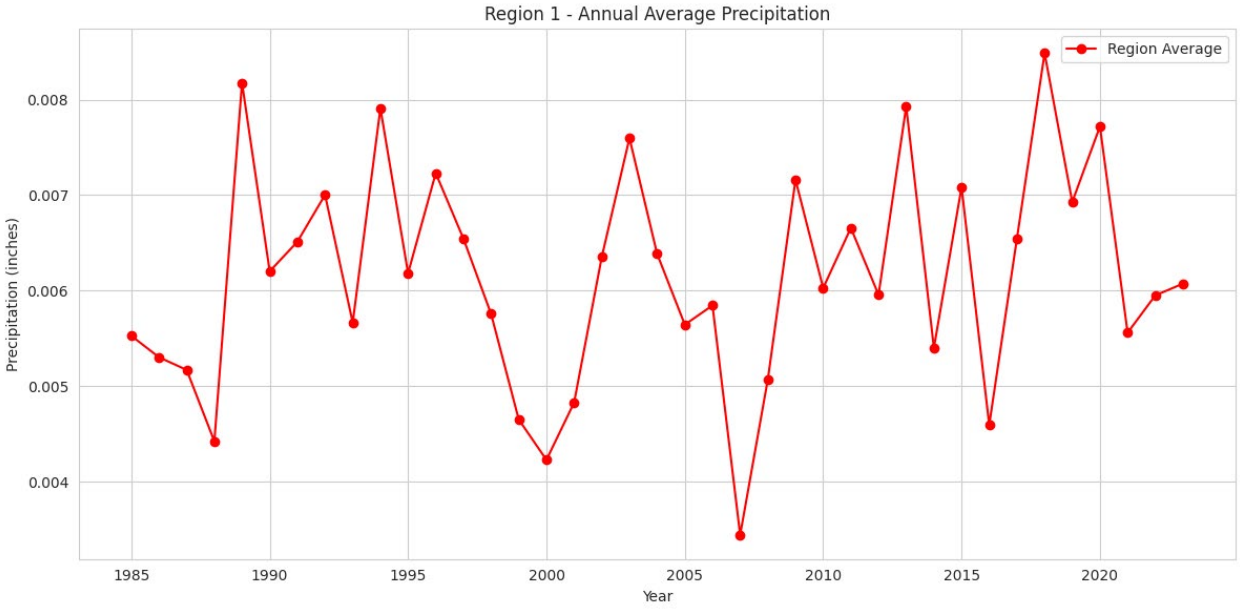

Annual Average Precipitation from all sites in Region 1

Region2:

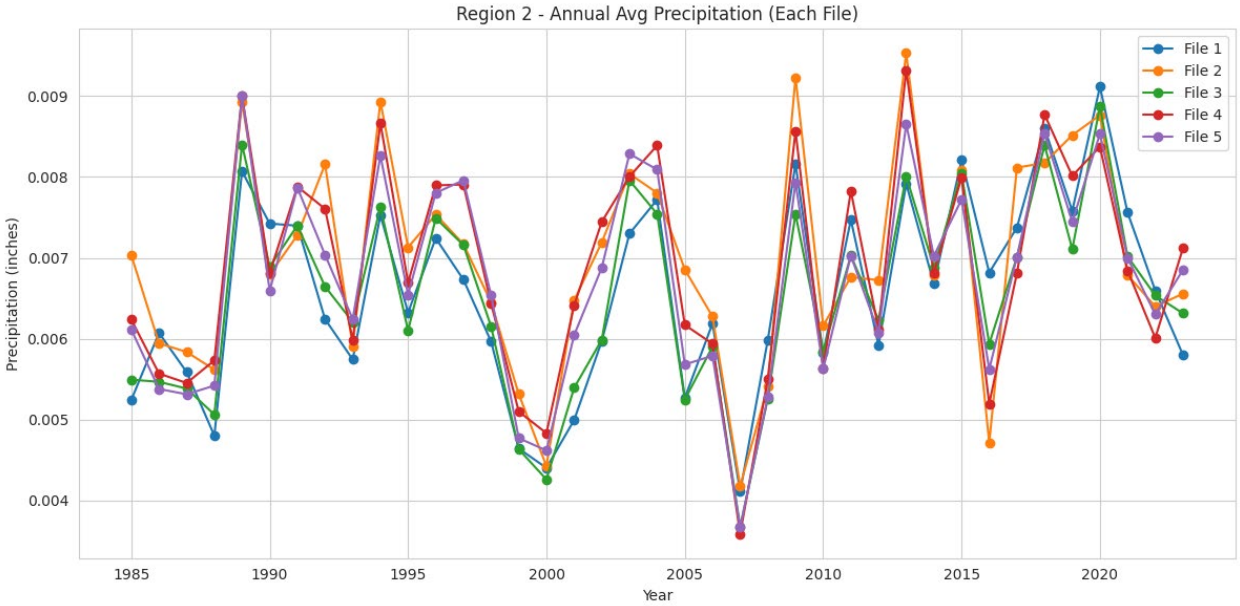

Annual Average Precipitation of each site in Region 2

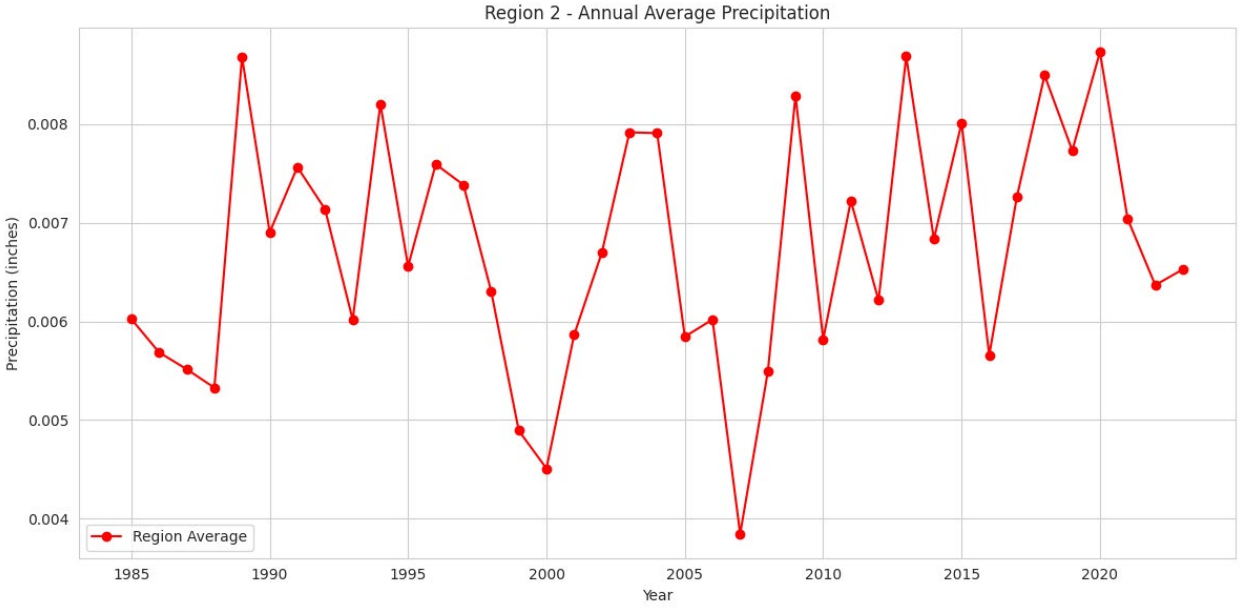

Annual Average Precipitation from all sites in Region 2

Region 3:

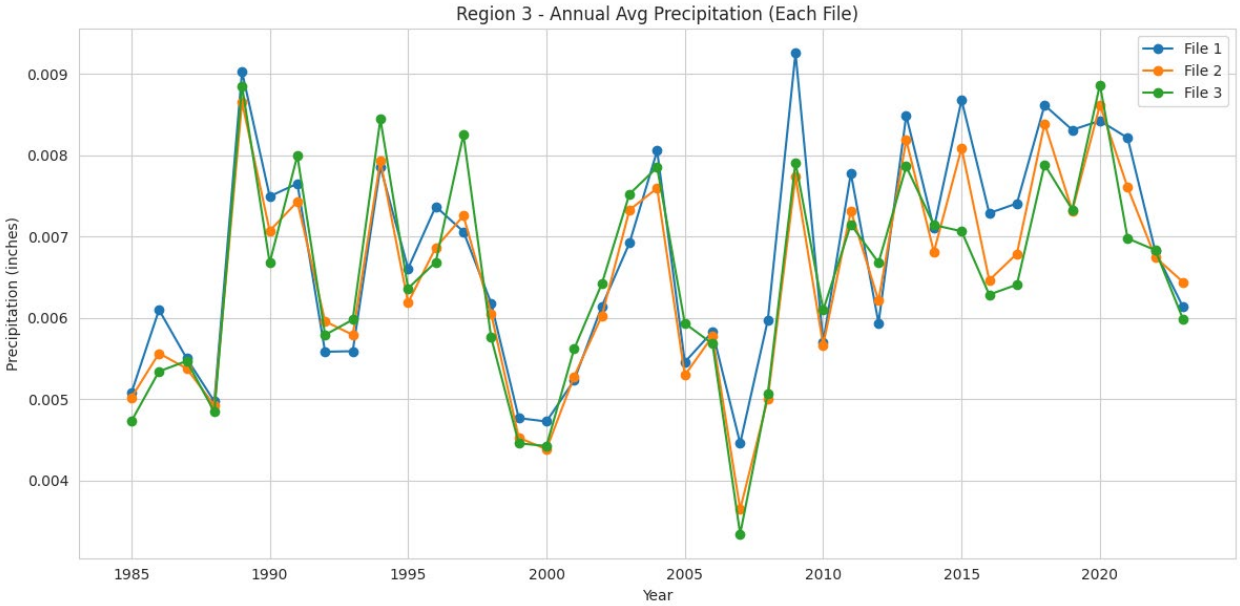

Annual Average Precipitation of each site in Region 3

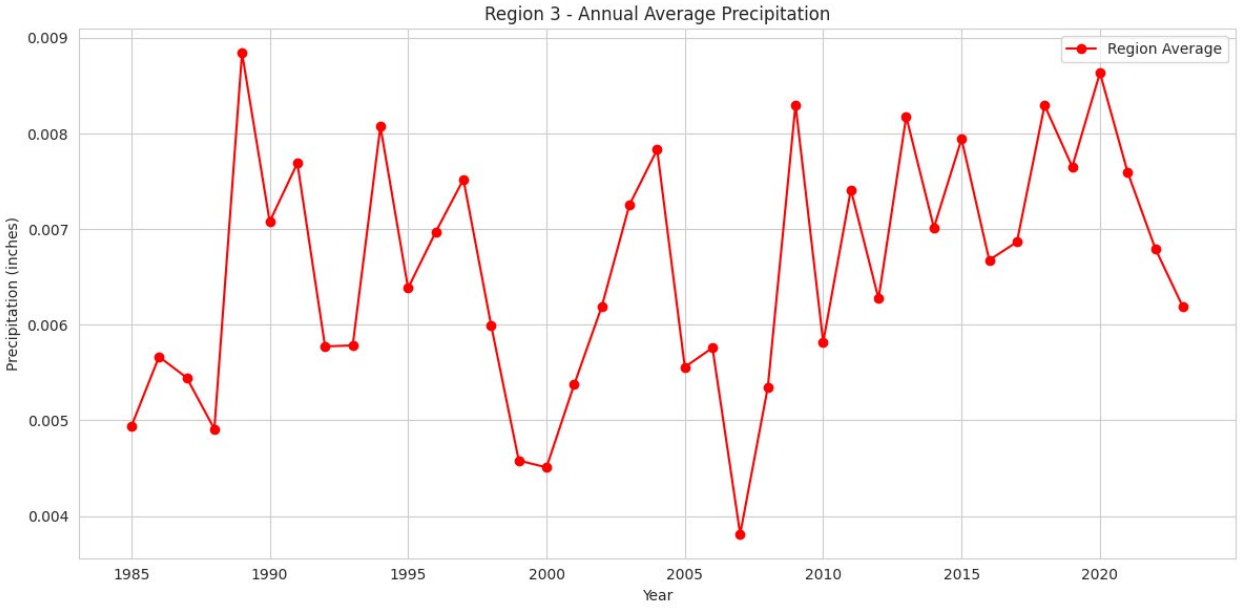

Annual Average Precipitation from all sites in Region 3

Region 4:

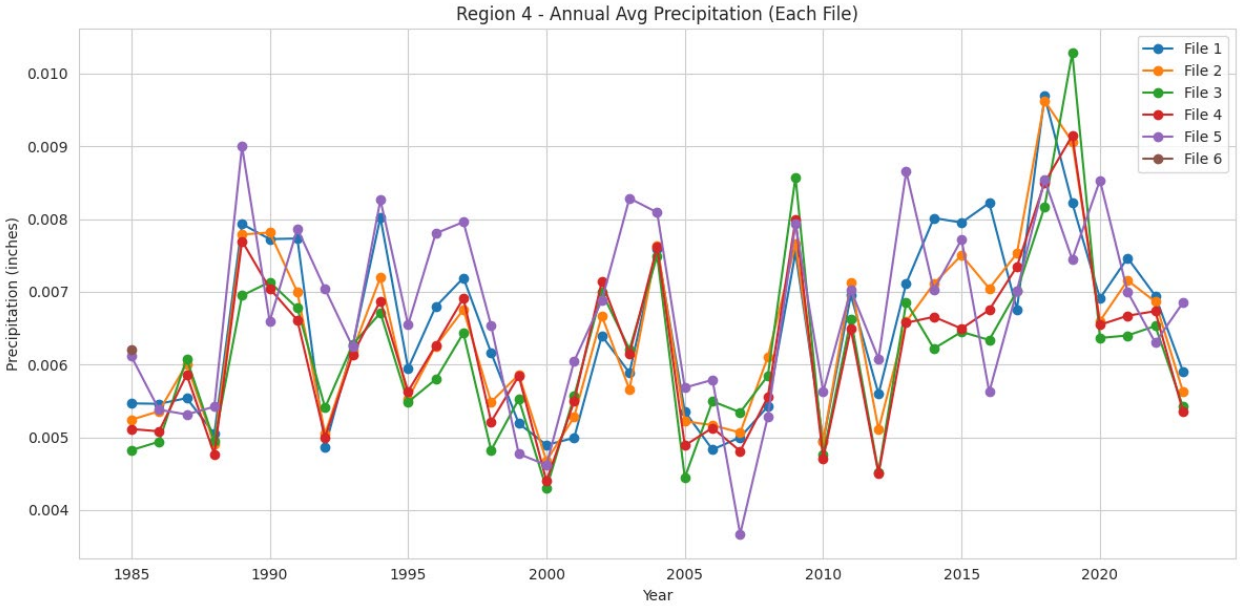

Annual Average Precipitation of each site in Region 4

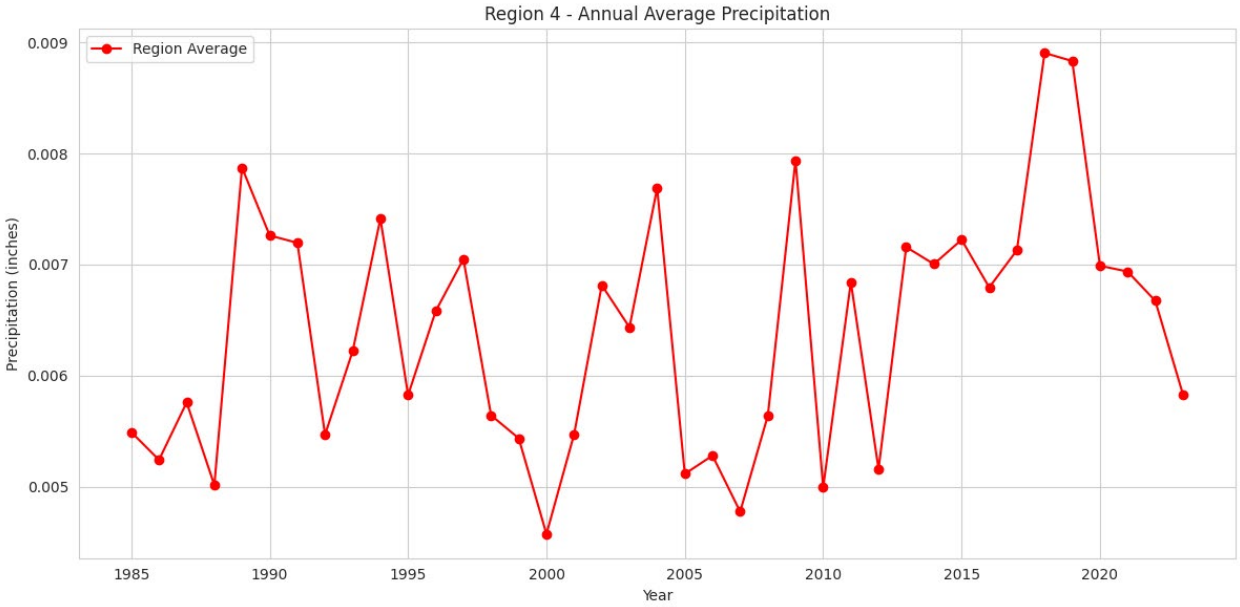

Annual Average Precipitation from all sites in Region 4

All regions:

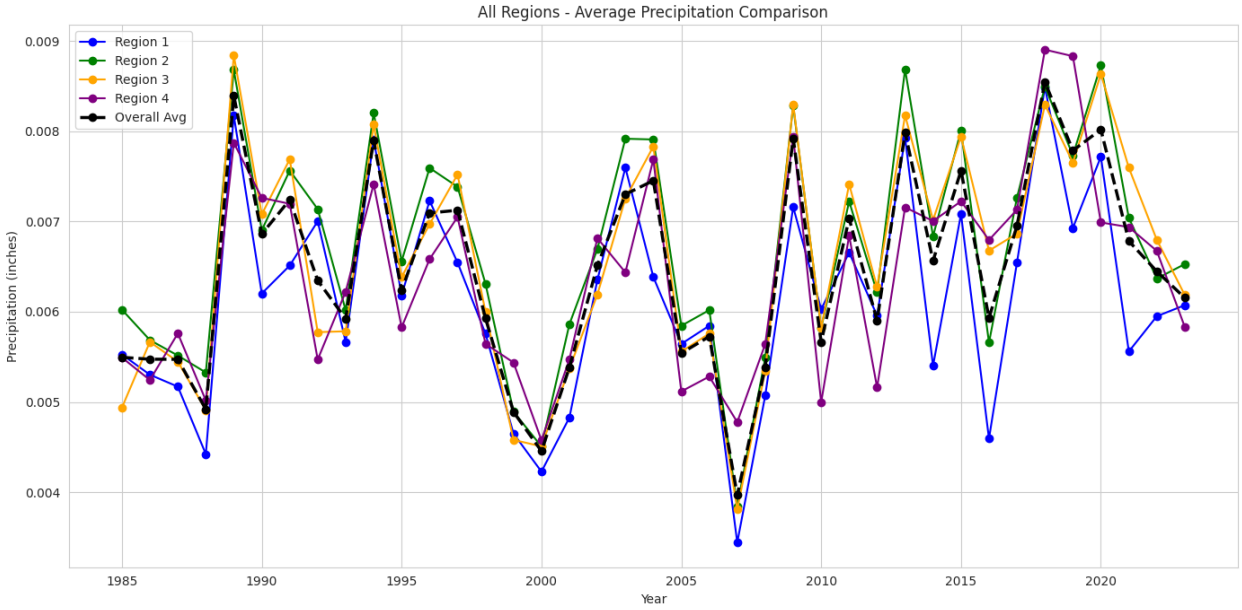
All Regions - Average Precipitation Comparison
Region 1
Region 2
Region 3
Region 4
Overall Avg
Precipitation (inches)
0.009
0.008
0.007
0.006
0.005
0.004
1985
1990
1995
2000
2005
2010
2015
2020
Year